Identifying Factors that Protect the Host from *Clostridium difficile* Infection

by

Jhansi Lakshmi Margaret Leslie

A dissertation submitted in partial fulfillment
of the requirements for the degree of
Doctor of Philosophy
(Microbiology and Immunology)
in the University of Michigan
2017

Doctoral Committee:

Professor Vincent B. Young, chair
Assistant Professor Irina Grigorova
Professor Philip C. Hanna
Professor Thomas Schmidt
Professor Michele S. Swanson

jlleslie@umich.edu
ORCID: 0000-0001-5600-210X

DEDICATION

For my family

ACKNOWLEDGEMENTS

This work would not have been possible without the support of many people over the years. I have been particularly lucky with the mentors in my life. Dr. Jay Solnick and his graduate student at the time, Dr. Michael Hornsby gave me my first chance to work in the lab, an opportunity that changed my life, for which I will always be grateful. Dr. Chris Polage introduced me to *C. difficile*, with the simple question “How do you feel about feces?” I am grateful for that as well as the advice and training I received while in his lab.

I have been equally fortunate in choosing my dissertation mentor, Vince for whom I have huge amount of respect and admiration. The rich and engaging environment he works so hard to provide for his trainees has been an amazing place to train. His curiosity and willingness to explore new fields as well as blunt honesty have made working in the lab both exciting and fun. I am also extremely grateful that Vince allowed me the freedom explore my scientific interests; I would not be the scientist I am today with out his guidance and training. Thank you.

The exceptional scientists that make up my thesis committee, Drs. Michele Swanson, Phillip Hanna, Irina Grigorova, and Thomas Schmidt also deserve huge thanks, as I learned so much from them at each of our meetings. Perhaps

the most important lesson imparted on me by them was to question my assumptions, chapter two would not have existed as it without that lesson. I also owe thanks to Dr. Patrick Schloss and his entire lab, my dissertation benefited greatly from my immersion in the Schloss lab.

The Young lab has been a warm and supportive environment from day one and each person who has been in the lab over the years has helped facilitate this project in some way. Particularly, our amazing lab managers over the years, Judith Opp, Kathy Wozniak, and Kimberly Vendrov, without their training, help and friendship most of the work that follows could not have been accomplished.

Drs. Casey Theriot and Anna Seekatz served both as my scientific role models and great friends during my training. Thank you both for taking the time to discuss ideas and share papers, it helped me grow tremendously. A special thank you to Drs. Niel and Sarah Baxter, who made graduate school fun.

Arguably the best part of prelims was meeting Matthew Jenior, a crucial collaborator on this endeavor and in my life. Your dedication and work ethic have been an inspiration. This work would not have been possible without you. Last but certainly not least, my family, who provide me with unconditional support and constant inspiration. I am more grateful than I have the words to express.

TABLE OF CONTENTS

LIST OF FIGURES

ABSTRACT

Clostridium difficile is the most prevalent single cause of nosocomial infection in the United States. A major risk factor for *Clostridium difficile* infection (CDI) is exposure to antibiotics. Antibiotics increase susceptibility to CDI by altering the gut microbial community, enabling increased germination of spores and growth of vegetative cells. Despite being a major risk factor, antibiotics are currently the principal treatment for the disease. The cycle of antibiotic usage associated with CDI is likely why twenty-five percent of patients with CDI fail antibiotic therapy and experience recurrent disease. An alternative treatment, such as limiting colonization with toxigenic *C. difficile* by prior colonization of susceptible patients with non-toxigenic strains of *C. difficile* has been utilized with some success in clinical trials. However the mechanisms underlying how prior colonization with *C. difficile* limits disease are unknown. The work described in this dissertation sought to determine the relative contribution of host and bacterial factors in mediating protection from CDI. Using a murine model of *C. difficile*, I present evidence in support of a novel paradigm of colonization resistance. In this model depletion of the amino acid glycine by prior colonization with one strain of *C. difficile* protects from lethal CDI by limiting germination of the incoming strain. Additionally, I show that unlike other gastrointestinal infections,

adaptive immunity is not required for clearance of *C. difficile*, rather clearance is associated the presence of two members of the *Lachnospiraceae* family in the indigenous untreated microbial community. Finally, I describe the use of human intestinal organoids to study CDI in the context of a complex human epithelium. Together these results underscore the importance of bacterial interactions in providing protection from colonization while attributes of the host and pathogen may alter the pathogenesis of the infection. These results are important because they provide new insights into this important nosocomial infection. Furthermore the role of glycine in providing colonization resistance provides a novel target for the development of next-generation probiotic therapies for CDI.

CHAPTER I

INTRODUCTION

Discovery and Epidemiology of *Clostridium difficile*

Clostridium difficile is a Gram-positive, spore-forming, anaerobic, bacillus. Originally named *Bacillus difficilis* for its morphology and its difficulty to cultivate, the species was first isolated in 1935 by Hall and O'Toole during a study characterizing changes in the maturing infant fecal bacterial community (1). Ominously, while the infants from whom this bacterium was isolated were seemingly healthy, the authors reported that spent culture media from this new species caused disease and even death in rabbits and guinea pigs. Almost forty years later, *C. difficile* emerged as a clinically important pathogen when it was linked to the development of pseudomembranous colitis in patients receiving antibiotics (2-4). We now know that colonization with C. *difficile* can result in asymptomatic carriage, mild diarrhea, pseudomembranous colitis, or even death. Currently, C. *difficile* infection (CDI) is the most prevalent hospital-acquired infection in the US, resulting in nearly 500,000 cases and 15,000 deaths a year (5).

CDI is a multistep infection (figure 1.1). First, alterations to the membership and/or function of gut microbiota leave the host susceptible to colonization (6-8). Colonization occurs via the fecal-oral route and can be

contracted from either infected individuals or from contaminated environmental sources. The metabolically dormant and ethanol-resistant spore is believed to be the primary transmissive form of the bacterium (9). Following ingestion, signals in the intestine such as glycine and the bile acid taurocholate induce germination of the spore into the metabolically active vegetative cell, which replicates in the large intestine (10-12). Finally, additional signals such as depletion of nutrients trigger sporulation and production of toxins, which mediate disease (13).

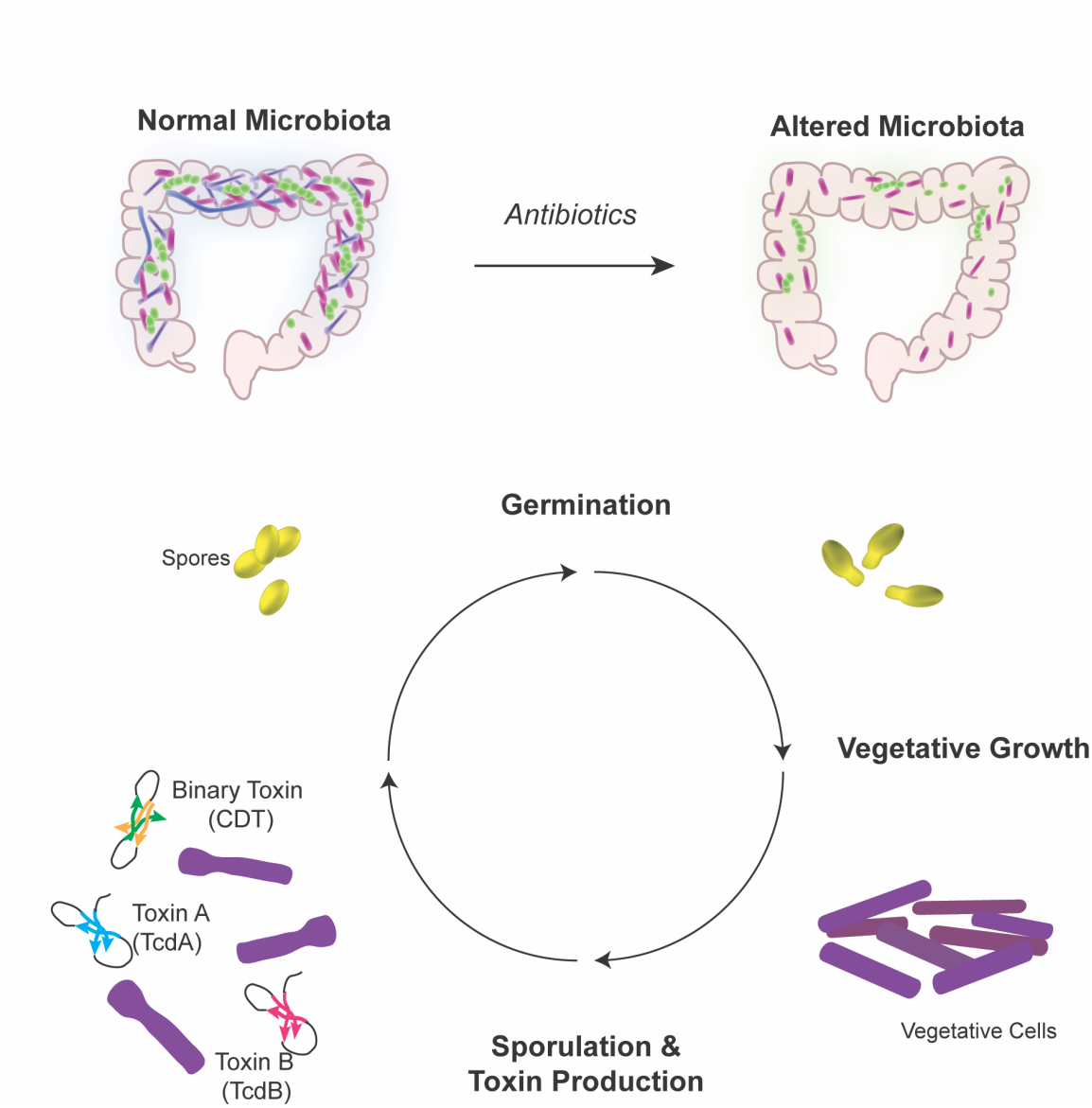

Figure 1.1: *Clostridium difficile* infection is a multistep disease
The intact gut microbiota protects from colonization with *C. difficile.* However following a perturbation such as antibiotic therapy, the altered community can be susceptible to colonization. *C. difficile* is believed to persist in the environment as a metabolically dormant spore. Upon ingestion and exposure to the correct environmental cues in the gut, the spore germinates into a vegetative cell that requires specific nutrients to replicate. Disease is mediated by its toxins (TcdA, TcdB and CDT), which are expressed during the later stage of growth. Sporulation is often observed concomitantly with toxin production in the later growth phase, completing the cycle.

C. difficile is a promiscuous pathogen, in that it can colonize and cause disease in many different animals including cats, dogs, pigs, horses and birds (14-17). While some data suggests transmission of *C. difficile* can occur between animals and humans, it remains to be proven if *C. difficile* is a truly a zoonotic disease or if colonization of animals and humans with the same strains merely points to high levels of environmental *C. difficile* (18, 19).

Major risk factors for acquiring CDI include: hospitalization, antibiotic exposure, and age over sixty-five years (20, 21). While clindamycin was first associated with the susceptibility to CDI, almost all classes of antibiotics have since been demonstrated to increase susceptibility in either humans or animal models of infection (22-25). Some classes of antibiotics impose a greater risk of developing CDI; limiting the use of antibiotics known to be associated with the development of CDI can reduce the incidence of the disease (24, 26, 27). Other factors that are associated with development of CDI include comorbidities such as inflammatory bowel disease, solid organ transplant and immune suppression (28-30). Proton pump inhibitors have also been proposed to increase risk for CDI, however the data on this association are less conclusive (31, 32). In addition to primary infection, recurrent infection is increasingly a problem with approximately one in five patients experiencing recurrent CDI (33). Patients that experience a first recurrence are increasingly likely to experience additional bouts of recurrent CDI (34). Although it is unknown why certain patients experience recurrence while others do not, failure of the microbiota to recover following antibiotics and or decreased humoral response to the toxins might play

a role (30, 35, 36). Currently the IDSA recommended therapy for treatment of both primary and recurrent CDI is the antibiotic vancomycin (37). Recently studies reporting a greater than 85% success rate for treatment of recurrent CDI with fecal microbial transplants has resulted in increased use of this therapy (38).

In the early 2000's the epidemiology of CDI changed, with a sharp increase in the incidence and severity of infection. This change is at least partially attributed to the emergence of a clade of *C. difficile* termed ribotype 027 (39). Ribotype 027's emerged in North America and went on to spread worldwide over the first decade of this century (40). These new strains of *C. difficile* were associated with more severe disease as well as increased relapse following treatment (41). Other clades of *C. difficile* such as the 078 have now also been associated with these phenotypes. Another major change in the epidemiology of CDI is the increased incidence of the disease in populations that were previously considered low-risk for infection, such as patients with no recent healthcare exposure (42, 43). It is unclear what is driving the worrying trend of increased community-associated CDI.

Currently, the incidence of CDI seems to have leveled, potentially due to changes in hospital policy such as better antibiotic stewardship (44). Interestingly, antibiotics seem to have been a strong influence on not only in terms of increasing susceptibility of the host to infection but also in terms of selection for the increase prevalence of strains that carry resistance to the same class of antibiotic. Nevertheless, CDI remains a serious health threat in the United States and throughout the world.

Pathogenesis

C. difficile is a genetically diverse species. Even between sub strains of *C. difficile* like the common laboratory strains 630 and 630Δerm there is much phenotypic variation (45). This diversity has led to controversy within the field when attempting to delineate the roles of the toxins as well as various other genes in the pathogenesis of infection (46-48). Additionally, relative to the commonly studied Gram-negative pathogens, the laborious process of generating clean mutations in both lab and clinical isolates has hampered determination of the specific roles of C. difficile genes in pathogenesis.

C. difficile causes disease via production of toxins. To date, all reported isolates carry up to three toxins (TcdA, TcdB and CDT). Strains that do not encode at least one of the three toxins do not cause disease (46, 49, 50). The primary virulence factors are the toxins carried within a 19.6kb region of the chromosome called the pathogenicity locus (Paloc) (51). Within the Paloc, the genes *tcdA* and *tcdB* encode the proteins toxin A (TcdA) and toxin B (TcdB), respectively. In addition to the toxins, the Paloc encodes an alternative sigma factor, *tcdR,* which positively regulates toxin production, as well as *tcdC,* a negative regulator of transcription (52-54). The final gene encoded in this locus is *tcdE*. TcdE is a putative phage-like holin, which is thought to facilitate secretion of the toxins (55). The Paloc genes can each be transcribed from their own promoters in addition to being transcribed as one polycistronic transcript (56, 57).

TcdA may be produced in higher quantities than TcdB, as transcripts of *tcdA* have been observed to be twice as abundant as *tcdB* transcript (57, 58).

Regulation of the Paloc is tied to many aspects of *C. difficile* metabolism. *In vitro* studies show that the master transcription factor CodY suppresses toxin production in the presence of high intracellular levels of branched chain amino acids (59). The amino acids cysteine, proline, as well as other easily metabolized carbon sources such as glucose also suppress toxin production (60-63). Conversely, toxin production is increased in stationary phase cultures suggesting that nutrient limitation also regulates the toxins.

Recent work by Jenior et al. showed that, in the context of different bacterial communities and thus varied metabolite milieus, the same strain of *C. difficile* expresses different levels of toxin, as measured by a cell cytotoxicity assay (64). This hints at a possible means by which individuals colonized with the same strain might experience varying severity of disease due to differences in the metabolites available to *C. difficile*. In addition, some strains of *C. difficile* regulate toxin production in response to their own population density through accessory gene regulator (*Agr*) mediated quorum signaling (65, 66). Integration of multiple environmental signals into regulation of its major virulence factors is fitting for a bacterium that relies so heavily on the status of the surrounding microbial community to carry out its life cycle. Furthermore, it suggests that the toxins many serve as a means for the bacterium to either acquire new nutrients sources or perhaps as an exit plan, as sporulation is thought to be timed with production of toxins.

The toxins TcdA and TcdB are large multi-domain proteins of approximately 308 and 270 KDa respectively. The proteins share a similar overall structure and within certain strains can have as much as 66% similarity (67). The region of most difference is the C-terminal domain, consisting of multiple olligopeptide repeats. This region is thought to mediate binding of the toxin to its cellular receptors. The currently identified receptors for TcdA are carbohydrates and the glycoprotein 96 (gp96) (68-70). However *in vitro* studies show that the C-terminal section of TcdA is not required for entry into the cell (71, 72). This suggests that another portion of the toxin is able to bind to mediate cell entry. Until recently the receptors for TcdB were unknown. In the last few years, three putative receptors have been identified: Wnt receptor frizzled family proteins (specifically FZD 1, 2 and 7), Chondroitin sulfate proteoglycan 4 (CSPG4), and Poliovirus receptor-like 3 (PLV3) (73-75). There is still controversy as to which of the three currently identified receptors actually contribute to disease in humans as CSPG4 is not actually expressed on the human colon epithelium (76). Determining the true receptors for the toxins will be crucial to understanding the pathogenesis of this infection. For example, whereas other bacterial causes of pseudomembranous colitis result in disease of the small bowel, a defining feature of CDI is that it is primarily a disease of the large bowel. At least one of the receptors, PLV3, is primarily expressed in the colon and not in the small intestine, which might explain the tissue tropism of CDI.

Following attachment, entry of the toxins into the cell was believed to be through clathrin-mediated endocytosis. While this is true of TcdB, TcdA can enter

the cell via both clathrin dependent and independent mechanisms (77). It is tempting to speculate that the different routes of entry might modulate the effect of the toxin on their cellular targets. Following endocytosis, the pH of the vesicle decreases, causing the hydrophobic translocation domain to insert into the membrane of the vesicle (78). Then the toxin's cysteine protease, with the aid of a host lipid inositol hexakisphosphate (InsP6) and zinc, cleaves off the N terminal enzymatic portion of the toxin (79-81).

The N-terminal domain is a glycosyltransferase. Once this domain is released from the holotoxin, it traffics to the apical cell membrane where it acts on its cellular targets: host GTPases such as Rho A, B, C, G Rac1-3 and Cd42 (82). Some strains of *C. difficile* have variations of TcdA and TcdB, that interact with slightly different cellular targets (83-86). Both TcdA and TcdB inactivate host GTPases via the transfer a glucose moiety onto either Thr37 or Thr35 of the GTPase, blocking its interaction with its effectors (87, 88). Rho family GTPases are integral to many cellular processes, such as regulating cytoskeletal structure and cell-cell contact; thus, inactivation results in many downstream effects (89). Broadly, glycosyltransferase-mediated inactivation of Rho family proteins can cause cytopathic effects, such as cell rounding, and death. While TcdA requires the glycoslytrasferase domain to cause cell death, at high concentrations TcdB can cause a necrotic cell death independent of its enzymatic activity (90, 91).

Some strains of *C. difficile,* most notably the ribotype 027 and 078 clades, express a third toxin called *C. difficile* transferase (CDT). This toxin is encoded in a 6.2 kb region of the chromosome termed the CdtLoc that is separate from the

Paloc. This locus is not carried by all strains of *C. difficile*; some strains completely lack the locus while others have *cdtR* but only retain a *cdtAB* pseudogene (92). The CdtLoc has three genes, *cdtR, ctdA*, and *cdtB*. *CdtR* encodes the transcriptional regulator of the locus, which additionally regulates the expression of TcdA and TcdB (93, 94). CDT is often called *C. difficile* binary toxin because it requires two components, CDTa and CDTb, to intoxicate cells. CDTb, the binding domain, is similar to *Clostridium perfringens* iota toxin; like iota toxin, CDTb utilizes lipolysis-stimulated lipoprotein cellular receptor for binding and internalization of CDT into host cells (95, 96). CDTa, the enzymatic portion of the toxin, binds a heptamer of CDTb. Following endocytosis and release into the host cell, CDTa mono-ADP-ribosylates globular actin(97). Ribosylation of actin disrupts microtubule structure, resulting in fingerlike projections from epithelial cells *in vitro*. To date the signals, that induce expression of CDT have yet to be fully characterized. While CDT is not required for virulence as strains that carry only CDT are avirulent in animal models, CDT can enhance virulence (98, 99). Another proposed role of CDT is enhancing colonization via increased adherence to the epithelium (100, 101). It should be noted that in animal models, no defect in initial colonization has been observed for strains that lack the binary toxin. In fact, the strains that lack all toxins colonize to the same level as strains with all three (7). This paradox begs the question of what if any role the toxins play in facilitating colonization. One study suggested that a 027 isolate, strain R20291, was able to persistently colonize a mouse while a historical strain that

lacked CDT was cleared (102). The role of the toxins in persistent colonization of the gut remains to be elucidated.

The Role of the Microbiome in CDI

The bacterial community that inhabits our gut plays a crucial role in the development of host physiology and health (103-105). In addition, the microbiota also provides protection from invading pathogens, an attribute termed colonization resistance (106, 107). In retrospect, the vital link between our resident gut bacteria and *C. difficile* was tantalizingly plain from its first discovery. *C. difficile* was recovered from the feces of infants, which we now know have relatively low diversity microbial communities that in some ways resemble the antibiotic-treated gut of an adult (108, 109). Understanding how the microbiota mediates colonization resistance is an active field of research. Our current grasp of the microbiota-mediated mechanisms that influence *C. difficile* colonization can be viewed through the framework of factors that influence the life cycle of *C. difficile* (figure 1.2).

The first step of *C. difficile* colonization following ingestion of a spore is germination within the intestine (110). Bile acids are key signals for germination (110, 111). Bile acid metabolism represents integration of both host and bacterial metabolism (112) . The primary bile acids chenodeoxycholate, cholate and their conjugated derivatives are synthesized in the liver and secreted into the small intestine. Most primary bile acids are reabsorbed by the terminal ileum, however residual primary bile acids are converted into secondary bile acids by

the gut microbiota (113). As a result, the large bowel typically has low levels of primary bile acids. In a conventional mouse, small intestinal content supports germination of *C. difficile* spores and outgrowth, while content from the cecum does not (114, 115). However, following antibiotic exposure, the level of the primary bile acids that facilitate germination are increased in the large bowel and feces, wherease levels of the secondary bile acids that inhibit outgrowth of vegetative cells are decreased (10, 11, 116, 117). Thus the pool of bile acids in the gut influences both the efficiency of germination as well as growth of the vegetative cell, ultimately impacting colonization. Treatment of a susceptible mouse with a single bacterium capable of converting primary bile acids to secondary bile acids, namely *Clostridium scindens,* is sufficient to partially restore colonization resistance (118, 119). However it is unclear if this phenotype occurs purely through modulation of the bile acid pool or if *C. scindens* provides protection via other means as well.

Following germination, the next requirement for colonization is the ability of the vegetative cell to find a suitable niche to propagate itself. As defined by Hutchison, an organism's niche includes all n-dimensional space that is defined by the resources required by an organism, such as the nutrients it utilizes to grow and replicate as well as the physical space it occupies (120). Rolf Freter applied the concept of an ecological niche as defined by nutrient availability to the microorganisms that inhabit the gut when he proposed the nutrient niche hypothesis, which posits that the composition of the gut microbiota is defined by interspecific competition for growth substrates (121). A correlate of this

hypothesis is that the colonization resistance is mediated by utilization of all available substrates by members of the microbiota. Thus, as the diversity of a community decreases, so should the level of colonization resistance. While a correlation between decreased diversity and increased susceptibility to CDI has frequently been remarked upon in the literature, diversity in and of itself is not likely to be responsible for providing colonization resistance (36). As an example, germ-free mice, which completely lack resident microbes, have no colonization resistance to *C. difficile* (122, 123). However, pre-colonizing germ-free mice with *Bacteroides thetaiotaomicron* (technically increasing diversity) increases levels of succinate in the gut resulting in higher levels of *C. difficile* upon challenge, thus arguably decreasing colonization resistance (124).

Many early studies exploring colonization resistance to C*. difficile* focused on the importance of the intact gut microbiota in preventing colonization (122, 125-128). They tested the hypothesis that intact community prevented colonization via utilization of the nutrients required by C*. difficile*. Recent studies have demonstrated that following administration of antibiotics there is a significant increase in the types of nutrients *C. difficile* can utilize for growth, such as sugar alcohols and amino acids (115, 129). However, a limitation of these studies is that most fail to directly prove that the members of the microbiota that are decreased following antibiotics actually limit colonization of *C. difficile* via competition for those specific nutrients. Thus while direct evidence in support of the nutrient niche hypothesis has been demonstrated with respect to other

bacteria such as *Escherichia coli*, it has yet to be fully supported with regard to *C. difficile* (130).

In addition to the general nutritional requirements for growth, a niche is also defined by the abiotic requirements such as the features that define the physical habitat of the organism. Beyond nutrients, the remaining aspects of *C. difficile's* niche space have been poorly defined. Recent work has sought to define localization of *C. difficile* in the intestine, however the data are conflicting. Some studies suggest that it colonizes close to the mucosa or even the crypts, while others suggest that it mainly resides in the outer mucus layer (131, 132). The question of where an organism lives seems mundane,, but it can be a crucial factor in explaining colonization resistance. In the case of certain Bacteroides, two different species are both able to colonize a germ-free mouse. However, pre-colonization with one strain precludes stable colonization with another strain of the same species. This phenotype was found to be associated with a specific locus, which enables localization of strains carrying those genes to the colonic crypts and thus saturation of that species' spatial niche (133). It is tempting to speculate that perhaps one of proteins that has been reported to facilitate *C. difficile* adhesion to the colonic epithelium, such as the surface layer protein (SlpA), may play a similar role (134, 135).

In addition to limiting the replicative ability of the vegetative cell, colonization of *C. difficile* may also be limited by inhibitors produced by other bacteria (136). Bacteriocins are small bactericidal proteins produced by bacteria often to inhibit closely related species (137). Some strains of *C. difficile* can

produce a R-type bacteriocin which when given prophylactically protects mice from colonization (138). A recent report of successful treatment of recurrent CDI using sterile fecal microbiota transplants also hints at the potential of molecules produced by the resident microbiota to directly inhibit *C. difficile* in the absence of viable bacteria (139).

Following colonization, the development of disease is ultimately dependent on both the activity of, and response to, *C. difficile* toxins. Much of the what we know regarding how the toxins interact with cells has been learned through the use of *in vitro* cell culture systems using epithelial cell lines such as Caco2, HT29, or Vero cells. However these systems lack much of the complexity inherent to an *in vivo* infection, such as the different cell types that make up the gastrointestinal tract or the ability to co-culture members of the microbiota. These are major limitations, since many studies show that the microbiota and/or microbial products play an important role in modulating the activity of the toxins and thus the course of disease. Certain strains of Bifidobacteria and Lactobacilli can decrease toxin-mediated cell rounding *in vitro*. This finding was dependent on incubation of viable *Bifidobacterium longum* with the toxins suggesting that the strain is either breaking down or secreting an inhibitor of the toxins (140). In a mouse model of EHEC, another toxin-mediated intestinal infection, acetate (a byproduct of microbial fermentation) protected mice from severe disease (141). Recently, potassium acetate mediated inhibition of histone deacetylase 6 was shown to protect from TcdA mediated inflammation (142). It would be interesting

to determine whether the short chain fatty acid acetate can protect from TcdA via a similar mechanism *in vivo.*

Elucidating the mechanisms that underlie microbiota-mediated colonization resistance and protection from disease is a critical area of investigation. Not solely because of the potential to derive novel therapeutics to treat CDI, but also because this knowledge will likely be necessary to combat antibiotic-resistant bacteria as we enter the post-antibiotic era.

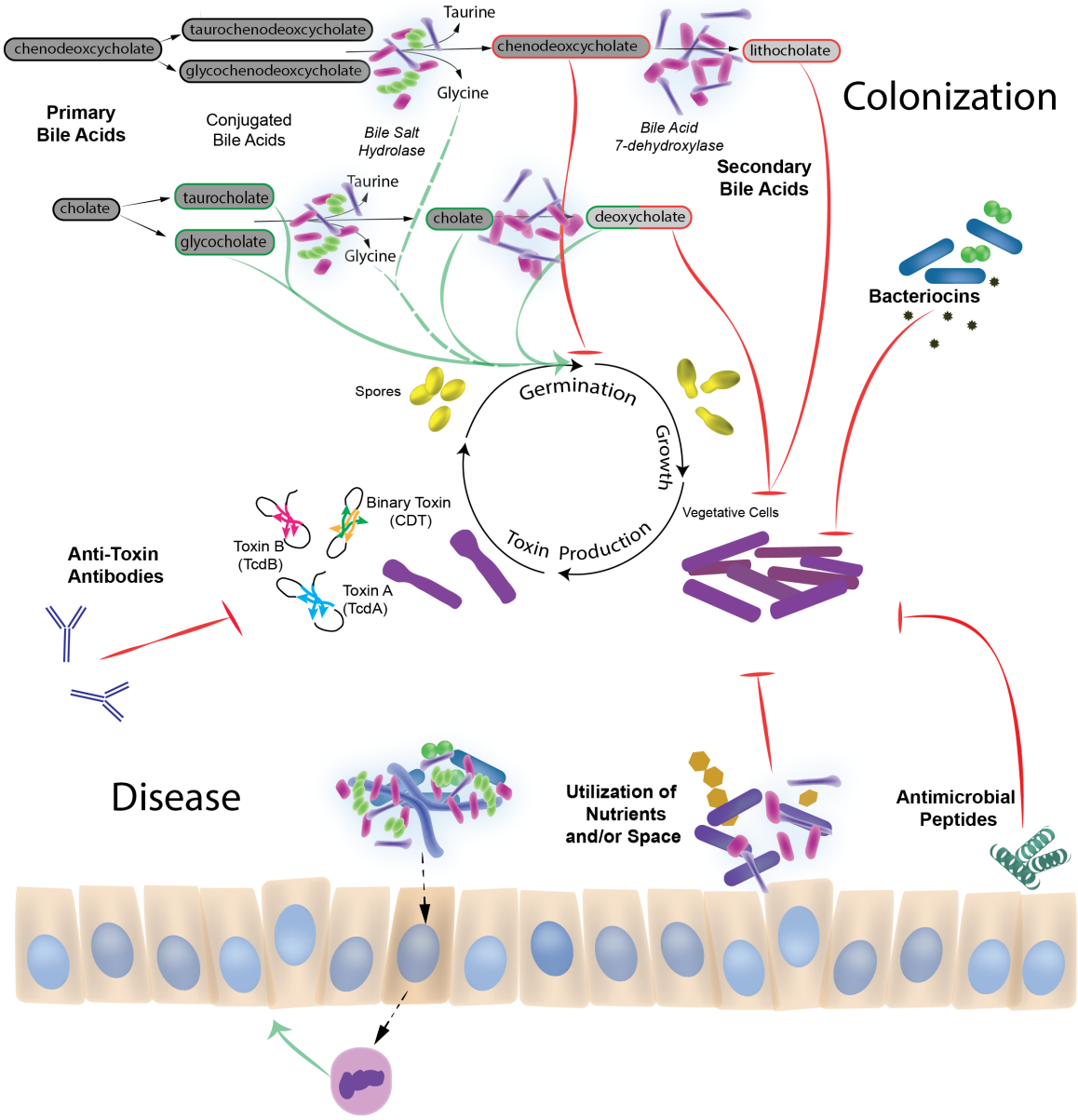

Figure 1.2. Mechanisms of protection from CDI
The mechanisms of protection from CDI can be viewed through the framework of the life cycle of *C. difficile*. Microbiota mediated protection primarily inhibits germination and outgrowth which impacts colonization. While host factors such as anti-toxin antibodies modulate disease. There are points of intersection, such as microbiota-derived signals that drive protective immune responses.

Host Response to Infection

The immune response to *C. difficile* governs the outcome of the infection. Toll like receptors (TLRs), which sense conserved microbial molecules, are critical regulators of both innate and adaptive immunity (143). TLR signaling in particular determines the response to acute infection. In the absence of MyD88, a critical node in TLR signaling, mice are more susceptible to severe CDI (144). After infection of MyD88-deficient mice, impaired neutrophil recruitment resulting in increased mortality (145). In addition to TLRs, signaling though the NOD like proteins, specifically NOD1, also facilitates neutrophil-mediated protection of acute infection (146). However the role of neutrophils in protection from CDI is still partially unresolved. In most models, the inability to recruit neutrophils results in severe disease; however, in rabbit ileal loops, inhibition of neutrophils protects the tissue from damage (147). Furthermore, there is a significant associated between elevated levels of Il-8, the chemokine primarily involved in recruitment of neutrophils, and severe disease in patients (148, 149). Perhaps the immune context and/or timing of recruitment relative to the infection potentiate the protective or harmful role of neutrophil recruitment during CDI. Whether this is the case is yet to be resolved. In addition to neutrophils, innate lymphoid cells (ILC) specifically interferon gamma producing ILC1, protect from severe disease in a murine model (150, 151). Recently eosinophils, a heretofore-neglected cell linage in terms of bacteria infections, have been linked to protection from CDI. Antibiotic perturbations of the microbiota decreased levels of the IL-17 family cytokine IL-25, leading to decreased eosinophils and

increased damage to the gut epithelium (152). Interestingly, binary toxin (CDT) can suppress the eosinophilic response, offering a potential explanation as to why some strains carrying binary toxin, like the 027 clade, might be associated with worse outcomes (99).

In addition to innate immunity, adaptive immunity is also critical to the pathogenesis of CDI. The majority of the research analyzing adaptive immunity and CDI has focused on the role of anti-toxin antibodies and protection from symptomatic disease. Early studies noted that patients who had deceased levels of serum IgG against TcdA were at increased risk for recurrent disease(30, 153). In animal models, passive immunization protects from disease (154, 155). Indeed, treatment of patients with monoclonal antibodies against TcdB reduces recurrent infections by 50% (156). Beyond a humoral response to the toxin, the impact of adaptive immunity on any other aspect of the infection is currently understudied.

Outline of the thesis

This thesis is based on the central hypothesis that resistance against *C. difficile* disease reflects the combined effects of host immunity and bacteria/bacteria competition. In chapter two, I describe a mechanism by which pre-colonization with one strain of *C. difficile* limits colonization of another via depletion of the amino acid glycine. While it was known that glycine enhances *C. difficile* vegetative growth in addition to being a required co-germinant, this is the first report of colonization resistance mediated by limitation of glycine (12,

157). In chapter three, the contribution of adaptive immunity to clearance of *C. difficile* is explored via restoration of adaptive immunity into immune-compromised infected mice. These experiments demonstrate that unlike infections caused by other gastrointestinal pathogens, adaptive immunity is not required for clearance of *C. difficile*. In chapter four, I characterize the use of intestinal organoids derived from human embryonic stem cells, as a tool to study the effects of *C. difficile* toxins on a more physiologically relevant epithelium. Finally, in chapter five, the implications of the findings in this thesis are discussed.

References

1. **Hall IC, O'Toole E.** 1935. Intestinal flora in new-born infants: With a description of a new pathogenic anaerobe, *Bacillus difficilis*. American Journal of Diseases of Children **49:**390-402.

2. **Tedesco FJ, Barton RW, Alpers DH.** 1974. Clindamycin-associated colitis: A prospective study. Annals of Internal Medicine **81:**429-433.

3. **Bartlett JG, Chang TW, Gurwith M, Gorbach SL, Onderdonk AB.** 1978. Antibiotic-associated pseudomembranous colitis due to toxin-producing *Clostridia*. New England Journal of Medicine **298:**531-534.

4. **Fekety R, Silva J, Toshniwal R, Allo M, Armstrong J, Browne R, Ebright J, Rifkin G.** 1979. Antibiotic-associated colitis: effects of antibiotics on *Clostridium difficile* and the disease in hamsters. Review of Infectious Diseases **1:**386-397.

5. **Lessa FC, Mu Y, Bamberg WM, Beldavs ZG, Dumyati GK, Dunn JR, Farley MM, Holzbauer SM, Meek JI, Phipps EC, Wilson LE, Winston LG, Cohen JA, Limbago BM, Fridkin SK, Gerding DN, McDonald LC.** 2015. Burden of *Clostridium difficile* infection in the United States. New England Journal of Medicine **372:**825-834.

6. **Reeves AE, Theriot CM, Bergin IL, Huffnagle GB, Schloss PD, Young VB.** 2010. The interplay between microbiome dynamics and pathogen dynamics in a murine model of *Clostridium difficile* Infection. Gut microbes **2:**145-158.

7. **Theriot CM, Koumpouras CC, Carlson PE, Bergin II, Aronoff DM, Young VB.** 2011. Cefoperazone-treated mice as an experimental platform to assess differential virulence of *Clostridium difficile* strains. Gut microbes **2:**326-334.

8. **Buffie CG, Jarchum I, Equinda M, Lipuma L, Gobourne A, Viale A, Ubeda C, Xavier J, Pamer EG.** 2011. Profound alterations of intestinal microbiota following a single dose of clindamycin results in sustained susceptibility to *Clostridium difficile*-induced colitis. Infection and immunity **80:**62-73.

9. **Deakin LJ, Clare S, Fagan RP, Dawson LF, Pickard DJ, West MR, Wren BW, Fairweather NF, Dougan G, Lawley TD.** 2012. The *Clostridium difficile* spo0A gene is a persistence and transmission factor. Infection and immunity **80:**2704-2711.

10. **Theriot CM, Koenigsknecht MJ, Carlson PE, Jr., Hatton GE, Nelson AM, Li B, Huffnagle GB, J ZL, Young VB.** 2014. Antibiotic-induced shifts in the mouse gut microbiome and metabolome increase susceptibility to *Clostridium difficile* infection. Nat Commun **5:**3114.

11. **Theriot CM, Bowman AA, Young VB.** 2016. Antibiotic-induced alterations of the gut microbiota alter secondary bile acid production and allow for *Clostridium difficile* spore germination and outgrowth in the large intestine. mSphere **1**.

12. **Sorg JA, Sonenshein AL.** 2008. Bile salts and glycine as cogerminants for *Clostridium difficile* spores. Journal of Bacteriology **190:**2505-2512.

13. **Edwards AN, Nawrocki KL, McBride SM.** 2014. Conserved oligopeptide permeases modulate sporulation initiation in *Clostridium difficile*. Infect Immun **82:**4276-4291.

14. **Stone NE, Sidak-Loftis LC, Sahl JW, Vazquez AJ, Wiggins KB, Gillece JD, Hicks ND, Schupp JM, Busch JD, Keim P, Wagner DM.** 2016. More than 50% of *Clostridium difficile* isolates from pet dogs in Flagstaff, USA, carry toxigenic genotypes. PLOS ONE **11:**e0164504.

15. **Madewell BR, Bea JK, Kraegel SA, Winthrop M, Tang YJ, Silva J.** 1999. *Clostridium difficile*: a survey of fecal carriage in cats in a veterinary medical teaching hospital. Journal of Veterinary Diagnostic Investigation **11:**50-54.

16. **Diab SS, Songer G, Uzal FA.** 2013. *Clostridium difficile* infection in horses: a review. Veterinary Microbiology **167:**42-49.

17. **Harvey RB, Norman KN, Andrews K, Hume ME, Scanlan CM, Callaway TR, Anderson RC, Nisbet DJ.** 2011. *Clostridium difficile* in Poultry and Poultry Meat. Foodborne Pathogens and Disease **8:**1321-1323.

18. **Knetsch CW, Connor TR, Mutreja A, van Dorp SM, Sanders IM, Browne HP, Harris D, Lipman L, Keessen EC, Corver J, Kuijper EJ, TD. L.** 2014. Whole genome sequencing reveals potential spread of *Clostridium difficile* between humans and farm animals in the Netherlands, 2002 to 2011. . Eurosurveillance **19**.

19. **Janezic S, Potocnik M, Zidaric V, Rupnik M.** 2016. Highly divergent *Clostridium difficile* strains isolated from the environment. PLoS ONE **11:**e0167101.

20. **Patel UC, Wieczorkiewicz JT, Tuazon J.** 2016. Evaluation of advanced age as a risk factor for severe *Clostridium difficile* infection. Journal of Clinical Gerontology and Geriatrics **7:**12-16.

21. **Jump RLP.** 2013. *Clostridium difficile* infection in older adults. Aging health **9:**403-414.

22. **Bignardi GE.** 1998. Risk factors for *Clostridium difficile* infection. Journal of Hospital Infection **40:**1-15.

23. **Gerding DN.** 2004. Clindamycin, cephalosporins, fluoroquinolones, and *Clostridium difficile*–associated diarrhea: this Is an antimicrobial resistance problem. Clinical Infectious Diseases **38:**646-648.

24. **Brown KA, Khanafer N, Daneman N, Fisman DN.** 2013. Meta-analysis of antibiotics and the risk of community-associated *Clostridium difficile* infection. Antimicrobial Agents and Chemotherapy **57:**2326-2332.

25. **Schubert AM, Sinani H, Schloss PD.** 2015. Antibiotic-induced alterations of the murine gut microbiota and subsequent effects on colonization resistance against *Clostridium difficile*. mBio **6**.

26. **Vardakas KZ, Trigkidis KK, Boukouvala E, Falagas ME.** 2016. *Clostridium difficile* infection following systemic antibiotic administration in randomised controlled trials: a systematic review and meta-analysis. International journal of antimicrobial agents **48:**1-10.

27. **Gross AE, Johannes RS, Gupta V, Tabak YP, Srinivasan A, Bleasdale SC.** 2017. The effect of a piperacillin/tazobactam shortage on antimicrobial prescribing and *Clostridium difficile* risk in 88 U.S. medical centers. Clin Infect Dis.

28. **Rodemann JF, Dubberke ER, Reske KA, Seo DH, Stone CD.** 2007. Incidence of *Clostridium difficile* Infection in Inflammatory Bowel Disease. Clinical Gastroenterology and Hepatology **5:**339-344.

29. **Khanna S, Pardi DS.** 2012. *Clostridium difficile* Infection: New Insights Into Management. Mayo Clinic Proceedings **87:**1106-1117.

30. **Kyne L, Warny M, Qamar A, Kelly C.** 2001. Association between antibody response to toxin A and protection against recurrent *Clostridium difficile* diarrhoea. Lancet **357:**189-193.

31. **Deshpande A, Pant C, Pasupuleti V, Rolston DDK, Jain A, Deshpande N, Thota P, Sferra TJ, Hernandez AV.** 2012. Association between proton pump inhibitor therapy and *Clostridium difficile* infection in a meta-analysis. Clinical Gastroenterology and Hepatology **10:**225-233.

32. **Faleck DM, Salmasian H, Furuya EY, Larson EL, Abrams JA, Freedberg DE.** 2016. Proton pump Inhibitors do not increase risk for *Clostridium difficile* infection in the intensive care unit. Am J Gastroenterol **111:**1641-1648.

33. **McFarland LV, Surawicz CM, Rubin M, Fekety R, Elmer GW, Greenberg RN.** 1999. Recurrent *Clostridium difficile* disease: epidemiology and clinical characteristics. Infection Control and Hospital Epidemiology **20:**43-50.

34. **Pépin J, Routhier S, Gagnon S, Brazeau I.** 2006. Management and outcomes of a first recurrence of *Clostridium difficile*-associated disease in Quebec, Canada. Clinical Infectious Diseases **42:**758-764.

35. **Seekatz AM, Rao K, Santhosh K, Young VB.** 2016. Dynamics of the fecal microbiome in patients with recurrent and nonrecurrent *Clostridium difficile* infection. Genome Medicine **8:**47.

36. **Chang JY, Antonopoulos DA, Kalra A, Tonelli A, Khalife WT, Schmidt TM, Young VB.** 2008. Decreased diversity of the fecal microbiome in recurrent

Clostridium difficile—associated diarrhea. Journal of Infectious Diseases **197:**435-438.

37. **Cohen SH, Gerding DN, Johnson S, Kelly CP, Loo VG, McDonald LC, Pepin J, Wilcox MH.** 2010. Clinical practice guidelines for *Clostridium difficile* infection in adults: 2010 update by the society for healthcare epidemiology of America (SHEA) and the infectious diseases society of America (IDSA). Infection Control & Hospital Epidemiology **31:**431-455.

38. **Dowle C.** 2016. Faecal microbiota transplantation: a review of FMT as an alternative treatment for *Clostridium difficile* infection. Bioscience Horizons: The International Journal of Student Research **9:**hzw007-hzw007.

39. **O'Connor JR, Johnson S, Gerding DN.** 2009. *Clostridium difficile* Infection Caused by the epidemic BI/NAP1/027 strain. Gastroenterology **136:**1913-1924.

40. **He M, Miyajima F, Roberts P, Ellison L, Pickard DJ, Martin MJ, Connor TR, Harris SR, Fairley D, Bamford KB, D'Arc S, Brazier J, Brown D, Coia JE, Douce G, Gerding D, Kim HJ, Koh TH, Kato H, Senoh M, Louie T, Michell S, Butt E, Peacock SJ, Brown NM, Riley T, Songer G, Wilcox M, Pirmohamed M, Kuijper E, Hawkey P, Wren BW, Dougan G, Parkhill J, Lawley TD.** 2013. Emergence and global spread of epidemic healthcare-associated *Clostridium difficile*. Nat Genet **45:**109-113.

41. **Rao K, Micic D, Natarajan M, Winters S, Kiel MJ, Walk ST, Santhosh K, Mogle JA, Galecki AT, LeBar W, Higgins PDR, Young VB, Aronoff DM.** 2015. *Clostridium difficile* Ribotype 027: relationship to age, detectability of Toxins A or B in stool with rapid testing, severe infection, and mortality. Clinical Infectious Diseases **61:**233-241.

42. **Wilcox MH, Mooney L, Bendall R, Settle CD, Fawley WN.** 2008. A case–control study of community-associated *Clostridium difficile* infection. Journal of Antimicrobial Chemotherapy **62:**388-396.

43. 2005. Severe *Clostridium difficile*-associated disease in populations previously at low risk--four states, 2005. MMWR. Morbidity and mortality weekly report **54:**1201-1205.

44. **Dingle KE, Didelot X, Quan TP, Eyre DW, Stoesser N, Golubchik T, Harding RM, Wilson DJ, Griffiths D, Vaughan A, Finney JM, Wyllie DH, Oakley SJ, Fawley WN, Freeman J, Morris K, Martin J, Howard P, Gorbach S, Goldstein EJC, Citron DM, Hopkins S, Hope R, Johnson AP, Wilcox MH, Peto TEA, Walker AS, Crook DW, Del Ojo Elias C, Crichton C, Kostiou V, Giess A, Davies J.** Effects of control interventions on *Clostridium difficile* infection in England: an observational study. The Lancet Infectious Diseases **17:**411-421.

45. **Collery MM, Kuehne SA, McBride SM, Kelly ML, Monot M, Cockayne A, Dupuy B, Minton NP.** 2016. What's a SNP between friends: The influence of

single nucleotide polymorphisms on virulence and phenotypes of *Clostridium difficile* strain 630 and derivatives. Virulence**:**1-15.

46. **Kuehne SA, Cartman ST, Heap JT, Kelly ML, Cockayne A, Minton NP.** 2010. The role of toxin A and toxin B in C*lostridium difficile* infection. Nature **467:**711-713.

47. **Lyras D, O'Connor JR, Howarth PM, Sambol SP, Carter GP, Phumoonna T, Poon R, Adams V, Vedantam G, Johnson S, Gerding DN, Rood JI.** 2009. Toxin B is essential for virulence of *Clostridium difficile*. Nature **458:**1176-1179.

48. **Carter GP, Rood JI, Lyras D.** 2010. The role of toxin A and toxin B in *Clostridium difficile*-associated disease. Gut Microbes **1:**58-64.

49. **Natarajan M, Walk ST, Young VB, Aronoff DM.** 2013. A clinical and epidemiological review of non-toxigenic *Clostridium difficile*. Anaerobe **22:**1-5.

50. **Kuehne SA, Cartman ST, Minton NP.** 2011. Both, toxin A and toxin B, are important in *Clostridium difficile* infection. Gut Microbes **2:**252-255.

51. **Monot M, Eckert C, Lemire A, Hamiot A, Dubois T, Tessier C, Dumoulard B, Hamel B, Petit A, Lalande V, Ma L, Bouchier C, Barbut F, Dupuy B.** 2015. *Clostridium difficile:* New Insights into the Evolution of the Pathogenicity Locus. Scientific Reports **5:**15023.

52. **Matamouros S, England P, Dupuy B.** 2007. *Clostridium difficile* toxin expression is inhibited by the novel regulator TcdC. Molecular Microbiology **64:**1274-1288.

53. **Mani N, Dupuy B.** 2001. Regulation of toxin synthesis in *Clostridium difficile* by an alternative RNA polymerase sigma factor. Proceedings of the National Academy of Sciences **98:**5844-5849.

54. **Moncrief JS, Barroso LA, Wilkins TD.** 1997. Positive regulation of *Clostridium difficile* toxins. Infection and Immunity **65:**1105-1108.

55. **Govind R, Vediyappan G, Rolfe RD, Dupuy B, Fralick JA.** 2009. Bacteriophage-mediated toxin gene regulation in *Clostridium difficile*. Journal of virology **83:**12037-12045.

56. **Dupuy B, Sonenshein AL.** 1998. Regulated transcription of *Clostridium difficile* toxin genes. Molecular Microbiology **27:**107-120.

57. **Hammond GA, Lyerly DM, Johnson JL.** 1997. Transcriptional analysis of the toxigenic element of *Clostridium difficile*. Microbial Pathogenesis **22:**143-154.

58. **Hundsberger T, Braun V, Weidmann M, Leukel P, Sauerborn M, Von Eichel-Streiber C.** 1997. Transcription Analysis of the Genes tcdA-E of the Pathogenicity Locus of *Clostridium difficile*. European Journal of Biochemistry **244:**735-742.

59. **Dineen SS, Villapakkam AC, Nordman JT, Sonenshein AL.** 2007. Repression of *Clostridium difficile* toxin gene expression by CodY. Molecular Microbiology **66:**206-219.

60. **Karlsson S, Burman LG, Åkerlund T.** 1999. Suppression of toxin production in *Clostridium difficile* VPI 10463 by amino acids. Microbiology **145:**1683-1693.

61. **Karlsson S, Lindberg A, Norin E, Burman LG, Akerlund T.** 2000. Toxins, butyric acid, and other short-chain fatty acids are coordinately expressed and down-regulated by cysteine in *Clostridium difficile*. Infection and immunity **68:**5881-5888.

62. **Karlsson S, Burman LG, Akerlund T.** 2008. Induction of toxins in *Clostridium difficile* is associated with dramatic changes of its metabolism. Microbiology (Reading, England) **154:**3430-3436.

63. **Antunes A, Martin-Verstraete I, Dupuy B.** 2011. CcpA-mediated repression of *Clostridium difficile* toxin gene expression. Molecular Microbiology **79:**882-899.

64. **Jenior ML, Leslie JL, Young VB, Schloss PD.** 2016. *Clostridium difficile* colonizes alternative nutrient niches during infection across distinct murine gut environments. bioRxiv**:**092304.

65. **Darkoh C, DuPont HL, Norris SJ, Kaplan HB.** 2015. Toxin synthesis by *Clostridium difficile* Is regulated through quorum signaling. mBio **6**.

66. **Darkoh C, Odo C, DuPont HL.** 2016. Accessory gene regulator-1 locus Is essential for virulence and pathogenesis of *Clostridium difficile*. mBio **7**.

67. **Voth DE, Ballard JD.** 2005. Clostridium difficile Toxins: Mechanism of Action and Role in Disease. Clinical Microbiology Reviews **18:**247-263.

68. **Pothoulakis C, Galili U, Castagliuolo I, Kelly CP, Nikulasson S, Dudeja PK, Brasitus TA, LaMont JT.** 1996. A human antibody binds to alpha-galactose receptors and mimics the effects of *Clostridium difficile* toxin A in rat colon. Gastroenterology **110:**1704-1712.

69. **Na X, Kim H, Moyer MP, Pothoulakis C, LaMont JT.** 2008. gp96 Is a human colonocyte plasma membrane binding protein for *Clostridium difficile* toxin A. Infection and Immunity **76:**2862-2871.

70. **Greco A, Ho JGS, Lin S-J, Palcic MM, Rupnik M, Ng KKS.** 2006. Carbohydrate recognition by *Clostridium difficile* toxin A. Nat Struct Mol Biol **13:**460-461.

71. **Gerhard R, Frenzel E, Goy S, Olling A.** 2013. Cellular uptake of *Clostridium difficile* TcdA and truncated TcdA lacking the receptor binding domain. Journal of medical microbiology **62:**1414-1422.

72. **Olling A, Goy S, Hoffmann F, Tatge H, Just I, Gerhard R.** 2011. The repetitive oligopeptide sequences modulate cytopathic potency but are not crucial for cellular uptake of *Clostridium difficile* toxin A. PloS one **6**.

73. **Tao L, Zhang J, Meraner P, Tovaglieri A, Wu X, Gerhard R, Zhang X, Stallcup WB, Miao J, He X, Hurdle JG, Breault DT, Brass AL, Dong M.** 2016. Frizzled proteins are colonic epithelial receptors for *C. difficile* toxin B. Nature **538:**350-355.

74. **Yuan P, Zhang H, Cai C, Zhu S, Zhou Y, Yang X, He R, Li C, Guo S, Li S, Huang T, Perez-Cordon G, Feng H, Wei W.** 2015. Chondroitin sulfate proteoglycan 4 functions as the cellular receptor for *Clostridium difficile* toxin B. Cell Res **25:**157-168.

75. **LaFrance ME, Farrow MA, Chandrasekaran R, Sheng J, Rubin DH, Lacy DB.** 2015. Identification of an epithelial cell receptor responsible for *Clostridium difficile* TcdB-induced cytotoxicity. Proceedings of the National Academy of Sciences **112:**7073-7078.

76. **Terada N, Ohno N, Murata S, Katoh R, Stallcup WB, Ohno S.** 2006. Immunohistochemical study of NG2 chondroitin sulfate proteoglycan expression in the small and large intestines. Histochemistry and Cell Biology **126:**483-490.

77. **Chandrasekaran R, Kenworthy AK, Lacy DB.** 2016. *Clostridium difficile* Toxin A undergoes clathrin-independent, PACSIN2-dependent endocytosis. PLOS Pathogens **12:**e1006070.

78. **Qa'Dan M, Spyres LM, Ballard JD.** 2000. pH-Induced conformational changes in *Clostridium difficile* toxin B. Infection and Immunity **68:**2470-2474.

79. **Reineke J, Tenzer S, Rupnik M, Koschinski A, Hasselmayer O, Schrattenholz A, Schild H, von Eichel-Streiber C.** 2007. Autocatalytic cleavage of *Clostridium difficile* toxin B. Nature **446:**415-419.

80. **Shen A, Lupardus PJ, Puri AW, Albrow VE, Gersch MM, Garcia KC, Bogyo M.** 2011. Defining an allosteric circuit in the cysteine protease domain of *Clostridium difficile* toxins. Nature structural & molecular biology **18:**364-371.

81. **Chumbler NM, Rutherford SA, Zhang Z, Farrow MA, Lisher JP, Farquhar E, Giedroc DP, Spiller BW, Melnyk RA, Lacy DB.** 2016. Crystal structure of *Clostridium difficile* toxin A. Nature microbiology **1:**15002.

82. **Jank T, Giesemann T, Aktories K.** 2007. Rho-glucosylating *Clostridium difficile* toxins A and B: new insights into structure and function. Glycobiology **17:**15R-22R.

83. **Lanis J, Barua S, Ballard J.** 2010. Variations in TcdB activity and the hypervirulence of emerging strains of Clostridium difficile. PLoS pathogens **6**.

84. **Drudy D, Fanning S, Kyne L.** 2007. Toxin A-negative, toxin B-positive *Clostridium difficile*. International Journal of Infectious Diseases **11:**5-10.

85. **Chaves-Olarte E, Löw P, Freer E, Norlin T, Weidmann M, von Eichel-Streiber C, Thelestam M.** 1999. A novel cytotoxin from *Clostridium difficile* serogroup F Is a functional hybrid between two other large clostridial cytotoxins. Journal of Biological Chemistry **274:**11046-11052.

86. **Quesada-Gomez C, Lopez-Urena D, Chumbler N, Kroh HK, Castro-Pena C, Rodriguez C, Orozco-Aguilar J, Gonzalez-Camacho S, Rucavado A, Guzman-Verri C, Lawley TD, Lacy DB, Chaves-Olarte E.** 2016. Analysis of TcdB proteins within the hypervirulent clade 2 reveals an impact of RhoA glucosylation on *Clostridium difficile* proinflammatory activities. Infect Immun **84:**856-865.

87. **Just I, Selzer J, Wilm M, Eichel-Streiber Cv, Mann M, Aktories K.** 1995. Glucosylation of Rho proteins by Clostridium difficile toxin B. Nature **375:**500-503.

88. **Just I, Wilm M, Selzer J, Rex G, von Eichel-Streiber C, Mann M, Aktories K.** 1995. The Enterotoxin from Clostridium difficile (ToxA) Monoglucosylates the Rho Proteins. Journal of Biological Chemistry **270:**13932-13936.

89. **Chen S, Sun C, Wang H, Wang J.** 2015. The role of Rho GTPases in toxicity of *Clostridium difficile* toxins. Toxins (Basel) **7:**5254-5267.

90. **Farrow MA, Chumbler NM, Lapierre LA, Franklin JL, Rutherford SA, Goldenring JR, Lacy DB.** 2013. *Clostridium difficile* toxin B-induced necrosis is mediated by the host epithelial cell NADPH oxidase complex. Proceedings of the National Academy of Sciences of the United States of America.

91. **Cowardin CA, Jackman BM, Noor Z, Burgess SL, Feig AL, Petri WA.** 2016. Glucosylation drives the innate inflammatory response to *Clostridium difficile* toxin A. Infection and Immunity **84:**2317-2323.

92. **Stare BG, Delmée M, Rupnik M.** 2007. Variant forms of the binary toxin CDT locus and tcdC gene in *Clostridium difficile* strains. Journal of Medical Microbiology **56:**329-335.

93. **Carter GP, Lyras D, Allen DL, Mackin KE, Howarth PM, O'Connor JR, Rood JI.** 2007. Binary toxin production in *Clostridium difficile* is regulated by CdtR, a LytTR family response regulator. Journal of Bacteriology **189:**7290-7301.

94. **Lyon SA, Hutton ML, Rood JI, Cheung JK, Lyras D.** 2016. CdtR Regulates TcdA and TcdB Production in *Clostridium difficile*. PLOS Pathogens **12:**e1005758.

95. **Papatheodorou P, Carette JE, Bell GW, Schwan C, Guttenberg G, Brummelkamp TR, Aktories K.** 2011. Lipolysis-stimulated lipoprotein receptor (LSR) is the host receptor for the binary toxin *Clostridium difficile* transferase (CDT). Proceedings of the National Academy of Sciences **108:**16422-16427.

96. **Hemmasi S, Czulkies BA, Schorch B, Veit A, Aktories K, Papatheodorou P.** 2015. Interaction of the *Clostridium difficil*e binary toxin CDT and its host cell receptor, lipolysis-stimulated lipoprotein receptor (LSR). Journal of Biological Chemistry **290:**14031-14044.

97. **Barth H, Aktories K, Popoff MR, Stiles BG.** 2004. Binary bacterial toxins: biochemistry, biology, and applications of common *Clostridium* and *Bacillus* proteins. Microbiology and molecular biology reviews : MMBR **68:**373-402, table of contents.

98. **Kuehne SA, Collery MM, Kelly ML, Cartman ST, Cockayne A, Minton NP.** 2014. Importance of Toxin A, Toxin B, and CDT in Virulence of an Epidemic *Clostridium difficile* Strain. The Journal of Infectious Diseases **209:**83-86.

99. **Cowardin CA, Buonomo EL, Saleh MM, Wilson MG, Burgess SL, Kuehne SA, Schwan C, Eichhoff AM, Koch-Nolte F, Lyras D, Aktories K, Minton NP, Petri WA, Jr.** 2016. The binary toxin CDT enhances *Clostridium difficile* virulence by suppressing protective colonic eosinophilia. Nat Microbiol **1:**16108.

100. **Schwan C, Stecher B, Tzivelekidis T, van Ham M, Rohde M, Hardt W-D, Wehland J, Aktories K.** 2009. *Clostridium difficile* toxin CDT induces formation of microtubule-based protrusions and increases adherence of bacteria. PLOS Pathogens **5:**e1000626.

101. **Carsten Schwana ASK, Thilo Nölkea, Lucas Schumacherb, Friedrich Koch-Nolteb, Mikhail Kudryashevc, Henning Stahlbergc, and Klaus Aktories.** 2014. *Clostridium difficile* toxin CDT hijacks microtubule organization and reroutes vesicle traffic to increase pathogen adherence. Proceedings of the National Academy of Sciences **111:**23132318.

102. **Lawley TD, Clare S, Walker AW, Stares MD, Connor TR, Raisen C, Goulding D, Rad R, Schreiber F, Brandt C, Deakin LJ, Pickard DJ, Duncan SH, Flint HJ, Clark TG, Parkhill J, Dougan G.** 2012. Targeted restoration of the intestinal microbiota with a simple, defined bacteriotherapy resolves relapsing *Clostridium difficile* disease in mice. PLoS Pathog **8:**e1002995.

103. **Cheesman SE, Neal JT, Mittge E, Seredick BM, Guillemin K.** 2011. Epithelial cell proliferation in the developing zebrafish intestine is regulated by the Wnt pathway and microbial signaling via Myd88. Proceedings of the National Academy of Sciences **108:**4570-4577.

104. **Chung H, Pamp SJ, Hill JA, Surana NK, Edelman SM, Troy EB, Reading NC, Villablanca EJ, Wang S, Mora JR, Umesaki Y, Mathis D, Benoist C, Relman DA, Kasper DL.** 2012. Gut immune maturation depends on colonization with a host-specific microbiota. Cell **149:**1578-1593.

105. **Ridlon JM, Kang D-J, Hylemon PB.** 2006. Bile salt biotransformations by human intestinal bacteria. Journal of Lipid Research **47:**241-259.

106. **Vollaard EJ, Clasener HA.** 1994. Colonization resistance. Antimicrobial Agents and Chemotherapy **38:**409-414.

107. **Stecher B, Berry D, Loy A.** 2013. Colonization resistance and microbial ecophysiology: using gnotobiotic mouse models and single-cell technology to explore the intestinal jungle. FEMS Microbiology Reviews **37:**793-829.

108. **Bäckhed F, Roswall J, Peng Y, Feng Q, Jia H, Kovatcheva-Datchary P, Li Y, Xia Y, Xie H, Zhong H, Khan Muhammad T, Zhang J, Li J, Xiao L, Al-Aama J, Zhang D, Lee Ying S, Kotowska D, Colding C, Tremaroli V, Yin Y, Bergman S, Xu X, Madsen L, Kristiansen K, Dahlgren J, Wang J.** Dynamics and stabilization of the human gut microbiome during the first year of life. Cell Host & Microbe **17:**690-703.

109. **Dethlefsen L, Relman DA.** 2011. Incomplete recovery and individualized responses of the human distal gut microbiota to repeated antibiotic perturbation. Proceedings of the National Academy of Sciences of the United States of America **108 Suppl 1:**4554-4561.

110. **Francis MB, Allen CA, Shrestha R, Sorg JA.** 2013. Bile acid recognition by the *Clostridium difficile* germinant receptor, CspC, is important for establishing infection. PLoS Pathogens **9:**e1003356.

111. **Wilson KH, Kennedy MJ, Fekety FR.** 1982. Use of sodium taurocholate to enhance spore recovery on a medium selective for *Clostridium difficile*. Journal of Clinical Microbiology **15:**443-446.

112. **Sayin Sama I, Wahlström A, Felin J, Jäntti S, Marschall H-U, Bamberg K, Angelin B, Hyötyläinen T, Orešič M, Bäckhed F.** 2013. Gut microbiota regulates bile acid metabolism by reducing the levels of tauro-beta-muricholic acid, a naturally occurring FXR antagonist. Cell Metabolism **17:**225-235.

113. **Ridlon JM, Kang DJ, Hylemon PB, Bajaj JS.** 2014. Bile acids and the gut microbiome. Curr Opin Gastroenterol **30:**332-338.

114. **Koenigsknecht MJ, Theriot CM, Bergin IL, Schumacher CA, Schloss PD, Young VB.** 2015. Dynamics and establishment of *Clostridium difficile* infection in the murine gastrointestinal tract. Infection and Immunity **83:**934-941.

115. **Theriot CM, Koenigsknecht MJ, Carlson PE, Hatton GE, Nelson AM, Li B, Huffnagle GB, Li J, Young VB.** 2014. Antibiotic-induced shifts in the mouse gut microbiome and metabolome increase susceptibility to *Clostridium difficile* infection. Nature communications **5:**3114-3114.

116. **Weingarden AR, Chen C, Bobr A, Yao D, Lu Y, Nelson VM, Sadowsky MJ, Khoruts A.** 2014. Microbiota transplantation restores normal fecal bile acid composition in recurrent *Clostridium difficile* infection. American Journal of Physiology - Gastrointestinal and Liver Physiology **306:**G310-G319.

117. **Sorg JA, Sonenshein AL.** 2010. Inhibiting the initiation of *Clostridium difficile* spore germination using analogs of chenodeoxycholic acid, a bile acid. J Bacteriol **192:**4983-4990.

118. **Buffie CG, Bucci V, Stein RR, McKenney PT, Ling L, Gobourne A, No D, Liu H, Kinnebrew M, Viale A, Littmann E, van den Brink MR, Jenq RR, Taur Y, Sander C, Cross J, Toussaint NC, Xavier JB, Pamer EG.** 2014. Precision microbiome reconstitution restores bile acid mediated resistance to *Clostridium difficile*. Nature **advance online publication**.

119. **Studer N, Desharnais L, Beutler M, Brugiroux S, Terrazos MA, Menin L, Schürch CM, McCoy KD, Kuehne SA, Minton NP, Stecher B, Bernier-Latmani R, Hapfelmeier S.** 2016. Functional intestinal bile acid 7α-Dehydroxylation by *Clostridium scindens* associated with protection from *Clostridium difficile* infection in a gnotobiotic mouse model. Frontiers in Cellular and Infection Microbiology **6**.

120. **Hutchinson GE.** 1957. Concluding Remarks. Cold Spring Harbor Symposia on Quantitative Biology **22:**415-427.

121. **Freter R, Brickner H, Botney M, Cleven D, Aranki A.** 1983. Mechanisms that control bacterial populations in continuous-flow culture models of mouse large intestinal flora. Infect Immun **39:**676-685.

122. **Wilson KH, Sheagren JN, Freter R, Weatherbee L, Lyerly D.** 1986. Gnotobiotic models for study of the microbial ecology of *Clostridium difficile* and *Escherichia coli*. J Infect Dis **153:**547-551.

123. **Onderdonk AB, Cisneros RL, Bartlett JG.** 1980. *Clostridium difficile* in gnotobiotic mice. Infect Immun **28:**277-282.

124. **Ng KM, Ferreyra JA, Higginbottom SK, Lynch JB, Kashyap PC, Gopinath S, Naidu N, Choudhury B, Weimer BC, Monack DM, Sonnenburg JL.** 2013. Microbiota-liberated host sugars facilitate post-antibiotic expansion of enteric pathogens. Nature **502:**96-99.

125. **Wilson KH, Silva J, Fekety FR.** 1981. Suppression of *Clostridium difficile* by normal hamster cecal flora and prevention of antibiotic-associated cecitis. Infection and Immunity **34:**626-628.

126. **Wilson KH, Sheagren JN.** 1983. Antagonism of toxigenic *Clostridium difficile* by nontoxigenic *C. difficile*. The Journal of Infectious Diseases **147:**733-736.

127. **Wilson KH, Perini F.** 1988. Role of competition for nutrients in suppression of *Clostridium difficile* by the colonic microflora. Infection and Immunity **56:**2610-2614.

128. **Wilson K, Freter R.** 1986. Interaction of *Clostridium difficile* and *Escherichia coli* with microfloras in continuous-flow cultures and gnotobiotic mice. Infection and immunity **54:**354-358.

129. **Jump RLP, Polinkovsky A, Hurless K, Sitzlar B, Eckart K, Tomas M, Deshpande A, Nerandzic MM, Donskey CJ.** 2014. Metabolomics Analysis Identifies Intestinal Microbiota-Derived Biomarkers of Colonization Resistance in Clindamycin-Treated Mice. PLoS ONE **9:**e101267.

130. **Maltby R, Leatham-Jensen MP, Gibson T, Cohen PS, Conway T.** 2013. Nutritional basis for colonization resistance by human commensal *Escherichia coli* strains HS and Nissle 1917 against *E. coli* O157:H7 in the mouse intestine. PLOS ONE **8:**e53957.

131. **Goulding D, Thompson H, Emerson J, Fairweather NF, Dougan G, Douce GR.** 2009. Distinctive profiles of infection and pathology in hamsters infected with *Clostridium difficile* strains 630 and B1. Infection and immunity **77:**5478-5485.

132. **Semenyuk EG, Poroyko VA, Johnston PF, Jones SE, Knight KL, Gerding DN, Driks A.** 2015. Analysis of bacterial communities during *Clostridium difficile* infection in the mouse. Infection and Immunity **83:**4383-4391.

133. **Lee S, Donaldson G, Mikulski Z, Boyajian S, Ley K, Mazmanian S.** 2013. Bacterial colonization factors control specificity and stability of the gut microbiota. Nature **501:**426-429.

134. **Merrigan MM, Venugopal A, Roxas JL, Anwar F, Mallozzi MJ, Roxas BAP, Gerding DN, Viswanathan VK, Vedantam G.** 2013. Surface-layer protein A (SlpA) Is a major contributor to host-cell adherence of *Clostridium difficile*. PLOS ONE **8:**e78404.

135. **Calabi E, Calabi F, Phillips AD, Fairweather NF.** 2002. Binding of *Clostridium difficile* surface layer proteins to gastrointestinal tissues. Infection and Immunity **70:**5770-5778.

136. **Lee J-S, Chung M-J, Seo J-G.** 2013. In Vitro Evaluation of Antimicrobial Activity of Lactic Acid Bacteria against *Clostridium difficile*. Toxicological Research **29:**99-106.

137. **Kommineni S, Bretl DJ, Lam V, Chakraborty R, Hayward M, Simpson P, Cao Y, Bousounis P, Kristich CJ, Salzman NH.** 2015. Bacteriocin production augments niche competition by enterococci in the mammalian gastrointestinal tract. Nature **526:**719-722.

138. **Gebhart D, Lok S, Clare S, Tomas M, Stares M, Scholl D, Donskey CJ, Lawley TD, Govoni GR.** 2015. A modified R-type bacteriocin dpecifically targeting *Clostridium difficile* prevents colonization of mice without affecting gut microbiota diversity. mBio **6**.

139. **Ott SJ, Waetzig GH, Rehman A, Moltzau-Anderson J, Bharti R, Grasis JA, Cassidy L, Tholey A, Fickenscher H, Seegert D, Rosenstiel P, Schreiber S.** 2017. Efficacy of sterile fecal filtrate transfer for treating patients with *Clostridium difficile* infection. Gastroenterology **152:**799-811.e797.

140. **Valdés-Varela L, Alonso-Guervos M, García-Suárez O, Gueimonde M, Ruas-Madiedo P.** 2016. Screening of *Bifidobacteria* and *Lactobacilli* able to antagonize the cytotoxic effect of *Clostridium difficile* upon intestinal epithelial HT29 monolayer. Frontiers in Microbiology **7**.

141. **Fukuda S, Toh H, Hase K, Oshima K, Nakanishi Y, Yoshimura K, Tobe T, Clarke JM, Topping DL, Suzuki T, Taylor TD, Itoh K, Kikuchi J, Morita H, Hattori M, Ohno H.** 2011. Bifidobacteria can protect from enteropathogenic infection through production of acetate. Nature **469:**543-547.

142. **Li Fang Lu DHK, Ik Hwan Lee, Ji Hong, Peng Zhang, I Na Yoon, Jae Sam Hwang, Ho Kim.** 2016. Potassium acetate blocks *Clostridium difficile* toxin A-induced microtubule disassembly by directly inhibiting histone deacetylase 6, thereby ameliorating inflammatory responses in the gut. Journal of Microbiology and Biotechnology **26:**693-699.

143. **Akira S, Takeda K, Kaisho T.** 2001. Toll-like receptors: critical proteins linking innate and acquired immunity. Nature immunology **2:**675-680.

144. **Lawley TD, Clare S, Walker AW, Goulding D, Stabler RA, Croucher N, Mastroeni P, Scott P, Raisen C, Mottram L, Fairweather NF, Wren BW, Parkhill J, Dougan G.** 2009. Antibiotic treatment of *Clostridium difficile* carrier mice triggers a supershedder state, spore-mediated transmission, and severe disease in Immunocompromised hosts. Infection and Immunity **77:**3661-3669.

145. **Jarchum I, Liu M, Shi C, Equinda M, Pamer E.** 2012. Critical role for MyD88-mediated neutrophil recruitment during *Clostridium difficile* colitis. Infection and immunity **80:**2989-2996.

146. **Hasegawa M, Yamazaki T, Kamada N, Tawaratsumida K, Kim Y-G, Núñez G, Inohara N.** 2011. Nucleotide-binding oligomerization domain 1 mediates recognition of *Clostridium difficile* and induces neutrophil recruitment and protection against the pathogen. Journal of immunology (Baltimore, Md. : 1950) **186:**4872-4880.

147. **Kelly CP, Becker S, Linevsky JK, Joshi MA, O'Keane JC, Dickey BF, LaMont JT, Pothoulakis C.** 1994. Neutrophil recruitment in *Clostridium difficile* toxin A enteritis in the rabbit. The Journal of Clinical Investigation **93:**1257-1265.

148. **Steiner TS, Flores CA, Pizarro TT, Guerrant RL.** 1997. Fecal lactoferrin, interleukin-1beta, and interleukin-8 are elevated in patients with severe *Clostridium difficile* colitis. Clinical and Diagnostic Laboratory Immunology **4:**719-722.

149. **Rao K, Erb-Downward JR, Walk ST, Micic D, Falkowski N, Santhosh K, Mogle JA, Ring C, Young VB, Huffnagle GB, Aronoff DM.** 2014. The systemic inflammatory response to *Clostridium difficile* infection. PLOS ONE **9:**e92578.

150. **Geiger TL, Abt MC, Gasteiger G, Firth MA, O'Connor MH, Geary CD, O'Sullivan TE, van den Brink MR, Pamer EG, Hanash AM, Sun JC.** 2014. Nfil3 is crucial for development of innate lymphoid cells and host protection against intestinal pathogens. The Journal of Experimental Medicine **211:**1723-1731.

151. **Abt Michael C, Lewis Brittany B, Caballero S, Xiong H, Carter Rebecca A, Sušac B, Ling L, Leiner I, Pamer Eric G.** Innate immune defenses mediated by two ILC subsets are critical for protection against acute *Clostridium difficile* infection. Cell Host & Microbe **18:**27-37.

152. **Buonomo EL, Cowardin CA, Wilson MG, Saleh MM, Pramoonjago P, Petri WA, Jr.** 2016. Microbiota-regulated IL-25 increases eosinophil number to provide protection during C*lostridium difficile* infection. Cell reports **16:**432-443.

153. **Kyne L, Warny M, Qamar A, Kelly C.** 2000. Asymptomatic carriage of *Clostridium difficile* and serum levels of IgG antibody against toxin A. The New England journal of medicine **342:**390-397.

154. **Corthier G, Muller MC, Wilkins TD, Lyerly D, L'Haridon R.** 1991. Protection against experimental pseudomembranous colitis in gnotobiotic mice by use of monoclonal antibodies against *Clostridium difficile toxin* A. Infect Immun **59:**1192-1195.

155. **Giannasca PJ, Zhang ZX, Lei WD, Boden JA, Giel MA, Monath TP, Thomas WD.** 1999. Serum antitoxin antibodies mediate systemic and mucosal protection from *Clostridium difficile* disease in hamsters. Infection and immunity **67:**527-538.

156. **Wilcox MH, Gerding DN, Poxton IR, Kelly C, Nathan R, Birch T, Cornely OA, Rahav G, Bouza E, Lee C, Jenkin G, Jensen W, Kim Y-S, Yoshida J, Gabryelski L, Pedley A, Eves K, Tipping R, Guris D, Kartsonis N, Dorr M-B.** 2017. Bezlotoxumab for prevention of recurrent *Clostridium difficile* infection. New England Journal of Medicine **376:**305-317.

157. **Karasawa T, Ikoma S, Yamakawa K, Nakamura S.** 1995. A defined growth medium for *Clostridium difficile*. Microbiology **141 (Pt 2):**371-375.

CHAPTER II

PROTECTION FROM LEATHAL *CLOSTIRIDUM DIFFICILE* INFECTION VIA INTRA-SPECIES COMPETITION FOR CO-GERMINANT

Introduction

Clostridium difficile a Gram-positive, spore-forming bacterium is the primary cause of infectious nosocomial diarrhea (1, 2). Susceptibility to *C. difficile* infection (CDI) results from perturbations of the gut microbial community, enabling increased germination of spores and outgrowth of vegetative *C. difficile* (3, 4). Following colonization and outgrowth, vegetative *C. difficile* produces toxins. The main toxins, TcdA and TcdB, are glycosyltransferases that inactivate cellular GTPases (5). Inactivation of these key cellular proteins results in damage of the colonic epithelium and inflammation manifesting as diarrhea and, in severe cases, toxic megacolon or even death. Currently the principal treatment for CDI are antibiotics (6). While antibiotics kill vegetative *C. difficile*, this therapy further disrupts the gut microbiota potentially delaying community recovery (7). It is hypothesized that delayed recovery of the gut microbiota is at least partially responsible for recurrence of disease as is experienced by 25% of patients (2).

Due to the high rate of recurrent infection associated with existing treatment for CDI, alternative approaches that spare or even restore the gut microbiota have been a focus of recent work. As is the case with many toxin-

mediated diseases early studies noted that generation of a humoral immune response to the toxins could be sufficient to protect against disease (8, 9). A recent clinical trial demonstrated that patients receiving monoclonal antibodies targeting the toxins, TcdA and TcdB, were 50% less likely to experience recurrent disease (10, 11). Unlike antibiotics, antibody therapy prevents illness while likely sparing the microbial community.

Recently, a non-toxigenic strain of *C. difficile* was demonstrated to successfully reduce the rate of recurrent CDI by 50% (12). The prevailing hypothesis is that the protection provided by the non-toxigenic strain is mediated by competitive exclusion via consumption of a subset of required resources such as nutrients, limiting the ability of toxigenic *C. difficile* to colonize the gut (13). However this has never been conclusively demonstrated to be true. Using a murine model of CDI, we sought to determine how pre-colonization with one strain of *C. difficile* might protect against lethal infection by another.

From our studies we determined that in the absence of adaptive immunity, pre-colonization with a less virulent strain of *C. difficile* is sufficient to provide protection from infection by a lethal strain. Using gnotobiotic mice we show that protection is mediated by limiting colonization of the highly virulent strain. Furthermore, we provide evidence that exclusion is not mediated on nutrient-based limitation of the vegetative form of the invading strain, but rather on depletion of the co-germinant glycine.

This work is important, as it is the first study to identify a mechanism though which pre-colonization with *C difficile*, a current clinical therapy, provides

protection from recurrent CDI. Furthermore limitation of germination associated with decreased levels of glycine in the gut is a novel paradigm for colonization resistance.

Experimental Procedures

Animals and housing

Both male and female mice age five to twelve weeks were used in these studies. The wild-type C57BL/6 specific-pathogen-free (SPF) mice were from a breeding colony originally derived from Jackson Laboratories over a decade ago. The Rag1$^{-/-}$ (B6.129S7-*Rag1*^{tm1Mom}/J) SPF mice were from a breeding colony started with mice from Jackson Laboratories in 2013. Germfree Rag1$^{-/-}$ mice were obtained from a colony established and maintained by the University of Michigan germfree facility.

Animals were housed with autoclaved cages, bedding, and water bottles. Mice were fed a standard irradiated chow (LabDiet 5LOD). All mice had access to food and water *ad libitum*. Cage changes were carried out in a biological safety cabinet. The frequency of cage changes varied depending on the experiment. To prevent cross-contamination between cages, hydrogen peroxide-based disinfectants in addition to frequent glove changes were utilized during all manipulation of SPF animals. A chlorine-based disinfectant was used during manipulation of the germfree mice. All mice were maintained under 12-hours of light and 12-hours of darkness in facilities maintained at temperature of 72° C +/- 4 degrees. Animal sample size was not determined by a statistical method.

Multiple cages of animals for each treatment were used to control for possible differences in the microbiota between cages. Mice were evaluated daily for signs of disease, those determined to be moribund were euthanized by CO_2 asphyxiation. The University Committee on the Care and Use of Animals at the University of Michigan approved this study. Animal husbandry was performed in an AAALAC-accredited facility.

Preparation of spores

Spore stocks of *C. difficile* strains 630 (ATCC BAA-1382) and VPI 10463 (ATCC 43255) were prepared as previously described by (3) with the following modifications, strains were grown overnight in 5mL of Columbia broth which was added to 40 mL of Clospore media (14).

Preparation of heat killed *C. difficile*

Heat-killed *C. difficile* strain 630 was made from an overnight culture grown anaerobically at 37°C in brain-heart infusion (BHI) broth supplemented with 0.01% cysteine. *C. difficile* strain 630 was enumerated by culturing for colony forming units (CFU) per mL of BHI. Following enumeration, the culture was removed from the chamber, spun down, and the pellet was washed and re-suspend in PBS. The solution was autoclaved at 121°C for 30 minutes at 15 PSI to kill the vegetative cells and inactivate any spores. The heat-killed *C. difficile* solution was equivalent to $2.7x10^{10}$ CFU/mL. In experiments using heat-killed *C. difficile,* mice were given 10^9 CFU equivalents in 0.05mL. A portion of the sample

was cultured on pre-reduced cycloserine-cefoxitin-fructose agar plates containing 0.1% taurocholate (TCCFA) to confirm that the inactivation was successful.

Infections

In experiments using both WT and Rag1$^{-/-}$ SPF mice, age and sex matched mice were co-housed starting at three weeks of age for thirty-three days through antibiotic administration. Upon infection, animals were separated into single genotype housing.

All SPF mice received the antibiotic cefoperazone (cat # 0219969501, MP Pharmaceuticals) dissolved in Gibco distilled water at concentration of 0.5 mg/mL administered *ad libitum* as the drinking water for either 10 or 5 days. The antibiotic water was changed every two days. Following completion of antibiotics, mice were given plain Gibco distilled water for two days before challenge with either spores or water (mock). *C. difficile* spores suspended in 50-100µL of Gibco distilled water were administered via oral gavage. The number of viable spores in each inoculum was enumerated by culturing for CFU per mL^{-1} on pre-reduced TCCFA. Over the course of the infection, mice were weighed routinely and stool was collected for quantitative culture.

In our persistent colonization model, forty-one days after primary infection mice were given an IP of clindamycin (Sigma, C5269) in sterile saline at concentration of 10 mg/kg to perturb the gut microbial community as described previously (3, 15). The next day mice were either mock challenged with water or with spores of *C. difficile* strain VPI 10463. In the short-term infection model,

mice were challenged with one strain and the following day challenged with the other. In the simultaneous co-infections, mice were challenged with different ratios of strain 630 and strain VPI 10463 within a total amount of 10^4 spores. At the conclusion of the experiments mice used in dual genotype experiments were genotyped using DNA from an ear snip using primers and cycling conditions as outlined by Jackson (https://www2.jax.org/protocolsdb/f?p=116:5:0::NO:5:P5_MASTER_PROTOCOL_ID,P5_JRS_CODE:27761,002216).

Quantitative culture from intestinal content

Fecal pellets or colonic content were collected from each mouse into a pre-weighed sterile tube. Following collection, the tubes were reweighed and passed into an anaerobic chamber (Coy Laboratories). In the chamber, each sample was diluted 1 to 10 (w/v) using pre-reduced sterile PBS and serially diluted. 100µL of a given dilution was spread on to pre-reduced TCCFA or when appropriate TCCFA supplemented with either 2 or 6µg/mL of erythromycin. Strain 630 is erythromycin resistant; use of 2µg/mL of erythromycin in TCCFA plates reduced background growth from other bacteria in the sample while TCCFA with 6µg/mL of erythromycin enabled selection of 630 (erythromycin resistant) from VPI 10463 (erythromycin sensitive). Plates were incubated at 37°C in the anaerobic chamber and colonies were counted at 18-24 hours. Plates that were used to determine if mice were negative for *C. difficile* were held for 48 hours.

Toxin activity assay

Intestinal content was collected from each mouse into a pre-weighted sterile tube and stored at -80°C. At the start of the assay each sample was diluted 1:10 weight per volume using pre-reduced sterile PBS. Following dilution, the sample was filter sterilized through a 0.22μm filter and the activity of the toxins was assessed using a Vero cell rounding-based cytotoxicity assay as described previously (16).

Histopathology evaluation

Mouse ceca and colon tissue were saved in histopathology cassettes and fixed in 10% formalin, followed by storage in 70% ethanol. McClinchey Histology Lab Inc. (Stockbridge, MI) prepared the tissue including embedding samples in paraffin, sectioning, and generation of haematoxylin and eosin stained slides. A board certified veterinary pathologist scored the slides blind to the experimental groups, using previously described criteria (15).

Anti-TcdA IgG ELISA

Blood was collected from mice via saphenous vein puncture into capillary blood collection tubes. Samples were spun down and serum was stored at -80°C. Levels of IgG specific to *C. difficile* TcdA were measured in serum from mice using a previously described ELISA protocol (17) with a few modifications. Briefly, 96-well EIA plates were coated with 100μl of purified *C. difficile* TcdA (List Laboratories, cat #152C) at 1μg/mL in 0.05M sodium bicarbonate buffer pH 9.6

overnight at 4°C. Mouse serum was diluted to 1:400 in blocking buffer and serially diluted 1:3. Each sample was run in duplicate. Negative controls included pre-immune sera from the mice in addition to wells that lacked serum. A positive control consisting of a monoclonal mouse anti-TcdA IgG antibody was run on each plate. The optical density at 410 nm was recorded on a VersaMax plate reader (Molecular Devices, Sunnyvale CA). The anti-Toxin A IgG titer was defined as the last dilution where both replicates had an OD_{410} greater than mean absorbance of all negative wells on the plate plus three times the standard deviation from that mean.

Serum neutralizing anti-toxin antibody assay

The serum neutralizing anti-toxin antibody assay was based on a previously described assay (9). With the following modifications: the concentration of purified TcdA or TcdB (List Laboratories) that resulted in 100% cell rounding was determined empirically, using the toxin activity assay. Vero cells were seeded at a density of 10^5 cells/0.075mL per well onto tissue culture treated plates. Four times the concentration of toxin that resulted in 100% cells rounding (64µg/mL for TcdA and 4µg/mL for TcdB) was incubated with serial dilutions of serum from mice. The serum toxin mixture was added to Vero cells and incubated overnight. The neutralizing titer was determined to be the last dilution with had less than 50% of round cells in the well. Each sample was run in duplicate and the results were averaged. Toxin only wells served as negative controls while goat anti-TcdA and B serum served as a positive control (TechLab

T5015). Sera obtained from mice prior to infection served as an additional negative control.

Scoring of clinical signs of disease

Mice were scored for signs of disease based on criteria previously described by (18). A member of the lab who had not been party to the experiment scored the mice before necropsy to avoid bias.

Quantitative PCR

Primers that differentiated strain VPI 10463 (IMG Genome ID: 2512047057) from strain 630 (GenBank: AM180355.1) were designed using publically available genomes. While the primers differentiated between the strains in pure culture they generated non-specific amplicon in the context of the microbiota and were only used in gnotobiotic experiments. VPI 10463 primers: Forward: 5'- TTTCACATGAGCGGACAGGC -3', Reverse: 5'-TCCGAAGGAGGTTTCCGGTT-3'. The expected product size is 153 nucleotides and the optimal annealing temperature was experimentally determined to be 56°C.

For quantitative PCR, DNA from fecal samples were diluted in ultrapure water such that such that 20 ng of DNA was added to each reaction. Each sample was run in triplicate. Samples were loaded into a Light cycler 480 multiwell plate, with FastStart Essential DNA Green master mix, 0.5μM of each primer. The plate was sealed with optically clear sealing tape briefly spun down

and run on the Roche LightCycler 96. The following conditions were used for qPCR: 95°C for 10 minutes, followed by thirty cycles of 95°C for 10 seconds, 56°C for 10 seconds, and 72°C for 10 seconds. A melt was run at the conclusion of the amplification.

Genomic DNA from VPI 10463, from a culture with a known amount of CFU was used to generate a standard curve. Negative controls included no template control wells in addition to dilutions of genomic DNA from strain 630.

Preparation of sterile cecal filtrate

The sterile cecal filtrate was prepared from SPF mice that were treated for ten-days with cefoperazone. Uninfected mice were sacrificed two or three days after the completion of the antibiotics (days 0 and 1 respectively of the infection model). Media was also made from infected mice, following our antibiotic regime, two days after the completion of antibiotics mice were infected with strain 630 and sacrificed one day later (day 1 post infection). Following euthanasia, the cecum was removed and the content was squeezed into a sterile 50mL conical. The conical was spun at 3000 rpm at room temperature for ten minutes to separate the solid matter from the liquid portion. The liquid portion of the sample was removed and diluted 1:2 by volume in sterile PBS (pH 7.4). The sample was spun again at 3000 rpm for 5 minutes at room temperature; the liquid portion was then filter sterilized using filters with successively smaller pore size (from 0.8μm, to 0.45μm, and finally a 0.22μm filter). Following passage through the 0.22μm filter, the media was frozen at -80°C until use. The media was tested for sterility

by inoculating into pre-reduced BHI in the anaerobic chamber; samples that gave rise to turbid growth within 48 hours were discarded.

Ex vivo vegetative growth

To determine if 24 hours of *C. difficile* strain 630 growth depletes the gut of the nutrients required for vegetative growth of strain VPI 10463, we used an *ex vivo* approach, utilizing sterile cecal filtrate from susceptible mice. Tubes of 180µL of day 0 cecal filtrate were thawed and allowed to equilibrate in the anaerobic chamber overnight. The inoculums were prepared from an overnight culture of *C. difficile* (strains 630 and VPI 10463) grown in BHI + 0.01% cysteine. Each culture was back diluted 1:10 and incubated at 37°C for two hours. After two hours had elapsed, 500µL of the culture was spun down for four minutes in the anaerobic chamber using a mini-centrifuge. To prevent the introduction of nutrients from carry over BHI, the supernatant was removed and the tubes were spun for an additional minute. Any remaining BHI was removed and the pellets were then suspended in 500µL of sterile anaerobic PBS. Both strains were then diluted 1:100 into sterile anaerobic PBS. 20µl of this 1:100 dilution was inoculated into the cecal filtrate. Vegetative CFU were enumerated at T=0, 24 hours by culturing on CCFA (which lacks the germinant taurocholate). Additionally samples were plated on BHI + 0.01% cysteine to check for any contamination. After 24 hours, the samples were removed from the chamber; cells were pelleted by centrifugation at 2,000g for five minutes. The supernatant was filter sterilized using a 0.22µm 96-well filter plate and the sterile flow through

was passed back into the chamber to equilibrate overnight. The following day, the VPI 10463 inoculum was prepared as described earlier and inoculated into the spent cecal filtrate. CFU were monitored by culturing sample at T=0, 6, and 24 hours on CCFA and BHI+0.01% cysteine.

Ex vivo germination assay

To determine if 24 hours of strain 630 growth altars the ability of VPI 10463 spores to germinate we performed an *ex vivo* germination assay based on a previously described method (19) with the following modifications. Rather than using complete cecal contents we used a sterile filtrate of cecal content from mice that were off of antibiotics for three days (day 1 cecal filtrate) or infected with *C. difficile* strain 630 for 24 hours (630 day 1 cecal filtrate). 180µL aliquots of the cecal filtrate were thawed and allowed to equilibrate in the anaerobic chamber overnight. The next day 10uL of spores from strain VPI 10463 were inoculated into the media. Controls included sterile PBS (Gibco cat#10010023), PBS + 0.1% sodium taurocholate, and PBS + 0.1% sodium taurocholate + 100mM glycine. Following inoculation, samples were incubated anaerobically at RT for 15 minutes, after which approximately half the volume was immediately plated on BHI + 0.1% Taurocholate +0.01% cysteine agar and the tubes were passed out of the chamber and placed in a water filled heat block set at 65°C for 20 minutes. The heating step kills off any vegetative cells. Additional controls included culturing the spore inoculum on BHI without taurocholate to check for presence of any vegetative cells in the stock as well as heating suspensions of

vegetative cells to confirm efficacy of heat killing. Following the 20 minutes incubation, tubes were passed back into the chamber and the remaining sample was plated on BHI + 0.1% Taurocholate +0.01% cysteine agar. The CFU recorded from the pre-heat plate represents the entire inoculum including remaining spores and any cells that germinated, while the post-heat plate represents only remaining spores.

Metabolomics

Quantification of relative *in vivo* metabolite concentrations was preformed by Metabolon (Durham, NC) as described previously(20).

DNA extraction

Genomic DNA was extracted from approximately 200-300 µl of fecal sample using the MoBio PowerSoil HTP 96 DNA isolation kit (formerly MoBio, now Qiagen) on the Eppendorf EpMotion 5075 automated pipetting system according to manufacturer's instructions.

Sequencing

The University of Michigan Microbial Systems Laboratory constructed amplicon libraries from extracted DNA as described previously(7). Briefly, the V4 region of the 16S rRNA gene was amplified using barcoded dual index primers as describe by Kozich et al. (21). The PCR reaction included the following: 5µl of 4µM stock combined primer set, 0.15µl of Accuprime high-fidelity Taq with 2µl of

10× Accuprime PCR II buffer (Life Technologies, #12346094), 11.85µl of PCR-grade water, and 1µl of template. The PCR cycling conditions were as follows: 95° for 2 minutes, 30 cycles of 95°C for 20 seconds, 55°C for 15 seconds, and 72°C for 5 minutes, and 10 minutes at 72°C. Following construction, libraries were normalized and pooled using the SequelPrep normalization kit (Life Technologies, #A10510-01). The concentration of the pooled libraries was determined using the Kapa Biosystems library quantification kit (KapaBiosystems, #KK4854) while amplicon size was determined using the Agilent Bioanalyzer high-sensitivity DNA analysis kit (#5067-4626). Amplicon libraries were sequenced on the Illumina MiSeq platform using the MiSeq Reagent 222 kit V2 (#MS-102-2003) (500 total cycles) with modifications for the primer set. Illumina's protocol for library preparation was used for 2 nM libraries, with a final loading concentration of 4pM spiked with 10% genomic PhiX DNA for diversity. The raw paired-end reads of the sequences for all samples used in this study can be accessed in the Sequence Read Archive under PRJNA388335.

Sequence curation and analysis

Raw sequences were curated using the mothur v.1.39.0 software package (22) following the Illumina MiSeq standard operating procedure. Briefly, paired end reads were assembled into contigs and aligned to the V4 region using the SLIVA 16S rRNA sequence database (release v128) (23), any sequences that failed to align were removed; sequences that were flagged as possible chimeras by UCHIME were also removed (24). Sequences were classified with a naïve

Bayesian classifier (25) using the Ribosomal Database Project (RDP) and clustered in to Operational Taxonomic Units (OTUs) using a 97% similarity cutoff with the Opticlust clustering algorithm (26).

The number of sequences in each sample was then rarefied to 9,000 sequences to minimize bias due to uneven sampling. Following curation in mothur, further data analysis and figure generation was carried out in R (v 3.3.3) using standard and loadable packages (27). The data and code for all analysis associated with this study are available at https://github.com/jlleslie/Intraspecific_Competition.

For the purpose of distinguishing between values that were detected at the limit of detection versus those that were undetected, all results that were not detected by a given assay were plotted at an arbitrary point below the limit of detection (LOD). However for statistical analysis, the value of LOD/√2 was substituted for undetected values. Wilcoxon ranked sum test was used to determine significant differences and when appropriate, reported p-values were corrected for multiple comparisons using the Benjamini–Hochberg correction.

Results

Development of murine model of persistent *C. difficile* colonization

The only single species bacterial preparation that has demonstrated efficacy in reducing recurrent CDI in humans is non-toxigenic *C. difficile* (12). However the mechanisms by which one strain of *C. difficile* prevents colonization of another are currently unknown. To begin to address this question we developed a model of persistent *C. difficile* colonization. Mice were made

susceptible to colonization via administration of the antibiotic cefoperazone. Following two days off of the antibiotic, mice were either mock challenged or challenged with *C. difficile* strain 630. Compared to mock-challenged animals, *C. difficile* infected animals displayed significant weight loss between days four to six post-challenge (figure 2.1A, $p<0.05$). After a week, infected mice remained highly colonized although there was a significant reduction in the fecal colony forming units (CFU) of *C. difficile* relative to levels observed in the feces on day one post-infection (figure 2.1 B, $p<0.01$). Contemporaneous with the decrease in colonization, infected animals recovered body weight until they were indistinguishable from the mock-infected animals (figure 2.1A). Additionally, the diversity of the gut microbiota increased within the first week of infection, a period corresponding to the recovery of weight and decrease in colonization (figure 2.1 D, right axis). Throughout the experiment, toxin was detected in the feces of most of the infected mice despite a lack of outward signs of disease (figure 2.1 A and C). Together these data demonstrate that *C. difficile* strain 630 can persistently colonize wild type mice as a minority member of the gut microbiota (figure 2.1 D, left axis).

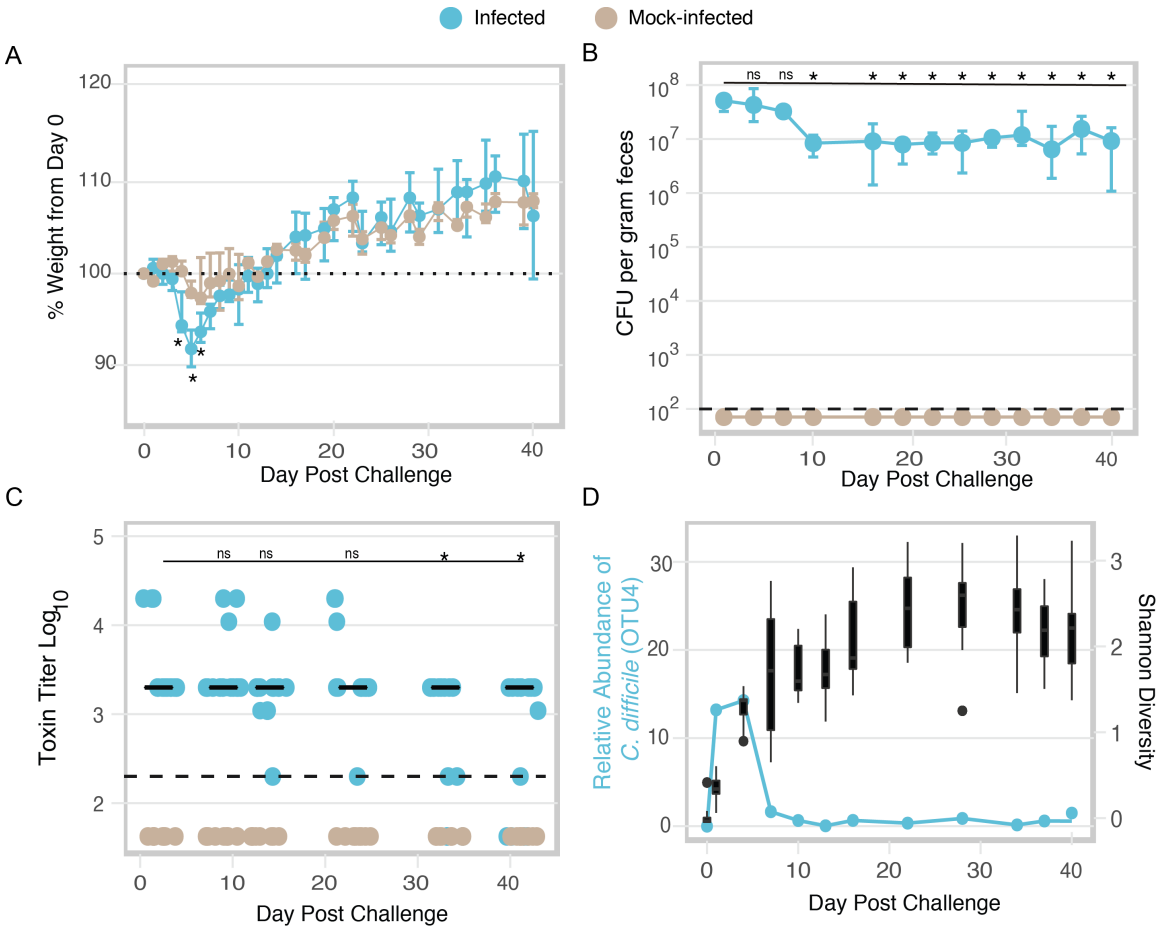

Figure 2.1. Murine model of persistent *C. difficile* colonization
A. Change in weight relative to day of infection for infected and mock challenged mice. Points represent median weight; bars are the upper and lower quartiles. Infected mice are colored blue while data from mock-infected animals are shown in tan. Following correction for multiple comparisons, weight loss in infected mice was only significantly different than mock-challenged mice on days 4, 5, and 6 post-infection, $p < 0.05$.
B. *C. difficile* colonization over time as determined by quantitative culture. Day 1 post-infection levels of *C. difficile* are significantly different from levels of colonization measured at day 10 post-infection through to day 40, $p < 0.01$. The hashed line represents the limit of detection of 100 CFU/g feces.
C. Fecal toxin activity remains detectable throughout the experiment. Toxin titer on day 33 and day 40 are significantly different from day 1 post-infection levels, $p<0.05$. The hashed line represents the limit of detection for this assay, 2.3.
D. Relative abundance of OTU 4 (*C. difficile*) over the course of the experiment (blue line) is plotted on the left axis while Shannon diversity of the infected mice over the course of the experiment is plotted on the right axis (black box plots).
Statistical significance for all data was calculated using a Wilcoxon test with a Benjamin- Hochberg correction for multiple comparisons.

Pre-colonization with *C. difficile* protects mice from challenge with a highly virulent strain.

To determine if a resident strain of C*. difficile* protects mice from challenge with a second strain in the context of perturbation to the gut microbiota, we administered a second antibiotic, clindamycin, to both the *C. difficile* infected and mock-infected mice. Intraperitoneal (IP) injection of clindamycin did not result in weight loss in either group of mice (figure 2.2 A) However, in the infected mice, levels of *C. difficile* strain 630 significantly increased following administration of clindamycin likely because the strain is resistant to the antibiotic (figure 2.2 B, $p< 0.001$) (28).

To control for possible variations in the microbiota across the cages, mice from 630-infected and mock-infected cages were split into two groups following the treatment with clindamycin. Approximately half the mice in a cage were challenged with 10^5 spores of *C. difficile* strain VPI 10463 while the rest of the mice were placed in a new cage and mock infected (figure 2.3 A). Strain VPI 10463 expresses both TcdA and TcdB and is lethal in this model of infection (15, 29).

Mice that that only received antibiotics and were not challenged with either strain of *C. difficile* (figure 2.3 B, tan dots) in addition to mice that were infected with strain 630 and then mock infected (figure 2.3 B, tan blue dots) were included as negative controls. Both groups maintained their weight throughout the treatments (figure 2.3B). Mice that had not been colonized with *C. difficile* strain 630 and were subsequently infected with *C. difficile* strain VPI 10463 lost a

significant amount of weight and had to be euthanized (figure 2.3 B, red dots). Surprisingly mice persistently colonized with *C. difficile* strain 630 were protected from challenge with the lethal strain (yellow dots) (figure 2.3 B, red vs. yellow $p<0.01$). Additionally, strain 630 pre-colonized mice had significantly lower toxin titers than the naïve mice challenge with strain VPI 10463 (figure 2.3 C, $p<0.05$). This finding was confirmed by the histopathology, as the summary score for the histopathology of the colon was significantly less in the 630 colonized mice challenged with VPI 10463 compared to the naïve mice challenged with VPI 10463 (figure 2.3 D, $p<0.01$).

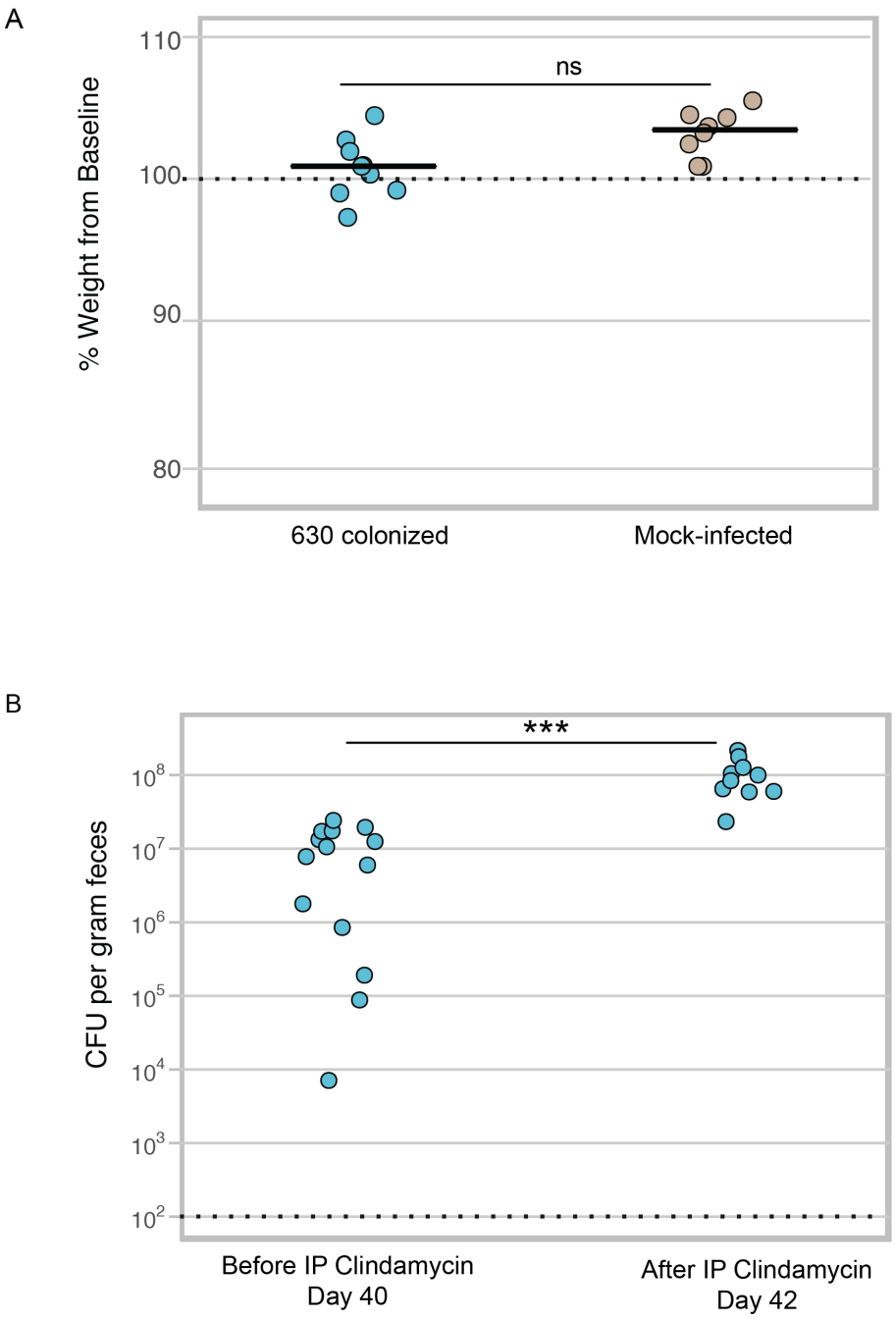

Figure 2.2 Effect of clindamycin on weight and colonization levels
A. Change in weight from the day mice were given clindamycin to the following day. Mock-infected mice (or naïve animals) are a reference point. There was not a significant difference between the infected or mock-infected mice following administration of clindamycin, $p > 0.05$.
B. *C. difficile* colonization in infected animals one day prior to administration of clindamycin and one day following. Clindamycin significantly increases levels of *C. difficile* strain 630 in infected mice, $p < 0.001$. For the data included in each figure, statistical significance was calculated using a Wilcoxon test.

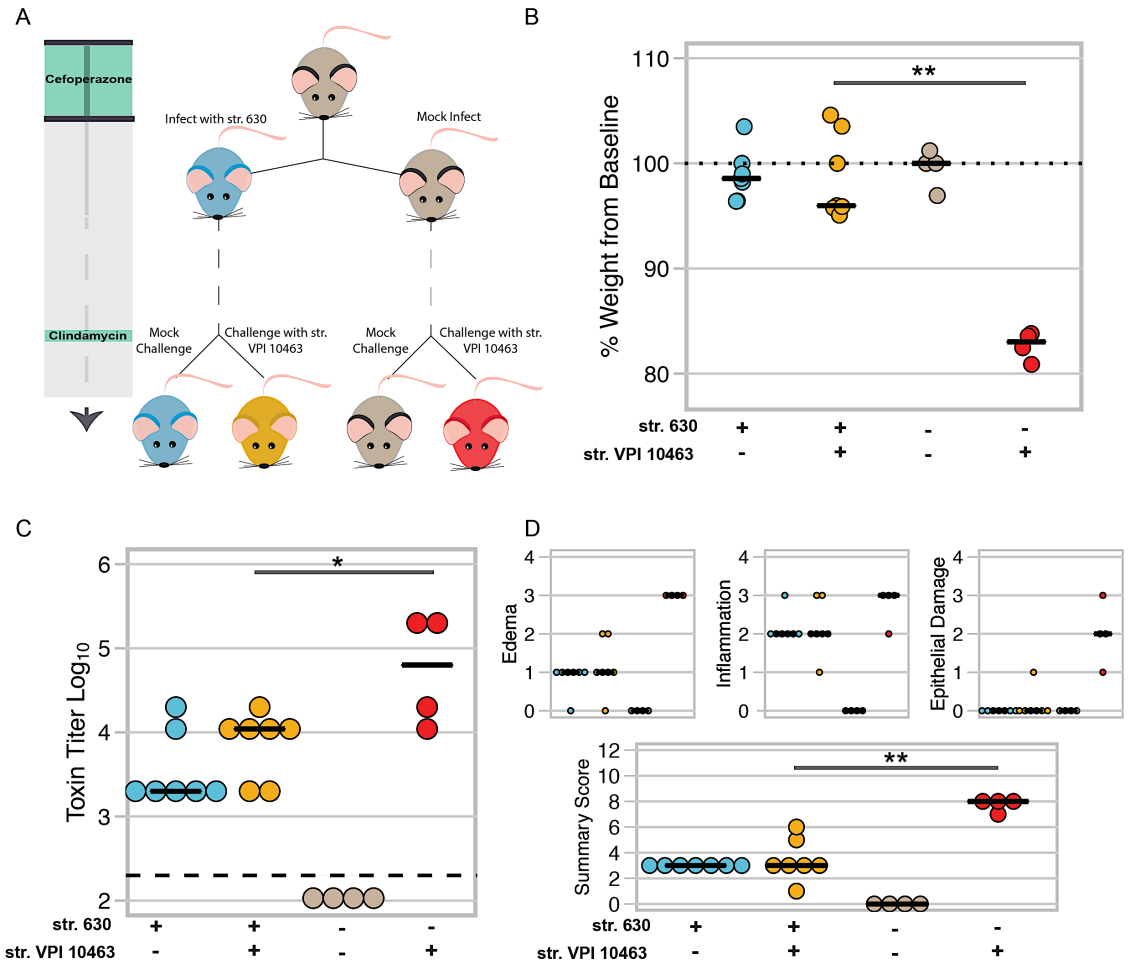

Figure 2.3. Mice pre-colonized with *C. difficile* strain 630 are protected from challenge with a lethal strain

A. Schematic of experimental conditions. Colors corresponding to treatment groups are carried throughout the figure.

B. Percent of day of challenge weight at time of necropsy. Mice colonized with *C. difficile* strain 630 and challenged with the lethal strain (VPI 10463) are protected from weight loss where as mice that had no exposure to *C. difficile* strain 630 experienced significant weight loss, p = 0.006061.

C. Toxin titer from intestinal content as measured by Vero cell rounding assay. Mice colonized with *C. difficile* strain 630 and then challenged with *C. difficile* strain VPI 10463 have a lower toxin titer relative to naïve mice challenged with VPI 10463, p = 0.04581. The hashed line represents the limit of detection for this assay, 2.3.

D. Histopathology scoring of the colon. Small panels depict scores for each component that makes up the summary score. VPI challenged 630 colonized vs. VPI challenged naive mice p-value = 0.008376.

For all data statistical significance between the *C. difficile* strain VPI 10463 challenged strain 630-colonized and VPI 10463 challenged naive mice was determined by Wilcoxon test.

Protection is associated with development of anti-toxin antibody responses, but antibody responses are not required for protection.

Since both strains express nearly identical forms of TcdA and TcdB, we questioned if protection might be due to the development of a humoral immune response to the toxins (9, 30). We found that mice previously infected with 630 developed a high anti-TcdA titer with a median titer of 32,400 (figure 2.4 A, 630 colonized vs. naïve mice $p< 0.01$). Using purified toxin, we determined that a portion of these antibodies were neutralizing as judged by their capacity to prevent TcdA mediated cell rounding (figure 2. 4 B). We suspect that we were unable to detect a neutralizing titer to TcdB due to the fact our total anti-TcdB IgG levels were much lower than anti-toxin A IgG (data not shown).

Since protection was correlated with both pre-colonization and the development of an adaptive immune response to the toxins, we next tested if adaptive immunity was the sole factor driving protection in our model. To do so, we utilized mice defective in recombination-activating gene 1 (RAG), which is critical in the development of B and T cells. $RAG1^{-/-}$ mice lack the adaptive arm of their immune system (31).

As observed with wild-type mice $RAG1^{-/-}$ mice, survive infection with strain 630 and can maintain persistent colonization (figure 2. 5). Following forty days of colonization, mice administered a dose of clindamycin via intraperitoneal injection and then challenged with the lethal strain VPI 10463. Strikingly, both the $RAG1^{-/-}$ and wild-type (WT) mice pre-colonized with strain 630 were protected following the challenge, while the naïve mice of both genotypes succumbed to the infection

(figure 2.6 A and B, naïve vs. colonized $p<0.05$). Scoring of the colonic pathology demonstrated that both the RAG1$^{-/-}$ and WT mice pre-colonized with 630 had less pathology relative to the naïve mice (figure 2.6 C, naïve vs. colonized $p<0.05$). These data demonstrate that, in the absence of adaptive immunity, pre-colonization with *C. difficile* is sufficient protect from lethal infection with another strain. Therefore adaptive immune responses are not required for protection from severe disease in mice pre-colonized with *C. difficile* strain 630.

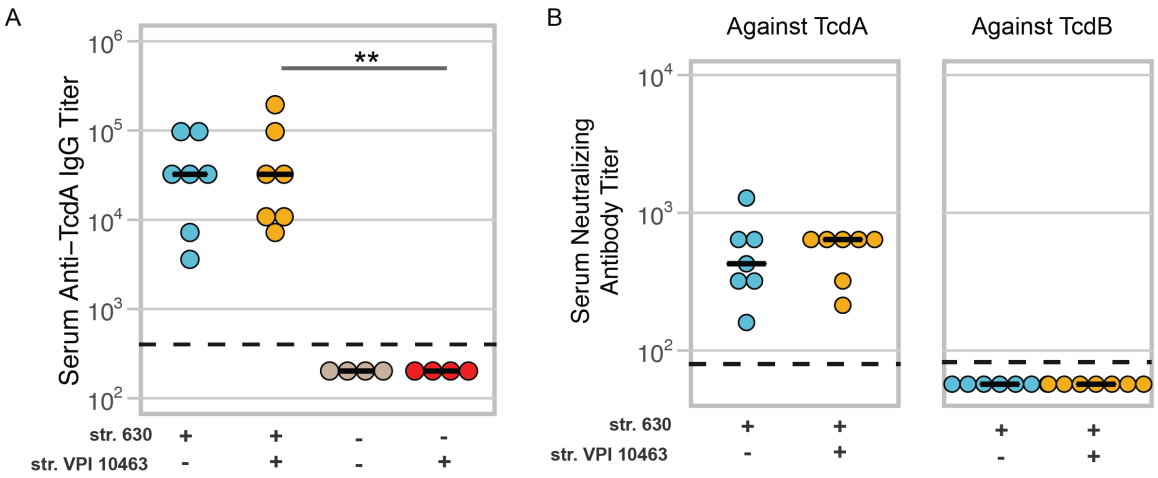

Figure 2.4. Mice colonized with *C. difficile* strain 630 develop serum IgG response directed against TcdA.
A. Titer of serum IgG against TcdA at conclusion of experiment as measured by ELISA. Limit of detection was a titer of 400, p = 0.008695. Statistical significance was calculated using a Wilcoxon test.
B. Neutralizing titer of serum against TcdA or TcdB at conclusion of experiment. Limit of detection was a titer of 80 for both toxins.

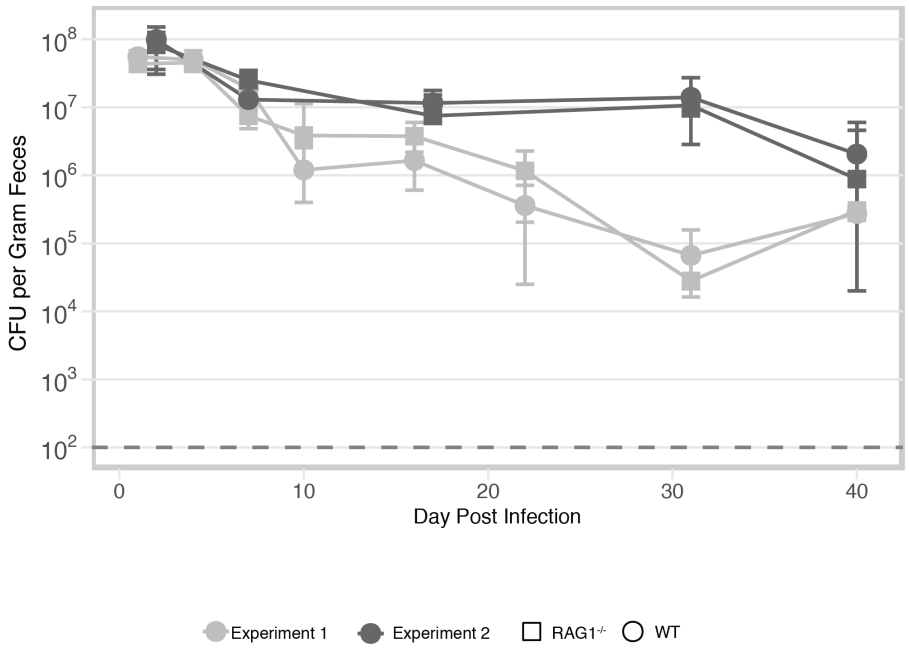

Figure 2.5. RAG1$^{-/-}$ mice can be persistently colonized by *C. difficile* strain 630.
C. difficile strain 630 colonization in infected RAG1$^{-/-}$ and WT mice. Points are the median CFU/g feces at a given day, while bars are the upper and lower quartiles. The different shapes correspond to mouse genotype, while color corresponds to experiment (data from two independent experiments are depicted).

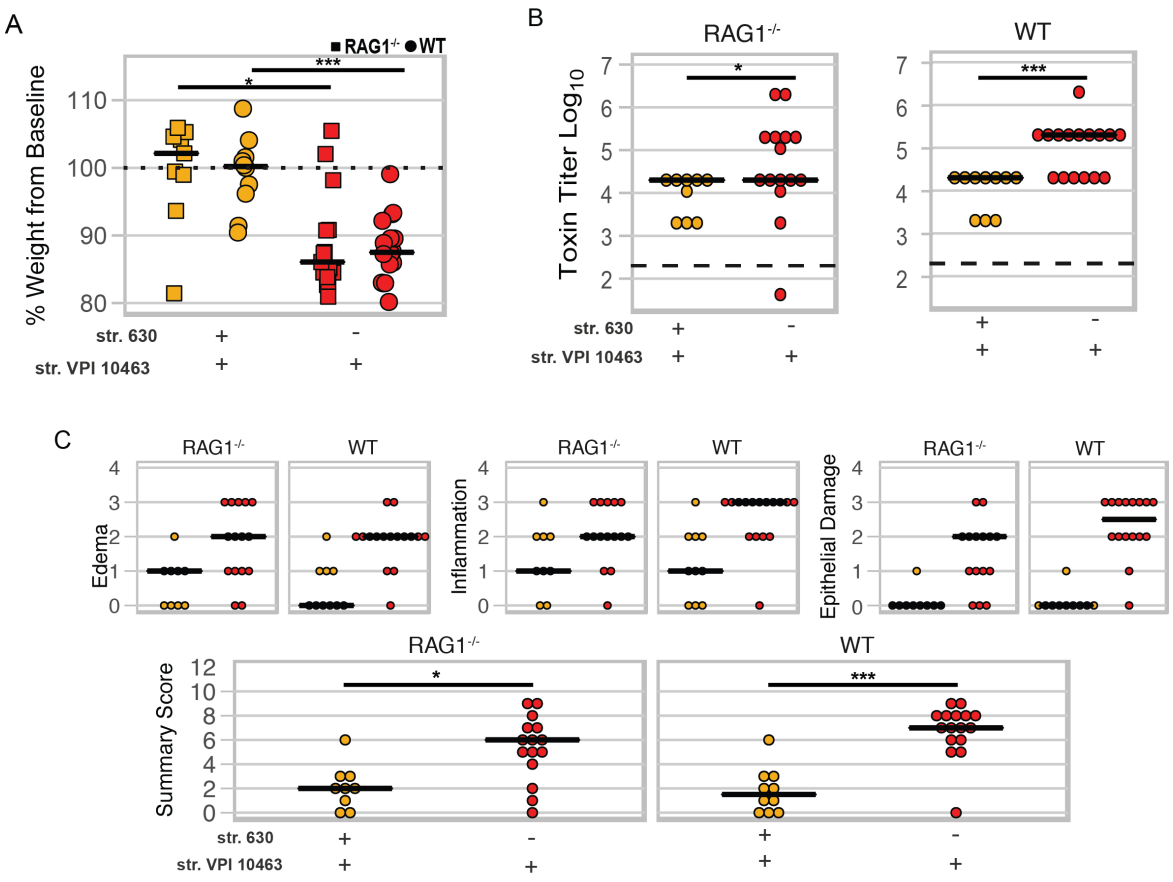

Figure 2.6. RAG1$^{-/-}$ mice pre-colonized with *C. difficile* are protected from challenge with a lethal strain of *C. difficile*

Figure 2.6. RAG1$^{-/-}$ mice pre-colonized with *C. difficile* are protected from challenge with a lethal strain of *C. difficile*

A. Percent of day of challenge weight at time of necropsy. Figure A shows the percent of body weight two days post challenge with the lethal strain relative to weight at time of infection. The dotted line at 100% indicates the value where animals neither gained nor lost weight. Both WT and RAG1$^{-/-}$ mice colonized with strain 630 and challenged with the highly virulent strain VPI 10463 are protected from weight loss where as mice that had no exposure to strain 630 experienced significant weight loss, VPI challenged 630 colonized RAG1$^{-/-}$ vs. VPI challenged naive RAG1$^{-/-}$ p=0.02016, VPI challenged 630 colonized WT vs. VPI challenged naive WT p=0.00021, no statistical difference was detected in comparisons of the same treatment between the two genotypes. Statistical significance was calculated using a Wilcoxon test with a Benjamini-Hochberg correction for multiple comparisons. Data are from two independently run experiments with multiple cages per each treatment group (same mice as in figure 2.5). Each point represents a mouse.

B. Toxin titer from intestinal content of mice in figure 2.6 A as measured by Vero cell rounding assay. Both WT and RAG1$^{-/-}$ mice colonized with strain 630 and then challenged with VPI 10463 have a lower toxin titer relative to naïve mice challenged with VPI 10463, 630 colonized RAG1$^{-/-}$ vs. naive RAG1$^{-/-}$ p=0.04319, 630 colonized WT vs. naive WT p=0.0007306.Statistical significance was calculated using a Wilcoxon test. Limit of detection was 2.3, however for visual clarity samples with an undetected toxin titer were plotted below the limit of detection.

C. Histopathology scoring of the colons of mice in figure 2.6 A. Small panels depict scores for each component that makes up the summary score. VPI challenged 630 colonized RAG1$^{-/-}$ vs. VPI challenged naive RAG1$^{-/-}$ p=0.0107, VPI challenged 630 colonized WT vs. VPI challenged naive WT p=0.0003011.Statistical significance was calculated using a Wilcoxon test.

Protection afforded by low virulence *C. difficile* strain develops rapidly and depends on exclusion of the lethal strain.

Protection afforded by the low virulence *C. difficile* strain develops rapidly and depends on exclusion of the lethal strain

Having ruled out the contribution by adaptive immunity in our model, we next sought to determine if protection required treatment with live *C. difficile*. Other groups have demonstrated that triggering of innate immune pathways with microbial associate molecular patterns, such TLR5 with flagella, protects against acute CDI (32, 33). Additionally, in other colitis models, both viable and heat-killed probiotic strains ameliorate disease via stimulation of host pathways (34). Thus we tested if defense against severe CDI could be conferred by via pre-treatment of mice with a high dose of strain 630 heat-killed via autoclave treatment. As we had not observed a role for adaptive immunity we shortened the model from forty-two days of pre-infection with strain 630 to one day. However, since we were additionally testing heat-killed vs. live *C. difficile* colonization we included RAG1$^{-/-}$ mice in this experiment to confirm findings from our persistent colonization model. Susceptible mice were infected with strain 630, given the equivalent of 10^9 CFU of heat-killed strain 630, or mock infected. Twenty-four hours later mice were all challenged with VPI 10463 (figure 2. 7 A). We observed no protective effect due to administration of heat-killed strain 630, indicating that protection requires colonization with *C. difficile* strain 630 not merely exposure to antigen (figure 2. 7 B, $p<0.05$ for all groups indicated). In this short infection model we also verified our finding that adaptive immunity is not necessary for protection, as both RAG1$^{-/-}$ and WT mice colonized with strain 630 were protected after just twenty-four hours of colonization (figure 2. 7 B). Mice

given viable strain 630 were highly colonized with this strain, while mice given heat-killed strain 630 or mock were not (figure 2.7 C, $p<0.01$ for all except WT 630 pre-colonized vs. mock, $p= 0.015$). However total levels of *C. difficile* (i.e. strain VPI 10463 and strain 630) between groups was not significantly different (figure 2.7 D, $p>0.7$). These data suggest that pre-colonization with strain 630 limits colonization by the lethal strain.

Since treatment with viable *C. difficile* strain 630 was required for protection, we examined whether this benefit was mediated through limiting levels of the more virulent strain. Using selective culturing, it is only possible to differentiate strain 630 from total *C. difficile,* as we were unable to identify an antibiotic that only strain VPI 10643 was resistant to. To overcome this limitation, we developed a quantitative PCR assay using primers that amplify a target in VPI 10463 that is absent in strain 630 (figure 2.8 A). Since these primers generated nonspecific amplicons when used in the context of the rest of the gut microbiota, we used them to follow colonization dynamics of strain VPI 10463 germ-free mice. $RAG1^{-/-}$ germ-free mice were either colonized with strain 630 or left germ-free; the following day, the germ-free mice in addition to one of the subset of 630-colonized mice were challenged with VPI 10463. Importantly, using this model we determined that the pre-colonization with strain 630 inhibits establishment of the lethal strain: we were unable to detect VPI 10463 genomic DNA in the mice that were co-infected, despite high overall levels of *C. difficile* measured by quantitative culture (figure 2.8 C, D, E). In the absence of a microbiota, strain

630 provided some protection from severe disease caused by VPI 10463, however sample size was too low to detect significance (figure 2.8 B).

Reports of patients infected with multiple strains of *C. difficile* suggest that, despite our results, infection with multiple strains can occur (35, 36). Thus we tested whether the order of colonization altered the ability of one strain to protect from challenge with another. We infected susceptible SPF wild type mice with strain VPI 10463 and then challenged them with strain 630 the following day, and vise versa. When administered as a second inoculum strain 630 was not able to rescue the mice from prior infection with the lethal strain (figure 2.9 A). However mice were infected with the two strains simultaneously, both strains were capable of colonizing regardless of the relative amount of each administered. While both strains were detectable when co-inoculated, protection was not observed unless strain 630 was the numerically dominant strain administered (figure 2.9 B). Interestingly, when infecting with different ratios of the two strains, the strains would not colonize past a threshold of approximately 10^8 CFU/gram feces, suggesting a population carrying capacity for *C. difficile* in the mouse gut. Together these data demonstrate that colonization with high levels of strain 630 can prevent establishment of the second strain.

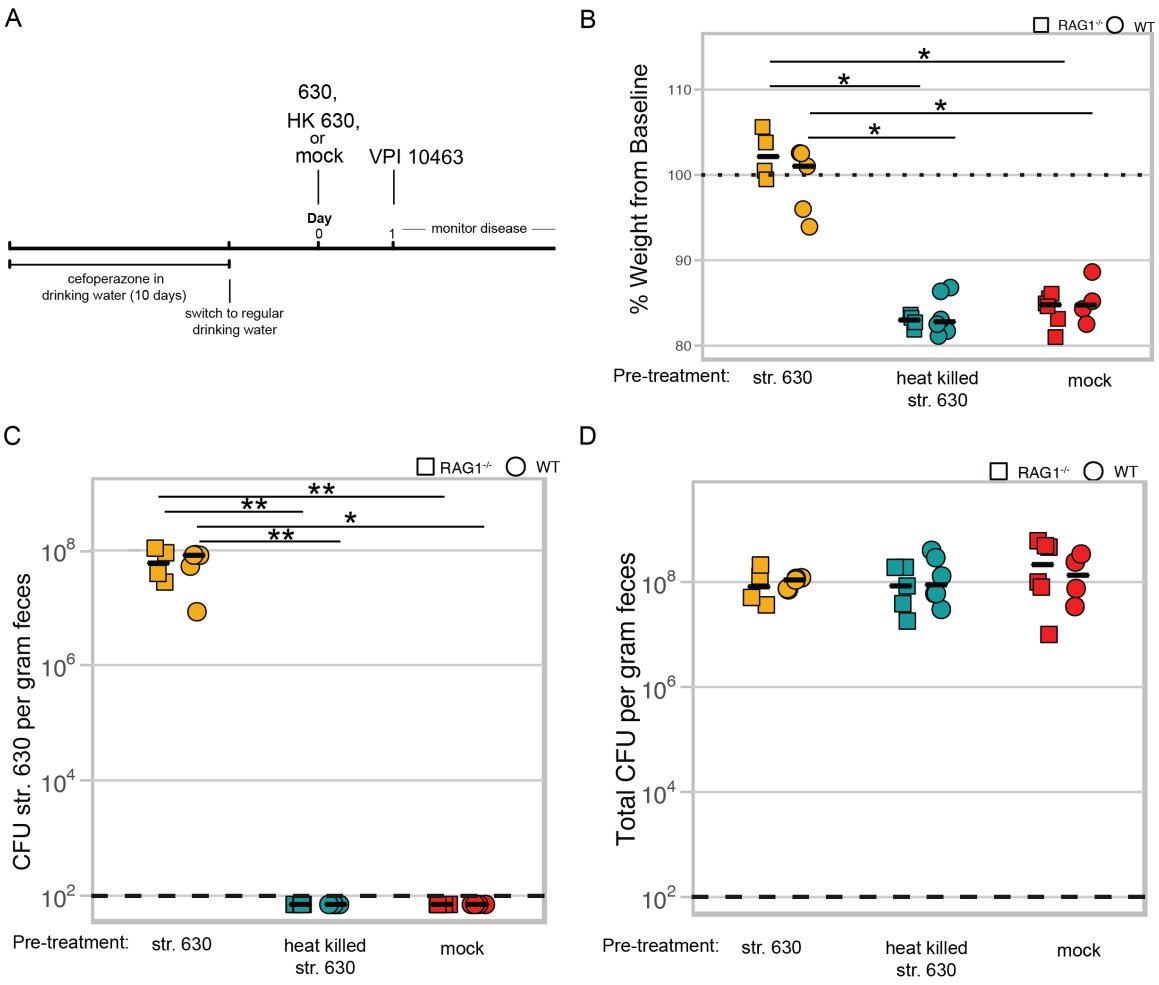

Figure 2.7. Heat-killed *C. difficile* strain 630 does not protect mice from challenge with lethal strain.

Figure 2.7. Heat-killed *C. difficile* strain 630 does not protect mice from challenge with lethal strain.
A. Schematic of shortened experimental timeline.
B. Percent of weight remaining relative to day of challenge in mice pre-treated with viable strain 630, heat-killed strain 630 or water (mock). All mice were infected with strain VPI 10463 one day following pre-treatment. Both RAG1$^{-/-}$ or WT mice given viable strain 630, did not loose weight following challenge with strain VPI 10463, $p<0.05$ vs. mock or heat-killed 630 treated mice. There was no significant difference between weight-loss in the mock vs. heat-killed 630 treatments for either genotype.
C. Levels of strain 630 in mice at conclusion of experiment. Levels of strain 630 were significantly different in mice given viable 630 compared to mice given heat-treated 630 or mock. RAG1$^{-/-}$mice given 630 vs. heat-treated 630, $p = 0.006$ or vs. mock, $p = 0.006$. WT mice given 630 vs. heat-treated 630, $p= 0.008$ or vs. mock, $p= 0.015$. There was no significant difference between colonization in the mock vs. heat-killed 630 treatments for either genotype. LOD is 100 CFU/g feces; undetected samples were plotted below the LOD for visual clarity.
D. Total levels of *C. difficile* colonization in mice at conclusion of experiment. There was no significant difference in total *C. difficile* colonization between any of the groups, $p>0.7$.
For all figures, squares represent RAG1$^{-/-}$ mice while circles represent wild-type (WT) mice. For the data included in each figure, statistical significance was calculated using a Wilcoxon test and corrected for multiple comparisons with a Benjamini- Hochberg correction.

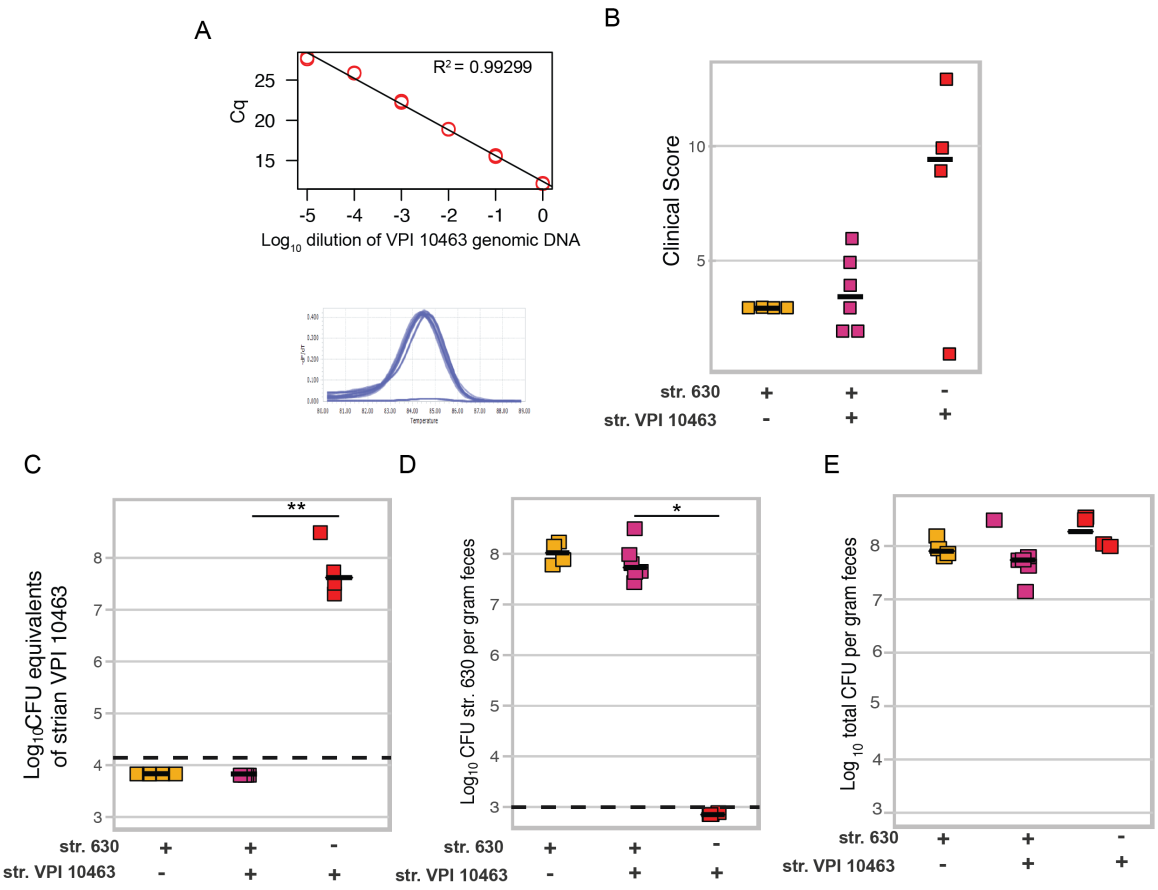

Figure 2.8. Pre-colonization with strain 630 excludes colonization by strain VPI 10463 in RAG1$^{-/-}$ germ-free mice

A. Validation of primers for VPI 10463. Plot of Cq (or crossing-threshold) vs. dilution of genomic DNA from VPI 10463, R^2 = 0.9929. The resulting PCR products formed one melt peak.

B. Clinical score of mice at time of necropsy.

C. CFU equivalents of strain VPI 10463 in mice as determined by qPCR using primers validated in 2.9 A. Mice pre-colonized with *C. difficile* strain 630 have undetectable levels of strain VPI 10463 using this assay, LOD is 1.39 X 10^4 CFU, p =0.005741. Samples that did not have amplification are plotted below the LOD for visual clarity.

D. CFU/gram of feces of *C. difficile* strain 630 across groups as determined by selective quantitative culture (630 is erythromycin resistant while VPI 10463 is sensitive to the antibiotic). Mice only challenged with VPI 10463 were not colonized with strain 630. LOD is 1000 CFU, p = 0.01142. Samples are plotted below the LOD for visual clarity.

E. Total CFU/gram of feces of *C. difficile* as determined by quantitative culture. Statistical significance was calculated using a Wilcoxon test.

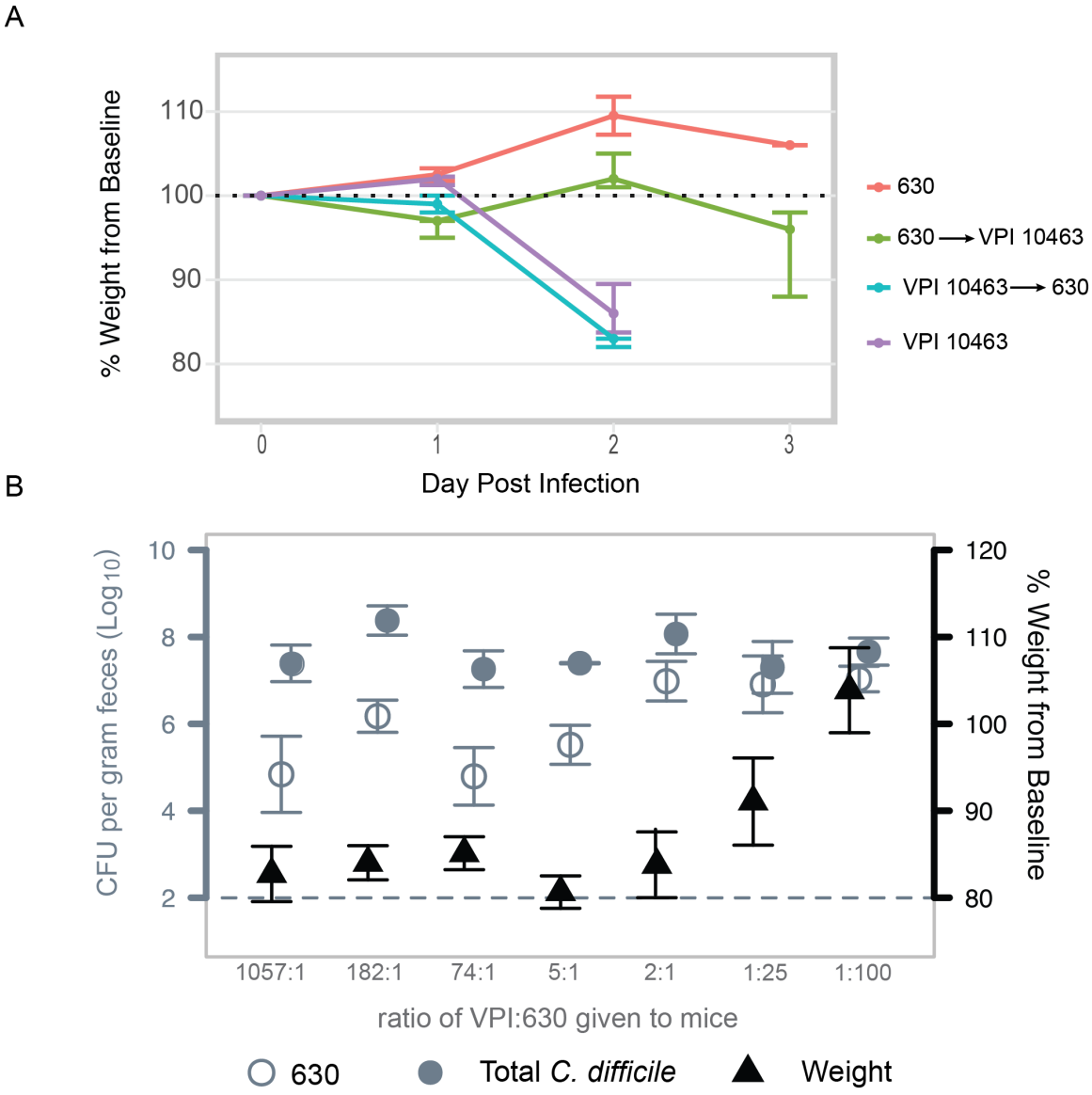

Figure 2.9. *C. difficile* strain 630 cannot rescue mice previously infected with strain VPI 10463

A. Wild-type mice were challenged with either strain 630 or strain VPI 10463, the following day mice were given the other strain. Treatment of mice colonized with strain VPI 10463 with strain 630 did not confer protection, n = 5 mice per experimental group.

B. Mice challenged simultaneously with both strain can be colonized by both strains. Left axis represents Log10 CFU of total C. difficile (closed circle) or strain 630 two days post challenge (open circle). Right axis depicts percent of baseline weight two days post challenge (triangle). Each different inoculum ratio was given to one cage of five mice. Points represent the median value for each treatment while the bars represent the upper and lower quartiles

Protection is associated with decreased availability of the amino acid glycine, a co-germinant

Others have reported that pre-colonization with one strain of *C. difficile* provides protection from challenge with a more virulent strain(37-39). In accordance with Freter's nutrient niche hypothesis, the prevailing hypothesis in the field is that consumption of nutrients by the first strain limits the ability of the invading strain to grow (37, 40). We tested this hypothesis in an *ex vivo* assay using sterile filtrates of cecal content from susceptible mice. Using this approach we found that when vegetative *C. difficile* were inoculated into susceptible mouse cecal filtrate, both strains (630 and VPI 10463) displayed significant growth after twenty-four hours (figure 2.10 A, $p< 0.01$). To test if one day of colonization was sufficient to reduce the nutrients required for growth, we tested if vegetative *C. difficile* strain VPI 10463 would grow in sterilized spent culture from one day of growth of strain 630. Spent culture media from twenty-four hour cultures of both 630 and VPI 10463 supported significant growth (figure 2.10 B). To test if nutrient utilization by strain 630 was different *in vivo,* we additionally tested growth of strain VPI 10463 in cecal filtrate made from mice that were infected with strain 630 for twenty-four hours (figure 2.10 C). This media also supported robust growth, demonstrating that in both batch culture and *in vivo*, twenty-four hours of colonization is not sufficient to reduce the nutrients required for growth of the invading strain. Additionally, as vegetative VPI 10463 replicated in the spent culture of strain 630, we ruled out the role of inhibition due to secreted

products like bacteriocins or even phage in this model. The lack of inhibiting products was confirmed by agar overlay assays (data not shown).

The primary infectious form of *C. difficile* is thought to be the environmentally stable spore (41). Recently groups have shown that *C. difficile* colonization can be decreased by reducing germination (42, 43). To date, the primary focus of studies evaluating germination of *C. difficile* spores have been on bile acids, specifically the primary bile acid taurocholate (44, 45). In the cefoperazone-treated murine model, we previously observed that susceptible mice have significantly increased levels of the bile acid taurocholate, a compound associated with enhanced germination (46). Since strain 630 cannot metabolize taurocholate, we sought other factors that may prevent colonization with a second strain (47).

Other metabolites that are significantly increased in susceptible mice are certain amino acids, including glycine (46). *C. difficile* can ferment glycine in a paired reaction to enhance growth in addition to utilizing this amino acid as a co-germinant (48-50). Using an untargeted metabolomics approach, we measured the relative levels of the glycine in cecum of conventional mice, which are resistant to infection, in addition to levels in the cecum of susceptible and 630 colonized animals (figure 2.11 A). Glycine is low in animals that have an intact community; however, following treatment with cefoperazone, glycine levels increases significantly. However, less than twenty-four hours of colonization with strain 630 significantly reduces glycine in the cecum relative to mock challenged susceptible animals. As we had already ruled out limitation of vegetative growth,

we asked if the decrease in glycine in mice colonized with strain 630 altered germination of VPI 10463 spores. For this purpose, we again utilized an *ex vivo* approach using sterile cecal filtrate from mice that had either been off cefoperazone for three days (D1 CF) or had been off of cefoperazone for two days followed by infection with strain 630 for twenty-four hours (630 D1 CF). PBS with both taurocholate and glycine served as a positive control while PBS alone and PBS with taurocholate were negative controls. Incubating spores in a given condition assessed germination for 15 minutes followed by heat-treatment to kill any cells that germinated. When germination occurs, the post-heat CFU is lower than the pre-heat amount; if there is minimal germination, the spores survive heating and CFU levels should remain constant between the pre and post time points.

Incubation of spores in PBS or PBS + taurocholate had minimal effects on the pre and post heat treatment CFU levels. However, heating the spores treated with PBS+ taurocholate + 100mM glycine significantly reduced CFU, indicating robust germination (figure 2.11B). A similar result was observed in D1 CF revealing that it also supports germination. However, when spores were incubated in 630 D1 CF, there was no significant difference in levels of pre and post CFU, indicating that 630 D1 CF does not support robust germination. To test whether decreased levels of glycine accounted for the poor germination, we attempted to restore germination by adding 100mM glycine to 630 D1 CF. The addition of 100mM glycine to 630 D1 CF resulted in germination (figure 2.11B). Together these results demonstrate that pre-colonization with 630 reduces levels

of glycine in the cecum, which in turn reduces the ability of a second strain to germinate and colonize.

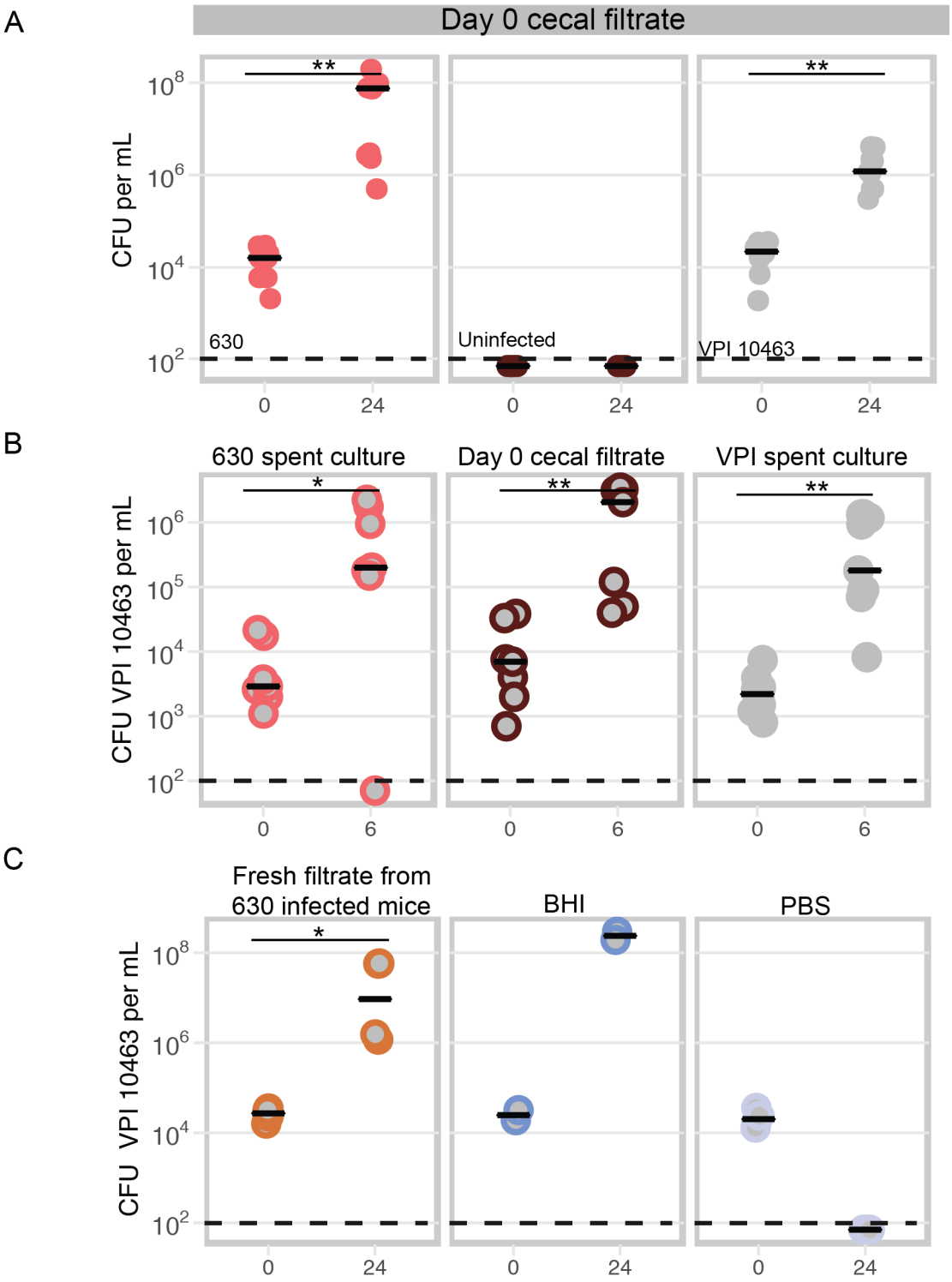

Figure 2.10. Exclusion of *C. difficile* strain VPI 10463 by pre-colonization with *C. difficile* strain 630 is not mediated by inhibition of vegetative growth.

Figure 2.10. Exclusion of *C. difficile* strain VPI 10463 by pre-colonization with *C. difficile* strain 630 is not mediated by inhibition of vegetative growth.

A. Sterile cecal filtrate from susceptible mice (day 0) was inoculated with vegetative cells of *C. difficile* strain 630, vehicle, or vegetative cells of *C. difficile* strain VPI 10463. Levels of colonization were monitored by quantitative culture at time zero and twenty-four hours. Cecal media supports robust growth of both strains, $p< 0.001$.

B. Filter sterilized spent culture from figure A was inoculated with vegetative strain VPI 10463 and colonization was monitored by quantitative culture at time zero and six hours. Spent culture media supports robust growth of strain VPI 10463. Strain VPI 10463 colonization at t =0 vs. t= 6 hours in 630 spent culture, $p= 0.02622$. Strain VPI 10463 colonization at t =0 vs. t= 6 hours in fresh media, $p= 0.0004095$. Strain VPI 10463 colonization at t =0 vs. t= 6 hours in VPI spent culture media, $p= 0.0005828$. Data from A and B represent two independent experiments using separate batches of cecal media run in at least quadruplicates.

C. Growth of *C. difficile* strain VPI 10463 in cecal media made from content from mice infected for twenty-four hours with *C. difficile* strain 630. Strain VPI 10463 colonization at t =0 vs. t= 24 hours, $p= 0.02857$. Statistical significance for all comparisons was calculated using a Wicoxon test.

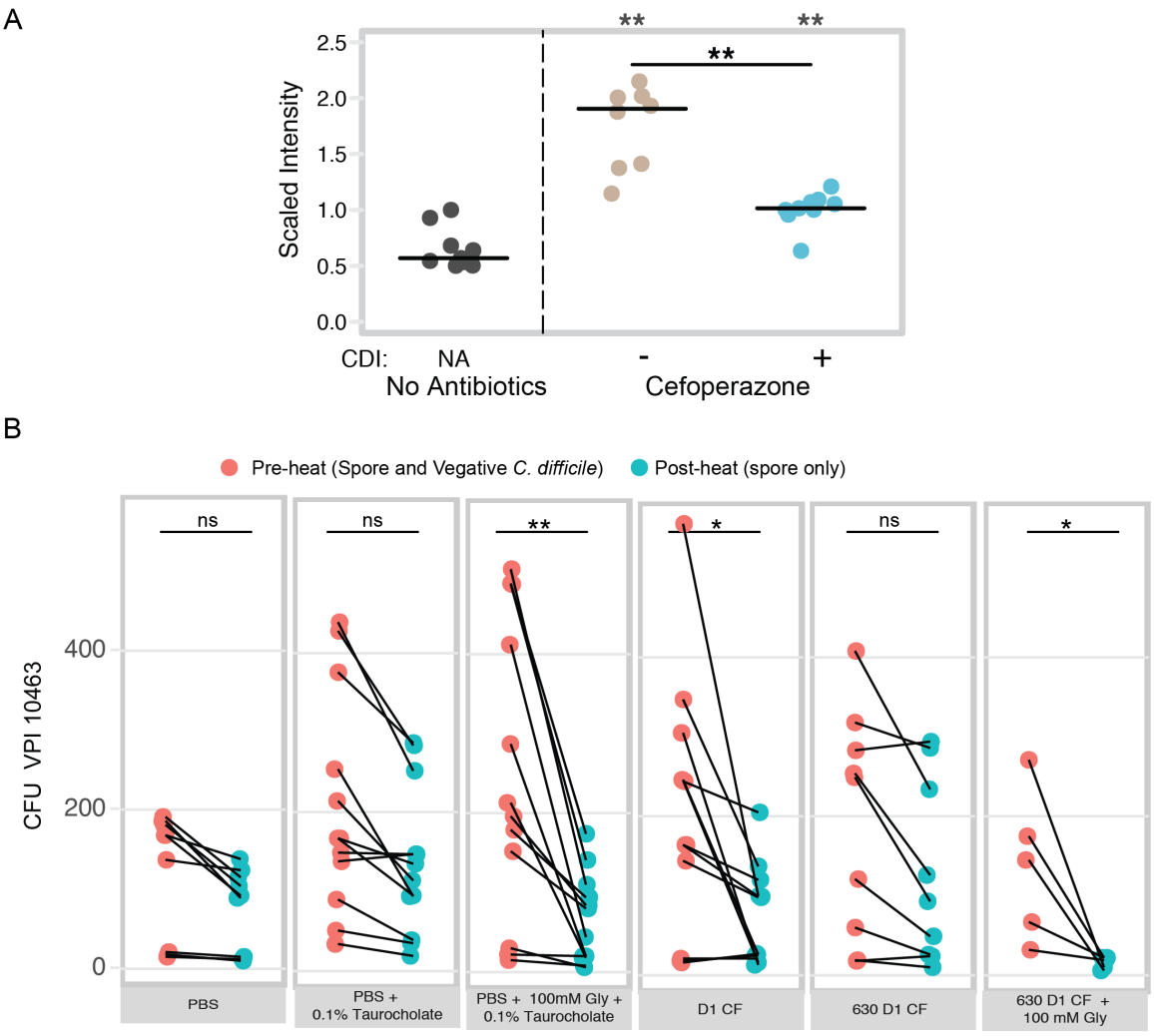

Figure 2.11. Colonization with *C. difficile* strain 630 significantly reduces the co-germinant glycine in cecal contents, leading to reduced germination of invading strain.

A. Relative concentration of glycine in cecal content of mice before antibiotics, after treatment with cefoperazone and one-day post infection with strain 630. Statistical significance for all comparisons was calculated using a Wilcoxon test with Benjamini- Hochberg correction. ** < 0.01

B. Germination of strain VPI 10463 spores following a fifteen-minute incubation in day one cecal filtrate (D1 CF) or cecal filtrates made from mice infected for twenty-four hours with strain 630 (630 D1 CF). PBS supplemented with 0.1% sodium taurocholate and 100mM glycine served as a positive control. Pink dots represent both the vegetative and any remaining spores before heating while the green dots represent the heat-resistant spores. * < 0.05, ** < 0.01. Statistical significance was calculated using a Wilcoxon test.

Discussion

The capacity of the gut microbiota to limit colonization by *C. difficile* has been appreciated for over three decades, however the mechanisms of colonization resistance remain to be fully elucidated (51-53). Many studies have applied on a top down approach to identify and build defined consortia that confer the same protection as the intact community (42, 43, 54). We took an alternative approach by building on the observation that administration of a single bacterium (non-toxigenic *C. difficile*) limited colonization (12, 39). We sought to determine how pre-colonization with one strain of *C. difficile* protects from infection by another. We began by testing the hypothesis that protection was a result of both intraspecific bacterial competition and the development of host immunity to *C. diffic*ile antigen. To do so, we utilized two well-characterized lab strains that despite being differentially virulent in our mouse model express nearly identical forms of both TcdA and TcdB (30, 55).

The multiple infection models, pre-colonization with a less virulent strain is sufficient to protect from challenge with a lethal strain of *C. difficile,* surprisingly even in the absence of adaptive immunity. Additionally, protection is dependent on high levels of colonization by the less virulent strain and is mediated by exclusion of the invading strain. The prevailing theory in the field has been that pre-colonization with one strain of *C. difficile* limits vegetative growth of the challenging strain. Our results challenge this model, as twenty-four hours of

growth by one strain is not sufficient to deplete nutrients to levels that limit vegetative growth.

While other bacterial therapies for *C. difficile* infection such as fecal microbial transplants can lead to clearance of *C. difficile* from the gut (7, 54) *C. difficile* strain 630 was not sufficient to protect mice already colonized with the lethal strain. Recently another group reported that a different toxigenic but low virulence strain of *C. difficile* could both protect and treat infection with VPI 10463 (56). This highlights an important consideration when designing bacterial based therapies for treatment of CDI, as unique strains have different relative fitness.

The major finding from this study is that reduction of glycine following colonization with one strain of *C. difficile* is sufficient to decrease germination of the second strain. This finding provides a novel target for the development of therapeutics that aim to restore colonization resistance.

References

1. **Asha NJ, Tompkins D, Wilcox MH.** 2006. Comparative analysis ofprevalence, risk factors, and molecular epidemiology of antibiotic-associated diarrhea due to *Clostridium difficile*, *Clostridium perfringens*, and *Staphylococcus aureus*. Journal of Clinical Microbiology **44:**2785-2791.

2. **Lessa FC, Mu Y, Bamberg WM, Beldavs ZG, Dumyati GK, Dunn JR, Farley MM, Holzbauer SM, Meek JI, Phipps EC, Wilson LE, Winston LG, Cohen JA, Limbago BM, Fridkin SK, Gerding DN, McDonald LC.**

2015. Burden of *Clostridium difficile* infection in the United States. New England Journal of Medicine **372:**825-834.

3. **Theriot CM, Koenigsknecht MJ, Carlson PE, Jr., Hatton GE, Nelson AM, Li B, Huffnagle GB, J ZL, Young VB.** 2014. Antibiotic-induced shifts in the mouse gut microbiome and metabolome increase susceptibility to *Clostridium difficile* infection. Nat Commun **5:**3114.

4. **Koenigsknecht MJ, Theriot CM, Bergin IL, Schumacher CA, Schloss PD, Young VB.** 2015. Dynamics and establishment of *Clostridium difficile* infection in the murine gastrointestinal tract. Infection and Immunity **83:**934-941.

5. **Carter GP, Rood JI, Lyras D.** 2010. The role of toxin A and toxin B in *Clostridium difficile*-associated disease. Gut Microbes **1:**58-64.

6. **Cohen SH, Gerding DN, Johnson S, Kelly CP, Loo VG, McDonald LC, Pepin J, Wilcox MH.** 2010. Clinical practice guidelines for *Clostridium difficile* infection in adults: 2010 update by the society for healthcare epidemiology of America (SHEA) and the infectious diseases society of America (IDSA). Infection Control & Hospital Epidemiology **31:**431-455.

7. **Seekatz AM, Theriot CM, Molloy CT, Wozniak KL, Bergin IL, Young VB.** 2015. Fecal microbiota transplantation eliminates *Clostridium difficile* in a murine model of relapsing disease. Infection and Immunity **83:**3838-3846.

8. **Kyne L, Warny M, Qamar A, Kelly C.** 2000. Asymptomatic carriage of *Clostridium difficile* and serum levels of IgG antibody against toxin A. The New England journal of medicine **342:**390-397.

9. **Giannasca PJ, Zhang ZX, Lei WD, Boden JA, Giel MA, Monath TP, Thomas WD.** 1999. Serum antitoxin antibodies mediate systemic and mucosal protection from *Clostridium difficile* disease in hamsters. Infection and immunity **67:**527-538.

10. **Lowy I, Molrine DC, Leav BA, Blair BM, Baxter R, Gerding DN, Nichol G, Thomas WDJ, Leney M, Sloan S, Hay CA, Ambrosino DM.** 2010. Treatment with monoclonal antibodies against *Clostridium difficile* toxins. New England Journal of Medicine **362:**197-205.

11. **Gupta SB, Mehta V, Dubberke ER, Zhao X, Dorr MB, Guris D, Molrine D, Leney M, Miller M, Dupin M, Mast TC.** 2016. Antibodies to Toxin B are protective against *Clostridium difficile* infection recurrence. Clinical Infectious Diseases.

12. **Gerding DN, Meyer T, Lee C, et al.** 2015. Administration of spores of nontoxigenic *Clostridium difficile* strain m3 for prevention of recurrent *C. difficile* infection: A randomized clinical trial. JAMA **313:**1719-1727.

13. **Borriello SP, Barclay FE.** 1985. Protection of hamsters against *Clostridium difficile* ileocaecitis by prior colonisation with non-pathogenic strains. Journal of Medical Microbiology **19:**339-350.

14. **Perez J, Springthorpe, V. S. & Sattar, S. A. .** 2011. Clospore: a liquid medium for producing high titers of semi-purified spores of *Clostridium difficile*. J. AOAC Int. **94:**618–626

15. **Reeves AE, Theriot CM, Bergin IL, Huffnagle GB, Schloss PD, Young VB.** 2010. The interplay between microbiome dynamics and pathogen dynamics in a murine model of *Clostridium difficile* Infection. Gut microbes **2:**145-158.

16. **Leslie JL, Huang S, Opp JS, Nagy MS, Kobayashi M, Young VB, Spence JR.** 2015. Persistence and toxin production by *Clostridium difficile* within human intestinal organoids result in disruption of epithelial paracellular barrier function. Infection and Immunity **83:**138-145.

17. **Trindade BC, Theriot CM, Leslie JL, Carlson Jr PE, Bergin IL, Peters-Golden M, Young VB, Aronoff DM.** 2014. *Clostridium difficile*-induced colitis in mice is independent of leukotrienes. Anaerobe **30:**90-98.

18. **Warren CA, van Opstal E, Ballard TE, Kennedy A, Wang X, Riggins M, Olekhnovich I, Warthan M, Kolling GL, Guerrant RL, Macdonald TL, Hoffman PS.** 2012. Amixicile, a novel inhibitor of pyruvate:ferredoxin oxidoreductase, shows efficacy against *Clostridium difficile* in a mouse infection model. Antimicrobial Agents and Chemotherapy **56:**4103-4111.

19. **Theriot CM, Bowman AA, Young VB.** 2016. Antibiotic-induced alterations of the gut microbiota alter secondary bile acid production and allow for

Clostridium difficile spore germination and outgrowth in the large intestine. mSphere **1**.

20. **Jenior ML, Leslie JL, Young VB, Schloss PD.** 2016. *Clostridium difficile* colonizes alternative nutrient niches during infection across distinct murine gut environments. bioRxiv**:**092304.

21. **Kozich JJ, Westcott SL, Baxter NT, Highlander SK, Schloss PD.** 2013. Development of a dual-index sequencing strategy and curation pipeline for analyzing amplicon sequence data on the MiSeq Illumina sequencing platform. Applied and Environmental Microbiology **79:**5112-5120.

22. **Schloss PD, Westcott SL, Ryabin T, Hall JR, Hartmann M, Hollister EB, Lesniewski RA, Oakley BB, Parks DH, Robinson CJ, Sahl JW, Stres B, Thallinger GG, Van Horn DJ, Weber CF.** 2009. Introducing mothur: Open-Source, Platform-Independent, Community-Supported Software for Describing and Comparing Microbial Communities. Applied and Environmental Microbiology **75:**7537-7541.

23. **Quast C, Pruesse E, Yilmaz P, Gerken J, Schweer T, Yarza P, Peplies J, Glöckner FO.** 2013. The SILVA ribosomal RNA gene database project: improved data processing and web-based tools. Nucleic Acids Research **41:**D590-D596.

24. **Edgar RC, Haas BJ, Clemente JC, Quince C, Knight R.** 2011. UCHIME improves sensitivity and speed of chimera detection. Bioinformatics **27:**2194-2200.

25. **Wang Q, Garrity GM, Tiedje JM, Cole JR.** 2007. Naive Bayesian classifier for rapid assignment of rRNA sequences into the new bacterial taxonomy. Appl Environ Microbiol **73:**5261-5267.

26. **Westcott SL, Schloss PD.** 2017. OptiClust, an improved method for assigning amplicon-based sequence data to operational taxonomic units. mSphere **2**.

27. **R Core Team.** 2017. R: A Language and Environment for Statistical Computing. R Foundation for Statistical Computing, Vienna, Austria.

28. **Kelly ML, Ng YK, Cartman ST, Collery MM, Cockayne A, Minton NP.** 2016. Improving the reproducibility of the NAP1/B1/027 epidemic strain R20291 in the hamster model of infection. Anaerobe **39:**51-53.

29. **Hammond GA, Johnson JL.** 1995. The toxigenic element of *Clostridium difficile* strain VPI 10463. Microb Pathog **19**.

30. **Lanis J, Barua S, Ballard J.** 2010. Variations in TcdB activity and the hypervirulence of emerging strains of Clostridium difficile. PLoS pathogens **6**.

31. **Mombaerts P, Iacomini J, Johnson RS, Herrup K, Tonegawa S, Papaioannou VE.** 1992. RAG-1-deficient mice have no mature B and T lymphocytes. Cell **68:**869-877.

32. **Jarchum I, Liu M, Lipuma L, Pamer EG.** 2011. Toll-like receptor 5 stimulation protects mice from acute Clostridium difficile colitis. Infection and immunity **79:**1498-1503.

33. **Jarchum I, Liu M, Shi C, Equinda M, Pamer E.** 2012. Critical role for MyD88-mediated neutrophil recruitment during *Clostridium difficile* colitis. Infection and immunity **80:**2989-2996.

34. **Sang L-X, Chang B, Wang B-Y, Liu W-X, Jiang M.** 2015. Live and heat-killed probiotic: effects on chronic experimental colitis induced by dextran sulfate sodium (DSS) in rats. International Journal of Clinical and Experimental Medicine **8:**20072-20078.

35. **van den Berg RJ, Ameen HA, Furusawa T, Claas EC, van der Vorm ER, Kuijper EJ.** 2005. Coexistence of multiple PCR-ribotype strains of *Clostridium difficile* in faecal samples limits epidemiological studies. J Med Microbiol **54:**173-179.

36. **Behroozian AA, Chludzinski JP, Lo ES, Ewing SA, Waslawski S, Newton DW, Young VB, Aronoff DM, Walk ST.** 2013. Detection of mixed populations of *Clostridium difficile* from symptomatic patients using capillary-

based polymerase chain reaction ribotyping. Infect Control Hosp Epidemiol **34:**961-966.

37. **Wilson KH, Sheagren JN.** 1983. Antagonism of toxigenic *Clostridium difficile* by nontoxigenic *C. difficile*. The Journal of Infectious Diseases **147:**733-736.

38. **Szczesny A, Martirosian G, Cohen S, Silva J.** 2005. Co-infection of hamsters with toxin A or toxin B-deficient *Clostridium difficile* strains. Polish journal of microbiology **54:**301-304.

39. **Nagaro K, Phillips S, Cheknis A, Sambol S, Zukowski W, Johnson S, Gerding D.** 2013. Nontoxigenic *Clostridium difficile* protects hamsters against challenge with historic and epidemic strains of toxigenic BI/NAP1/027 *C. difficile*. Antimicrobial agents and chemotherapy **57:**5266-5270.

40. **Freter R, Brickner H, Botney M, Cleven D, Aranki A.** 1983. Mechanisms that control bacterial populations in continuous-flow culture models of mouse large intestinal flora. Infect Immun **39:**676-685.

41. **Lawley TD, Clare S, Walker AW, Goulding D, Stabler RA, Croucher N, Mastroeni P, Scott P, Raisen C, Mottram L, Fairweather NF, Wren BW, Parkhill J, Dougan G.** 2009. Antibiotic treatment of *Clostridium difficile* carrier mice triggers a supershedder state, spore-mediated transmission, and severe disease in Immunocompromised hosts. Infection and Immunity **77:**3661-3669.

42. **Buffie CG, Bucci V, Stein RR, McKenney PT, Ling L, Gobourne A, No D, Liu H, Kinnebrew M, Viale A, Littmann E, van den Brink MR, Jenq RR, Taur Y, Sander C, Cross J, Toussaint NC, Xavier JB, Pamer EG.** 2014. Precision microbiome reconstitution restores bile acid mediated resistance to *Clostridium difficile*. Nature **advance online publication**.

43. **Studer N, Desharnais L, Beutler M, Brugiroux S, Terrazos MA, Menin L, Schürch CM, McCoy KD, Kuehne SA, Minton NP, Stecher B, Bernier-Latmani R, Hapfelmeier S.** 2016. Functional intestinal bile acid 7 α -Dehydroxylation by *Clostridium scindens* associated with protection from *Clostridium difficile* infection in a gnotobiotic mouse model. Frontiers in Cellular and Infection Microbiology **6**.

44. **Sorg JA, Sonenshein AL.** 2010. Inhibiting the initiation of *Clostridium difficile* spore germination using analogs of chenodeoxycholic acid, a bile acid. J Bacteriol **192:**4983-4990.

45. **Wilson KH, Kennedy MJ, Fekety FR.** 1982. Use of sodium taurocholate to enhance spore recovery on a medium selective for *Clostridium difficile*. Journal of Clinical Microbiology **15:**443-446.

46. **Theriot CM, Koenigsknecht MJ, Carlson PE, Hatton GE, Nelson AM, Li B, Huffnagle GB, Li J, Young VB.** 2014. Antibiotic-induced shifts in the mouse gut microbiome and metabolome increase susceptibility to *Clostridium difficile* infection. Nature communications **5:**3114-3114.

47. **Scaria J, Chen J-W, Useh N, He H, McDonough SP, Mao C, Sobral B, Chang Y-F.** 2014. Comparative nutritional and chemical phenome of *Clostridium difficile* isolates determined using phenotype microarrays. International Journal of Infectious Diseases **27:**20-25.

48. **Sorg JA, Sonenshein AL.** 2008. Bile salts and glycine as cogerminants for *Clostridium difficile* spores. Journal of Bacteriology **190:**2505-2512.

49. **Karasawa T, Ikoma S, Yamakawa K, Nakamura S.** 1995. A defined growth medium for *Clostridium difficile*. Microbiology **141 (Pt 2):**371-375.

50. **Bouillaut L, Self WT, Sonenshein AL.** 2013. Proline-dependent regulation of *Clostridium difficile* Stickland metabolism. Journal of bacteriology **195:**844-854.

51. **Wilson KH, Silva J, Fekety FR.** 1981. Suppression of *Clostridium difficile* by normal hamster cecal flora and prevention of antibiotic-associated cecitis. Infection and Immunity **34:**626-628.

52. **Wilson KH, Sheagren JN, Freter R, Weatherbee L, Lyerly D.** 1986. Gnotobiotic models for study of the microbial ecology of *Clostridium difficile* and *Escherichia coli*. J Infect Dis **153:**547-551.

53. **Wilson KH, Perini F.** 1988. Role of competition for nutrients in suppression of *Clostridium difficile* by the colonic microflora. Infection and Immunity **56:**2610-2614.

54. **Lawley TD, Clare S, Walker AW, Stares MD, Connor TR, Raisen C, Goulding D, Rad R, Schreiber F, Brandt C, Deakin LJ, Pickard DJ, Duncan SH, Flint HJ, Clark TG, Parkhill J, Dougan G.** 2012. Targeted restoration of the intestinal microbiota with a simple, defined bacteriotherapy resolves relapsing *Clostridium difficile* disease in mice. PLoS Pathog **8:**e1002995.

55. **Theriot CM, Koumpouras CC, Carlson PE, Bergin II, Aronoff DM, Young VB.** 2011. Cefoperazone-treated mice as an experimental platform to assess differential virulence of *Clostridium difficile* strains. Gut microbes **2:**326-334.

56. **Etienne-Mesmin L, Chassaing B, Adekunle O, Mattei LM, Bushman FD, Gewirtz AT.** 2017. Toxin-positive *Clostridium difficile* latently infect mouse colonies and protect against highly pathogenic *C. difficile*. Gut.

CHAPTER III

THE GUT MICROBIOTA MEDIATES CLEARANCE OF *CLOSTRIDIUM DIFFICILE* INFECTION INDEPENDENT OF ADAPTIVE IMMUNITY

Summary

Clostridium difficile, a Gram-positive, anaerobic bacterium is the leading single cause of nosocomial infections in the United States. A major risk factor for *C. difficile* infection (CDI) is prior exposure to antibiotics, which increase susceptibility to CDI by altering the microbial community enabling colonization. The importance of the gut microbiota in providing protection from CDI is underscored by the reported 80-90% success rate of fecal microbial transplants in treating recurrent infection. Adaptive immunity, specifically humoral immunity, is also sufficient to protect from both acute and recurrent CDI. However the role of the adaptive immune system in modulating *C. difficile* colonization has yet to be resolved. In this study we sought to determine if adaptive immunity decreases *C. difficile* colonization. Using murine models of CDI, we found that adaptive immunity is dispensable for clearance of *C. difficile*. Furthermore, Random Forest analysis of the indigenous untreated microbial community identified community profiles that predicted animals that would go on to clear the infection with 76% accuracy. These findings indicate that the indigenous gut microbiota and not adaptive immunity limits *C. difficile* colonization within the murine gastrointestinal

tract. Adaptive immune response, while able to mitigate acute disease by limiting toxin-mediated damage, has no effect on pathogen colonization. This research has implications for the design of preclinical studies testing the efficacy of vaccines on levels of colonization, as inherent differences in the baseline community structure of animals within cages may bias findings.

Introduction

The anaerobic bacterium *Clostridium difficile,* is a significant cause of morbidity and mortality in the US with an estimated 500,000 cases yearly (1). A major risk factor for *C. difficile* infection (CDI) is prior exposure to antibiotics (2). Antibiotics increase susceptibility to CDI by altering the membership of the microbial community and thus the metabolome of the gut, enabling colonization (3). Colonization with *C. difficile* can manifest in a range of clinical syndromes ranging from asymptomatic colonization to inflammatory colitis characterized by diarrhea with abdominal pain, and in severe cases death. In addition to primary infection, one in five patients treated for CDI experience recurrent disease (1).

Disease is mediated by the production of two toxins, TcdA and TcdB, which are the major virulence factors for *C. difficile* (4). TcdA and TcdB are large multi-domain proteins, that inactivate cellular rho-family GTPases via the addition of a glucose molecule (5). Inactivation of these key regulatory proteins in epithelial cells results in disruption of tight junctions, increased paracellular flow, and, eventually, cell death (6).

The importance of the gut microbiota in providing protection from CDI is underscored by the reported 80-90% success rate of fecal microbial transplants in preventing recurrent infection (7-9). Other than microbiome-mediated prevention of colonization, adaptive immunity, specifically humoral immunity, also provides protection from both acute and recurrent CDI, likely via antibody-mediated neutralization of *C. difficile* toxins TcdA and TcdB (10-12). However, the role of the adaptive immune system in modulating *C. difficile* colonization has yet to be resolved.

In this study we sought to determine if adaptive immunity decreases *C. difficile* colonization. We found that adaptive immunity is dispensable for clearance of *C. difficile*. Instead, the indigenous microbial community membership that exists prior to antibiotic administration and infection predicted which animals went on to clear the infection.

Experimental Procedures

Animal Husbandry

Male and female C57BL/6 specific-pathogen-free (SPF) mice age five to twelve weeks were used in these studies. The wild type mice were from a breeding colony at the University of Michigan, originally derived from Jackson Laboratories over a decade ago. The Rag1$^{-/-}$ (B6.129S7-*Rag1*^{tm1Mom}/J) mice were from a breeding colony started with mice from Jackson Laboratories in 2013. Animals were housed in filter top cages with corncob bedding and nestlet enrichment. Water bottles were autoclaved empty and filled in a biological safety

cabinet with either sterile water or antibiotic dissolved in sterile water. Mice were fed a standard irradiated chow (LabDiet 5LOD) and had access to food and water *ad libitum*. Cage changes were carried out in a biological safety cabinet. The frequency of cage changes varied depending on the experiment. To prevent cross-contamination between cages, hydrogen peroxide-based disinfectants in addition to frequent glove changes were utilized during all manipulation of the animals. The mice were maintained under 12-hours of light/dark cycle in facilities maintained at temperature of 72°C +/- 4 degrees. Animal sample size was not determined by a statistical method. Multiple cages of animals for each treatment were used to control for possible differences in the microbiota between cages. Mice were evaluated daily for signs of disease. Euthanasia was carried out via CO_2 asphyxiation when mice were determined to be moribund or at the conclusion of the experiment. Animal studies were conducted under the approval of The University of Michigan Committee on the Care and Use of Animals; husbandry was performed in an AAALAC-accredited facility.

Preparation of spores

Spore stocks of *C. difficile* strain 630 (ATCC BAA-1382) were prepared as previously described with the following modifications; strains were grown overnight in 5mL of Columbia broth, which was added to 40mL of Clospore media (3, 13).

Infections

In experiments comparing colonization in WT and Rag1$^{-/-}$ mice, age and sex matched mice were co-housed for thirty-three days starting at three weeks of age and continuing through cefoperazone administration. Upon infection, animals were separated into single genotype housing. Mice were made susceptible to infection by providing *ad libitum* drinking water with the addition of 0.5mg/mL cefoperazone (cat # 0219969501, MP Pharmaceuticals) in Gibco distilled water. The antibiotic water was changed every two days and was provided for 10 days. Following two days of supplying drinking water without antibiotic, mice were challenged with either spores or water (mock). *C. difficile* spores suspended in 50µL of Gibco distilled water were administered via oral gavage. The number of viable spores in each inoculum was enumerated by plating for colony forming units (CFU) per mL^{-1} on pre-reduced taurocholate cycloserine cefoxtin fructose agar (TCCFA). Over the course of the infection, mice were weighed routinely and stool was collected for quantitative culture. Mice were infected with between 10^2 and 10^4 CFU.

Quantitative culture

Fresh voided fecal pellets were collected from each mouse into a pre-weighed sterile tube. Following collection, the tubes were reweighed and passed into an anaerobic chamber (Coy Laboratories). In the chamber, each sample was diluted 1 to 10 (w/v) using pre-reduced sterile PBS and serially diluted. 100uL of a given dilution was spread on to pre-reduced TCCFA or when appropriate

TCCFA supplemented with either 2 or 6µg/mL of erythromycin. Strain 630 is erythromycin resistant; use of erythromycin in TCCFA plates reduced background growth from other bacteria in the sample. Plates were incubated anaerobically at 37°C and colonies were enumerated at 18-24 hours. Plates that were used to determine if mice were negative for *C. difficile* were held and rechecked at 48 hours.

Splenocytes recovery and transfer

Spleens from individual animals were aseptically harvested from donor mice. Following harvest, the organ was gently ground up using sterile glass slides to remove the cells from the capsule. Cells were suspended in filter-sterilized RPMI complete media consisting of RPMI + 1 L-glutamine (Gibco 11875-093) supplemented with 10% FBS (Gibco 16140-071), 1% 100x Penicillin-Streptomycin (Gibco 15070-063), 1% 1M HEPES (Gibco 15630-080), 1% 100x non-essential amino acids (Gibco 11140-050), 1% 100mM Sodium Pyruvate (Gibco 11360-070) and 0.05mL of 1M 2-Mercaptoethanol (Sigma M3148). The cell suspension was passed through 40µm cell strainer to remove large debris. Cells were pelleted by centrifugation at 15000 rpm for five minutes at 4°C. Following the spin, the pellet was broken up with red blood cells RBC lysing buffer (Sigma R7757) and incubated with the solution for no more than five minutes. Lysis was stopped with the addition of more RMPI complete media and cells were enumerated manually using a haemocytometer. Following enumeration, the cells were pelleted again by centrifugation at 15000 rpm for 5

minutes at 4°C and re-suspended in Leibovitz's L-15 (Corning 10-045-CV) media. Recipient mice were injected into the peritoneal cavity with 2 x 10^7 cells in 0.25mL L-15 media. Mice that received vehicle were injected with 0.25mL of L-15 media only.

Blood collection

Blood was collected from either from the saphenous vein for pre-treatment time points or via heart puncture at the experimental endpoint. Collections from the saphenous veined utilized capillary tubes (Sarstedt microvette CB300 Z) while blood collected via heart puncture utilized a polymer gel based separator tube (BD Microtainer SST). Following collection, tubes were spun according to manufacture's instructions, serum was aliquoted and stored at -80°C until use.

Total IgG ELISA

Total serum IgG levels were measured using the IgG (Total) Mouse Uncoated ELISA Kit (ThermoFisher Scientific Cat# 88-50400). Each sample was diluted 500-fold in assay buffer and run in duplicate with Southern Biotech TMB Stop Solution (Cat# 0412-01) used as the stop solution. Optical density values were measured at 450nm and 570nm on a VersaMax plate reader (Molecular Devices, Sunnyvale, CA) and corrected by subtracting the 570nm measurement from the 450nm measurement. A 4-Parameter Standard Curve was used to calculate sample concentration values.

Anti-*C. difficile* TcdA IgG ELISA

Titers of serum IgG specific to *C. difficile* TcdA (toxin A) was measured by ELISA as previously described, with the following modifications (14). Serum from $Rag1^{-/-}$ mice that received an adoptive transfer was diluted 1:50 in blocking buffer with subsequent serial dilutions to a final dilution of 1:12150. Serum from the wild-type mice was diluted 1:1200 in blocking buffer with subsequent serial dilutions to a final dilution of 1:874800. Each sample was run in duplicate. Each plate had the following negative controls: all reagents except serum, all reagents except toxin and pre-immune serum if applicable. Additionally, each plate had a positive control consisting of toxin coated wells reacted with mouse TcdA monoclonal antibody clone TCC8 diluted 1:5000 in blocking buffer (antibodies-online.com). The optical density at 410nm and 650nm was recorded on a VersaMax plate reader (Molecular Devices, Sunnyvale CA). The absorbance for each sample was corrected by subtracting the OD_{650} reading from the OD_{410} reading. The anti-TcdA IgG titer for each sample was defined as the last dilution with a corrected OD_{410} greater than average corrected OD_{410} of the negative control wells plus three times the standard deviation of those wells.

DNA Extraction

Genomic DNA was extracted from approximately 200-300 µl of fecal sample using the MoBio PowerSoil HTP 96 DNA isolation kit (formerly MoBio,

now Qiagen) on the Eppendorf EpMotion 5075 automated pipetting system according to manufacturer's instructions.

Sequencing

The University of Michigan Microbial Systems Laboratory constructed amplicon libraries from extracted DNA as described previously (15). Briefly, the V4 region of the 16S rRNA gene was amplified using barcoded dual index primers as describe by Kozich et al. (16). The PCR reaction included the following: 5µl of 4µM stock combined primer set, 0.15µl of Accuprime high-fidelity Taq with 2µl of 10× Accuprime PCR II buffer (Life Technologies, #12346094), 11.85µl of PCR-grade water, and 1µl of template. The PCR cycling conditions were as follows: 95°C for 2 minutes, 30 cycles of 95°C for 20 seconds, 55°C for 15 seconds, and 72°C for 5 minutes, and 10 minutes at 72°C. Following construction, libraries were normalized and pooled using the SequelPrep normalization kit (Life Technologies, #A10510-01). The concentration of the pooled libraries was determined using the Kapa Biosystems library quantification kit (KapaBiosystems, #KK4854) while amplicon size was determined using the Agilent Bioanalyzer high-sensitivity DNA analysis kit (#5067-4626). Amplicon libraries were sequenced on the Illumina MiSeq platform using the MiSeq Reagent 222 kit V2 (#MS-102-2003) (500 total cycles) with modifications for the primer set. Illumina's protocol for library preparation was used for 2 nM libraries, with a final loading concentration of 4pM spiked with 10 % PhiX for diversity. The

raw paired-end reads of the sequences for all samples used in this study can be accessed in the Sequence Read Archive under PRJNA388335.

Sequence Curation and Analysis

Raw sequences were curated using the mothur v.1.39.0 software package (17) following the Illumina MiSeq standard operating procedure. Briefly, paired end reads were assembled into contigs and aligned to the V4 region using the SLIVA 16S rRNA sequence database (release v128) (18), any sequences that failed to align were removed; sequences that were flagged as possible chimeras by UCHIME were also removed (19). Sequences were classified with a naïve Bayesian classifier (20) using the Ribosomal Database Project (RDP) and clustered in to Operational Taxonomic Units (OTUs) using a 97% similarity cutoff with the Opticlust clustering algorithm (21).

The number of sequences in each sample was then rarefied to 10,000 sequences to minimize bias due to uneven sampling. For feature selection the, the shared file was filtered to remove any OTU that was in less than six samples across the entire data set. The mothur implementation of LefSe (linear discriminant analysis effect size) was used to determine OTUs that differentiated IgG positive verses $RAG1^{-/-}$ mice given vehicle nineteen days post transfer (22). Following curation in mothur, further data analysis and figure generation was carried out in R (v 3.3.3) using standard and loadable packages (23). The data and code for all analysis associated with this study are available at https://github.com/jlleslie/AdaptiveImmunity_and_Clearance.

Most of the analysis relied on the R package vegan (24). This includes, determining the axes for the multidimensional scaling (MDS) plots using Bray-Curtis dissimilarity calculated from sequence abundance. Additionally, vegan was used to determine significance between groups using ANOSIM, calculation of Inverse Simpson index, and Bray-Curtis dissimilarity between samples. Final figures were modified and arranged in Adobe Illustrator CC. For the purpose of distinguishing between values that were detected at the limit of detection versus those that were undetected, all results that were not detected by a given assay were plotted at an arbitrary point below the LOD. However for statistical analysis, the value of LOD/$\sqrt{2}$ was substituted for undetected values. Wilcoxon ranked sum test was used to determine significant differences and, when appropriate, reported p-values were corrected for multiple comparisons using the Benjamini–Hochberg correction.

Random Forest Analysis

Random Forest analysis was performed using R (v.3.2.3) using the randomForest package (25, 26). Model parameters ntree and mtry were tuned based on the input datasets in order to achieve optimal classification without over-fitting (27). Briefly, ntree was calculated by multiplying the total number of OTUs included in the analysis by a ratio of the quantity of samples in each classification category. Additionally, mtry was defined as the square root of the number of OTUs. The informative cutoff for Mean Decease Accuracy (MDA) values was determined by the absolute value of the lowest MDA measured (28).

Testing for significant difference in OTU relative abundance following feature selection was performed using Wilcoxon signed-rank test with Benjamini–Hochberg correction.

Results

Reconstitution of adaptive immunity does not impact C*. difficile* colonization

We sought to determine the contribution of adaptive immunity in clearance of *C. difficile*. To address this question we asked if reconstitution of adaptive immunity via transfer of splenocytes from wild-type mice into RAG1$^{-/-}$ mice, which are deficient in both B and T cells, is sufficient to clear *C. difficile*. Reports of immunization with various *C. difficile* antigen suggests that antibodies to these antigens may decrease colonization, so we additionally asked if transfer of cells from mice immunized via natural infection with *C. difficile* might facilitate clearance (29, 30). Splenocytes were collected from wild type mice that were either naïve or colonized with *C. difficile* strain 630 for three weeks (figures 3.1 A, 3.2 A). The development of humoral immune responses to *C. difficile* in the donor mice was confirmed by the detection of high titers of anti-TcdA IgG in the serum while uninfected mice had undetectable levels of anti-TcdA serum IgG (figure 3.2 B. $p < 0.01$).

To determine the effect of reconstitution of adaptive immunity on *C. difficile* colonization, the recipient mice (RAG1$^{-/-}$) were colonized with *C. difficile* strain 630 prior to the adoptive transfer. Donor splenocytes were administered to

the recipient RAG1$^{-/-}$ mice two days after *C. difficile* challenge. Recipient mice were randomly assigned to one of three groups that either received splenocytes from naïve wild type donors, splenocytes from infected wild type donors, or vehicle (figure 3.1 A). To confirm the successful engraftment of the WT cells, we measured total serum IgG in the recipient mice three-weeks post transfer. The mice that received splenocytes had significantly higher levels of total serum IgG post-transfer compared to the mice that received vehicle (figure 3.2 C, $p < 0.05$). Of the mice that received splenocytes, two did not develop any detectable serum IgG. There was no difference in the levels of total serum IgG between the mice that received splenocytes from infected donors versus uninfected donors ($p > 0.05$). Furthermore, we verified that we successfully transferred anti-*C. difficile* immunity, as anti-TcdA IgG was detected only in the serum of mice that received splenocytes from the infected donors (figure 3.2 D, $p < 0.01$).

Following adoptive transfer, levels of *C. difficile* in the feces were monitored for three weeks. We observed clearance of *C. difficile* from mice that were housed in a single cage. However, clearance of *C. difficile* did not occur in any of the animals in the two other cages within that same treatment group (figure 3.3 A). Three-weeks post transfer there was no significant difference in levels of colonization in any of the groups (figure 3.3 B, $p > 0.05$). Notably, in the cage that cleared the infection, one mouse had undetectable levels of serum IgG while the other three mice in the cage had detectable levels (figure 3.3 C). Together these results do not support the model that presence of adaptive immunity is required for clearance of *C. difficile*.

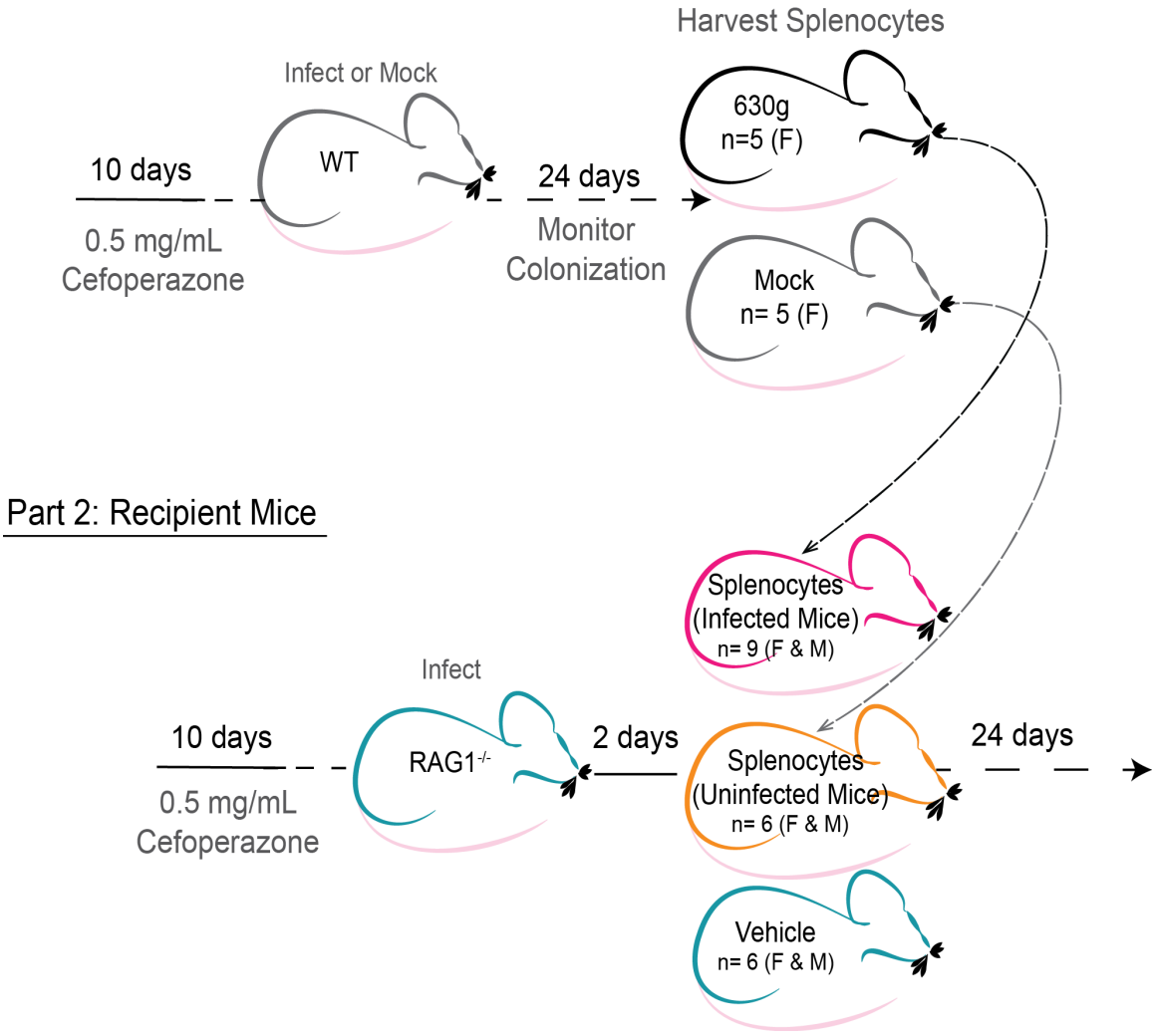

Figure 3.1. Schematic of the experimental timeline.
The timeline observed for the mice from which the splenocytes were harvested is outlined in Part 1 (donor mice). Splenocytes from the donors were injected into infected RAG1-/- mice as outlined in Part 2 (recipient mice).

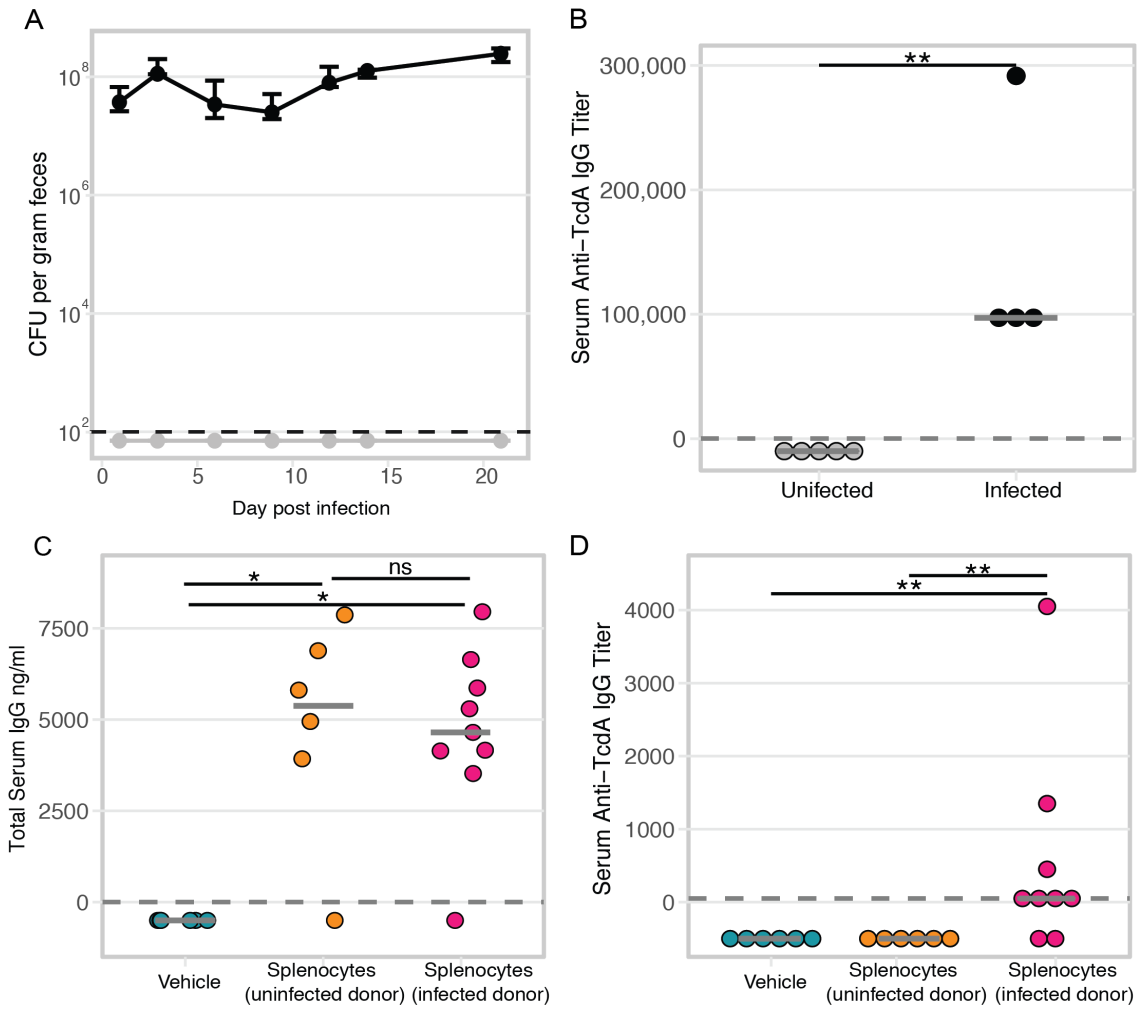

Figure 3.2 Adoptive transfer of splenocytes into RAG$^{1-/-}$ mice results in reconstitution of humoral immunity.

A. *C. difficile* colonization in donor mice. Circles represent the median CFU/g feces for each cage while the error bars denote upper and lower quartiles.Grey represents the cage of mock-infected mice that were never colonized, while black points represent the infected mice. The black-hashed line represents the limit of detection, which was 100 CFU/g feces. All undetected results are plotted below the LOD line for visual clarity.

B. Anti-TcdA IgG titers in wild-type donor mice ($p = 0.009$).

C. Total serum IgG in the recipient Rag1$^{-/-}$ mice twenty-four days post injection of splenocytes (Vehicle vs. Uninfected Donor Splenocytes $p= 0.011$; Uninfected Donor Splenocytes vs. Infected Donor Splenocytes $p= 0.814$.

D. Anti-TcdA IgG titers in recipient Rag1$^{-/-}$ mice twenty-four days post transfer of splenocytes (Vehicle vs. Infected Donor Splenocytes $p= 0.008$; Uninfected Donor Splenocytes vs. Infected Donor Splenocytes $p= 0.008$. Statistical significance was calculated using a Wilcoxon test with Benjamini–Hochberg correction for multiple comparisons. Dashed line represents the limit of detection, while solid bars represent the median. Undetected results are plotted below the LOD line for visual clarity, and a value equal to the LOD/$\sqrt{2}$ was used for statistical tests.

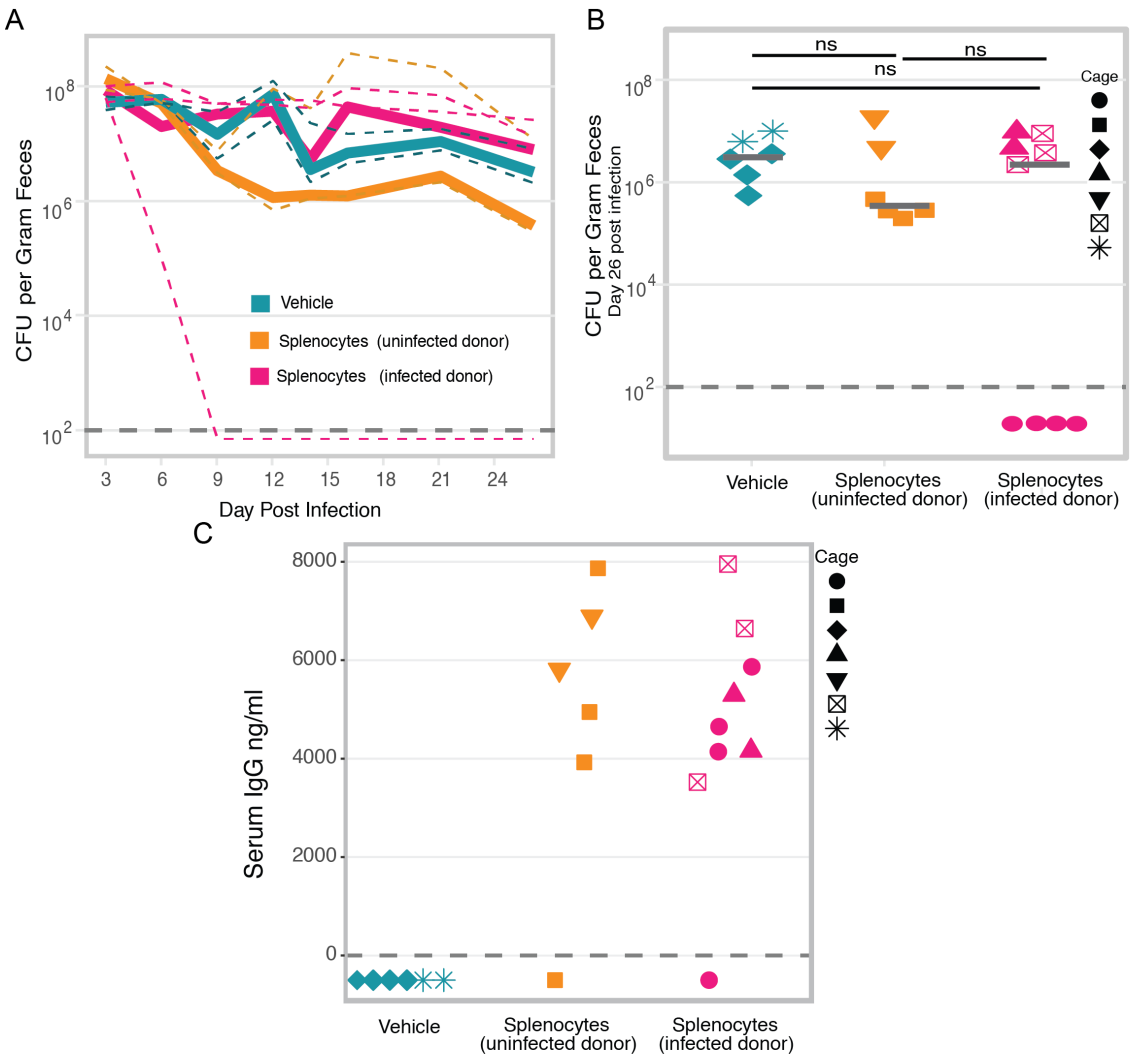

Figure 3.3. Clearance of *C. difficile* colonization is not associated with restoration of adaptive immunity.

A. Time course of intestinal colonization levels with *C. difficile* colored by treatment group. Solid lines represent the median CFU of *C. difficile* per gram of feces. Dashed lines represent median colonization within each cage.

B. Colonization on day 26-post infection (day 24-post adoptive-transfer) colored by treatment group (p=0.835). For A and B: The dark-grey dashed line represents the limit of detection. For all data, statistical significance was calculated using a Wilcoxon test with Benjamini–Hochberg correction for multiple comparisons.

C. Same data as in figure 3.2 C however shapes represent animals within one cage. Note that one of the fuchsia circles had no detectable serum IgG. The hashed lined represents the LOD of 1.56 ng/mL, all undetected results are plotted below the LOD line for visual clarity.

Specific OTUs are altered in mice with reconstituted adaptive immunity

The range in the levels of colonization we observed within each treatment group suggested that something other than adaptive immunity might modulate levels of *C. difficile*. The gut microbial community is crucial in protecting from initial colonization and for facilitating clearance of *C. difficile* (31). We examined the gut microbial community structure of the mice over the course of the experiment by using 16S rRNA gene amplicon sequencing. Visualization of the Bray-Curtis dissimilarity between the day one post infection communities (before the adoptive transfer) using multidimensional scaling revealed that the mice that cleared *C. difficile* had a distinct community compared to the mice that remained colonized (figure 3.4, ANOSIM, $p = 0.02$, $R = 0.7363$). This result suggests that gut microbiota, rather than the adoptive transfer of splenocytes, enables clearance of *C. difficile*.

The microbiota and the immune system have been previously shown to modulate one another through numerous complex interactions (32, 33). In the cefoperazone mouse model of infection, the diversity of microbiota begins to recover by two weeks following cessation of the antibiotic (34). Therefore we asked if reconstitution of adaptive immunity altered the recovery of the community following antibiotics and infection with *C. difficile*. Our first approach sought to determine if we could detect changes in the overall community composition of the mice. We calculated the Bray-Curtis dissimilarity between each mouse's day twenty-one sample (nineteen days after the adoptive transfer) and their pre-antibiotic sample. We hypothesized that the addition of adaptive

immunity might prevent the microbiota from returning to the same structure as was observed before adoptive transfer. Thus, we investigated whether the mice that received splenocytes might have higher Bray-Curtis dissimilarity values compared to the vehicle group. Since we were unable to confirm that we successfully restored adaptive immune function in two of mice that received splenocytes, we excluded them from the rest of analysis as our questions hinged on immune status-gut microbiota interactions (figure 3.3 C). Additionally could not calculate this metric for a couple of mice due to the lack of pre-antibiotic samples. Comparing the Bray-Curtis dissimilarity results between the three treatment groups revealed no significant differences between any of the groups (figure 3.5 A, $p > 0.05$). We also wondered if addition of adaptive immunity might alter alpha-diversity so we calculated the inverse Simpson index of each fecal community at day nineteen post transfer (day twenty-one post infection). We did not observe any significant differences between the treatment groups by these means (figure 3.5 B, $p > 0.05$). This suggested that by broad metrics of community structure, the perturbation of antibiotics and infection with *C. difficile* potentially mask any trends related to reconstitution of adaptive immunity.

While we saw no significant differences in the recovery of the community structure or alpha diversity at day twenty-one post infection, we wondered if perhaps the abundance of only a few OTUs were altered by reconstitution of the adaptive immune system. For this analysis we grouped all of the mice that received splenocytes and developed detectable levels of serum IgG at day twenty-six post infection together and called them IgG positive. The mice that

only received vehicle and thus had undetectable levels of serum IgG were designated the IgG negative group. Using sequence abundance from day twenty-one post infection samples, LefSe identified twenty-seven OTUs with LDA values greater than two. The ten OTUs with the highest LDA values were primarily enriched in the IgG negative mice (figure 3.6 A). OTU 3, which is classified as *Akkermansia,* had the highest LDA value. This OTU was found at a significantly lower abundance in the IgG positive mice compared to the IgG negative mice. A decrease in the abundance of *Akkermansia* following reconstitution of adaptive immunity via adoptive transfer of from wild-type mice into RAG1$^{-/-}$ has been previously reported by another group (35).

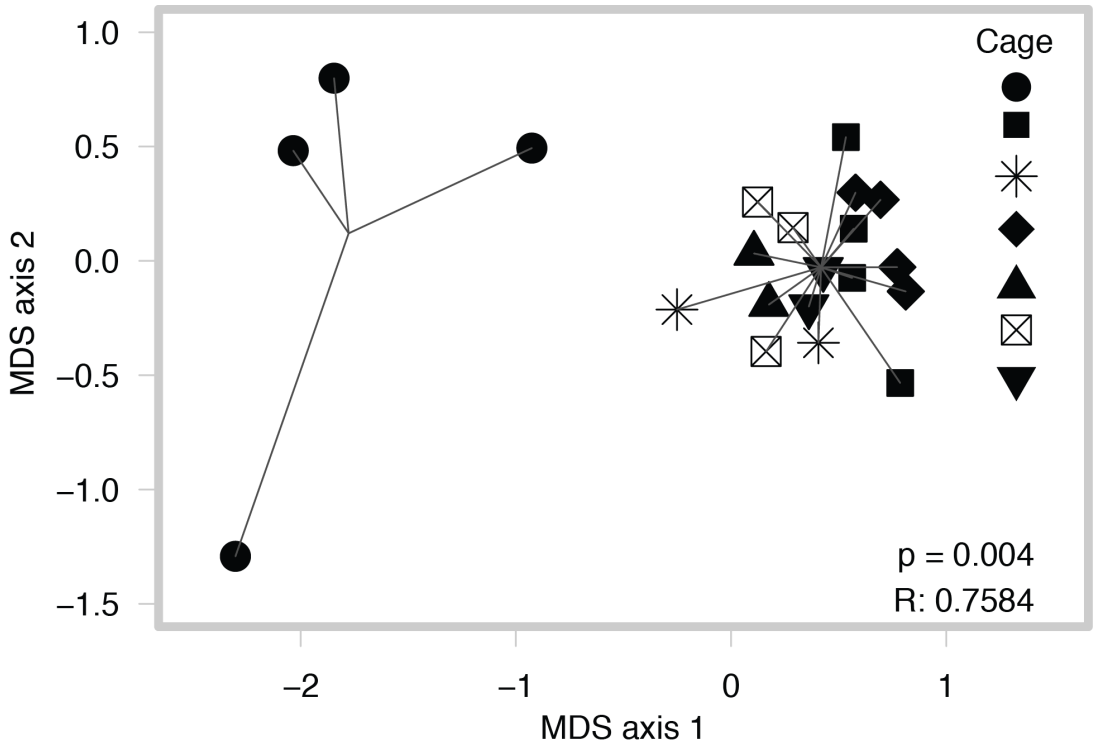

Figure 3.4. Clearance of *C. difficile* colonization is associated with significantly different pre-transfer gut microbiota

Multidimensional scaling (MDS) plot of Bray-Curtis dissimilarity index comparing communities in mice at day one-post infection. Cages that cleared infection are shown as black dots, while other cages are represented by the other shapes (p=0.004). Significance was determined with ANOSIM in R (v3.2.3) from vegan (v2.4-3).

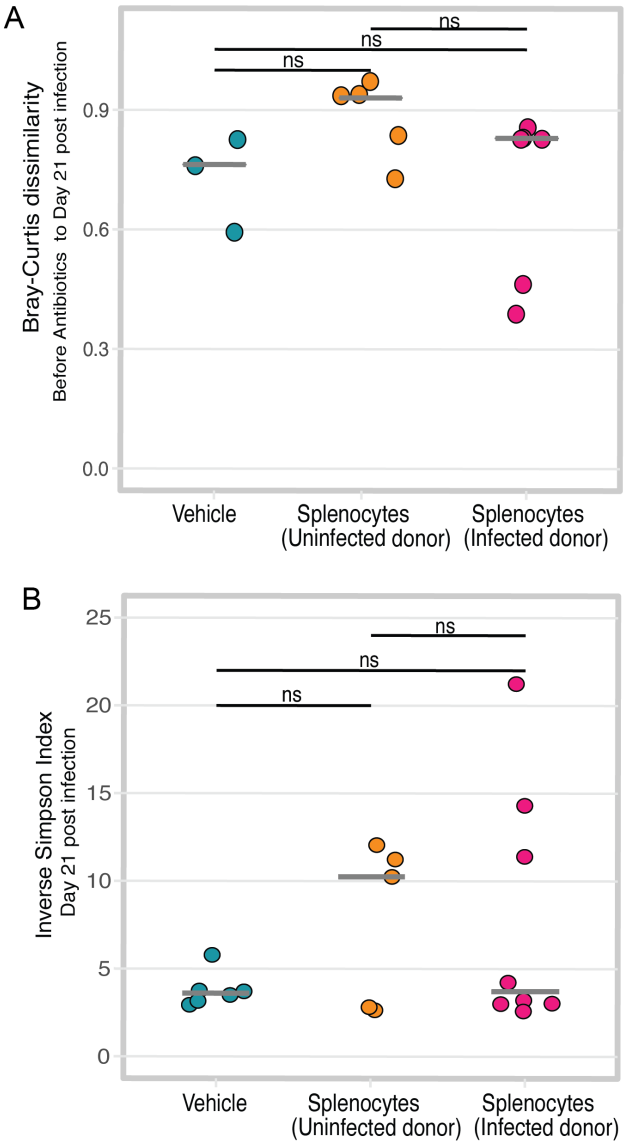

Figure 3.5. Reconstitution of adaptive immunity does not alter gut microbial diversity in our model

A. Bray-Curtis dissimilarity between each mouse's pre-antibiotic and day 21-post infection communities (Uninfected donor splenocytes vs. Infected donor splenocytes p= 0.082, Uninfected donor splenocytes vs. vehicle p= 0.149, Infected donor splenocytes vs. vehicle p= 0.714).

B. Inverse Simpson diversity of communities day 21-post infection communities (Uninfected donor splenocytes vs. Infected donor splenocytes p= 0.9433, Uninfected donor splenocytes vs. vehicle p=0.7546, Infected donor splenocytes vs. vehicle p= 0.6623). Statistical significance was calculated using a Wilcoxon test with Benjamini–Hochberg correction for multiple comparisons

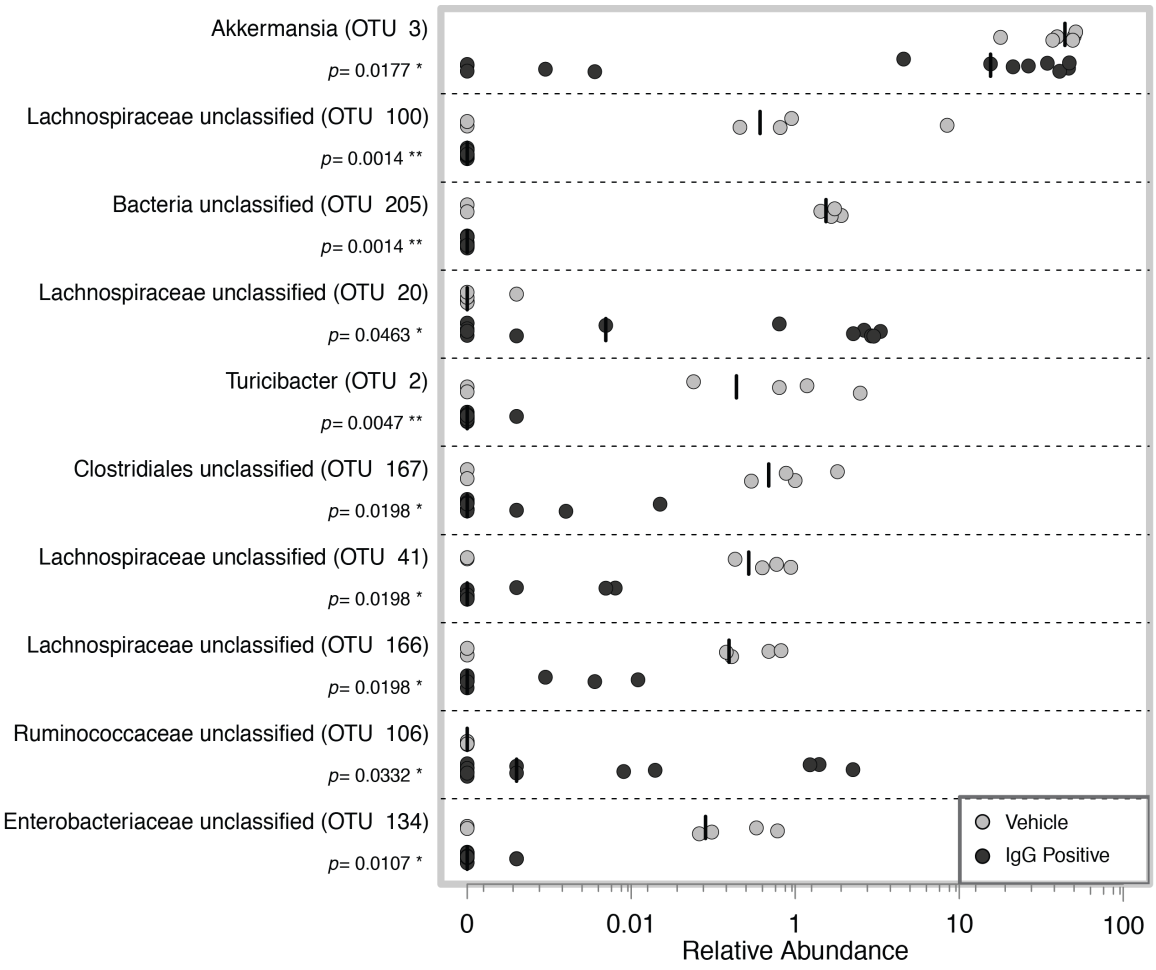

Figure 3.6. Effect of reconstitution of adaptive immunity on the specific OTUs
Relative abundance of the top ten OTUs with the highest LDA distinguishing between vehicle treated Rag1$^{-/-}$ and IgG positive mice. Each dot represents a single mouse. Bars represent the median.

Structure of the fecal microbiota before antibiotics is associated with clearance in both WT and RAG1$^{-/-}$ mice.

To test if the gut microbial community is sufficient to provide clearance of *C. difficile*, we co-housed RAG1$^{-/-}$ mice with WT mice (figure 3.7). For this experiment, we did not perform splenocyte transfer so that the RAG1$^{-/-}$ mice remained without adaptive immunity. After a little over a two weeks of co-housing, the two groups of mice consisting of both wild-type mice into RAG1$^{-/-}$ had significantly different community structures as demonstrated by the MDS plot of the Bray-Curtis dissimilarities (figure 3.8 A, ANOSIM, $p = 0.046$, $R = 0.161$). When the mice were analyzed by genotype rather than by co-housing group we found that gut communities of the two genotypes of mice were not significantly different (figure 3.8 B, ANOSIM, $p = 0.085$, $R = 0.1224$). During the infection we again observed some mice cleared while others remained colonized. In this experiment the two cages of mice that cleared were both from the same cohousing group (figure 3.7 and 3.8 C). At the conclusion of the experiment the two cages that remained colonized had significantly higher levels of *C. difficil*e compared to the mice that cleared (figure 3.8 C, $p<0.01$). Cleared or colonized mice did not belong to any one genotype but rather to the same co-housing group (figure 3.8 C, D). These results in addition to our previous experiment demonstrate that clearance of *C. difficile* is independent of adaptive immunity.

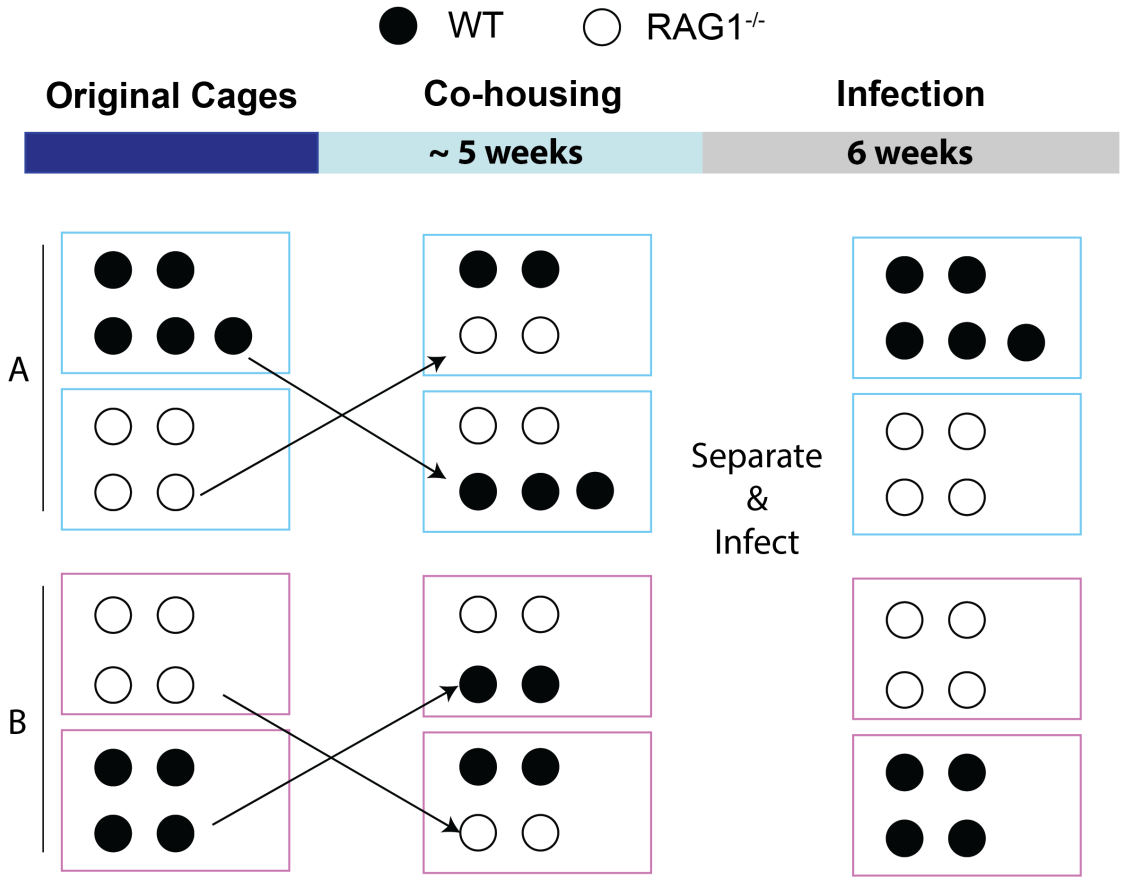

Figure 3.7. Schematic of co-housing experiment.
Open circles represent RAG1$^{-/-}$ mice while closed circles represent the wild-type mice. Mice were co-housed for thirty-three days starting before antibiotics up to infection. The colors of the boxes represent gender as well as grouping of mice. Group A denoted by the blue boxes are male RAG1$^{-/-}$ and WT mice that were cohoused before infection while group B, denoted by the purple boxes, represents the female RAG1$^{-/-}$ and WT mice that were cohoused.

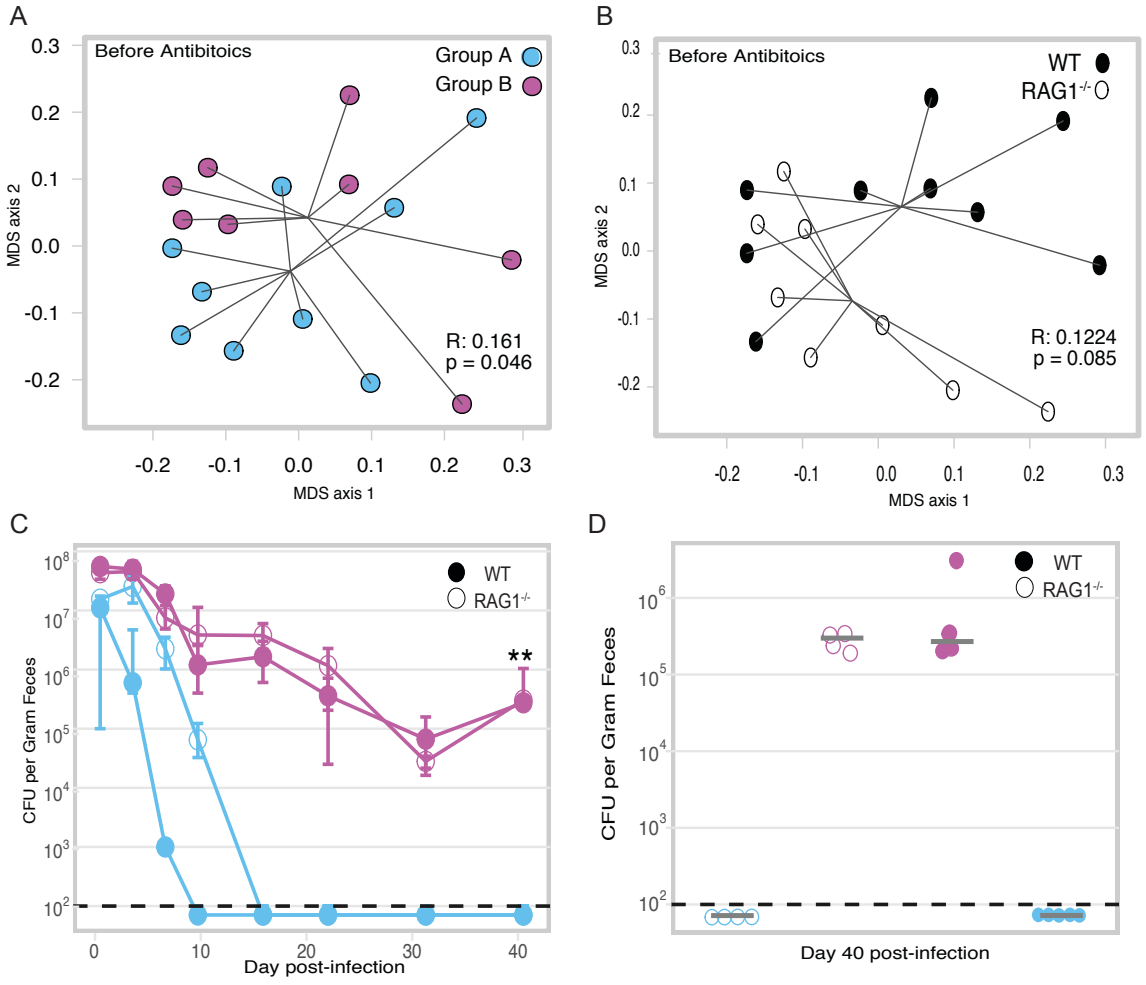

Figure 3.8. Altered microbiota is correlated with clearance in co-housed mice
A. Multidimensional scaling MDS plot of Bray-Curtis dissimilarity between the fecal microbiota of the group A (blue) vs. group B (purple) mice before antibiotic-pretreatment (p=0.046). Significance was determined with ANOSIM in R (v3.2.3) from vegan (v2.4-3).
B. RAG$^{1-/-}$ and WT pre-treatment communities are not significantly different when analyzed by genotype (same plot as A, clustered by genotype rather than co-housing groups).
C. Median temporal *C. difficile* colonization by cage with interquartile ranges. The colors refer back to figure 3.7 and represent co-housing groups prior to infection (p=0.002).
D. *C. difficile* colonization at 40 days post-infection for each cage. The dashed line represents the limit of detection. Undetected results are plotted below the LOD line for visual clarity. A value equal to the LOD/$\sqrt{2}$ was used for statistical tests. Statistical significance for B was calculated using a Wilcoxon test.

Random Forest feature selection identifies OTUs in the pre-antibiotic community that differentiates mice that will remain persistently colonized vs. clear *C. difficile* infection.

Following our previous analyses we made the consistent observation that structure of the gut microbiome was associated with clearance of *C. difficile*, even prior to antibiotic treatment (figure 3.8 A). We questioned if specific OTUs present in the mice before any intervention that might differentiated mice that would go on to clear the infection. For this analysis, we pooled data from three independent experiments (the two described earlier and a third experiment including only WT mice) where cages of mice had spontaneously cleared *C. difficile* (figure 3.9 A). We utilized Random Forest for feature selection to identify OTUs that could classify mice as "cleared" or "colonized" based on their pre-intervention microbiota. Using the pre-treatment community we could classify mice with 76.9% accuracy. Nine out of the top ten OTUs that most contributed to classification were from the Firmicutes phylum (figure 3.9 B and C). Three OTUs in particular (OTUs 52, 93, and 26) ranked highest in their ability to discriminate between the groups. OTUs 52 and 93 were significantly increased in abundance in mice that would go on to clear while OTU 26 was enriched in mice that would remain persistently colonized. Therefore we tested if those three OTUs alone were sufficient to classify the mice. Generating a new Random Forest model using only those three OTUs, we found that classification improved. Utilizing the median out-of bag error for 100 forest iterations, these three OTUs discriminated between colonized and cleared mice with 98.08% accuracy.

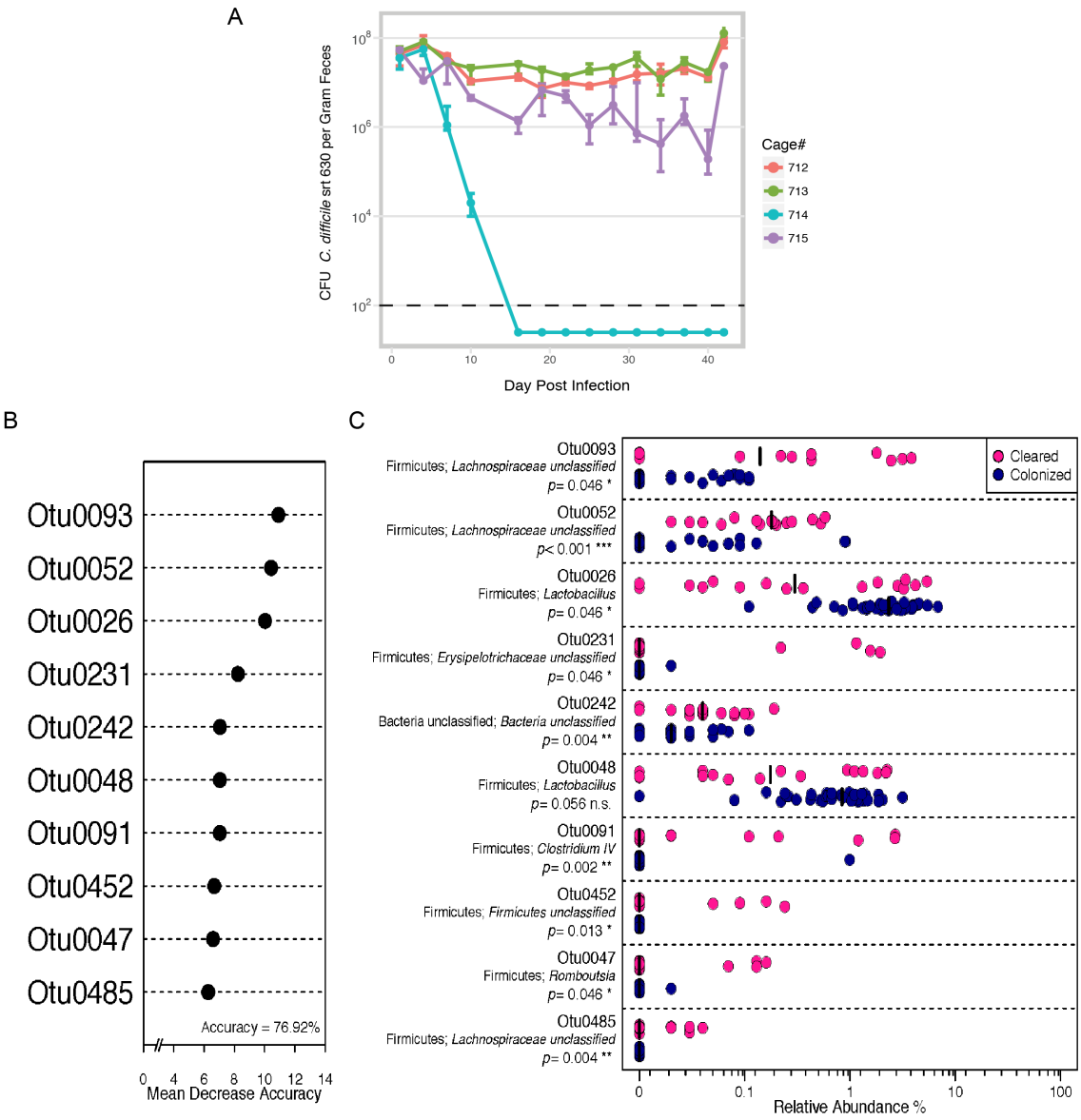

Figure 3.9. Intact community predicts outcome of *C. difficile* infection

A. Colonization of *C. difficile* in wild type mice included in Random Forest analysis.
Circles represents the median CFU/g feces for each cage while the error bars denote upper and lower quartiles. Colors represent the different cages of mice. The black-hashed line represents the limit of detection, which was 100 CFU/g feces. All undetected results are plotted below the LOD line for visual clarity.

B.Top ten OTUs with highest mean decrease in accuracy from the Random Forest classifier.

C. Relative abundance of OTUs from A that distinguish between mice that cleared *C. difficile* and those that remained colonized. Black bars represent the median. Statistical significance was calculated using a Wilcoxon test with Benjamini–Hochberg correction.

Discussion

In this study we tested if adaptive immunity was required for clearance for the gastrointestinal pathogen *C. difficile*. Results from multiple experimental models lead us to conclude that adaptive immunity is dispensable for clearance of *C. difficile* in mice. This finding is in contrast to the paradigm observed in other gastrointestinal infections. For example, infection with the attaching-effacing pathogen *Citrobacter rodentium* provides a framework by which adaptive immunity plays a role in clearance (36, 37). In addition to the potential direct effects, adaptive immunity may have on the bacterium itself, it is known that there is a complex interaction loop between the microbiota and host immune response. Both the innate and adaptive arms of the immune system regulate membership of the gut microbial community while the gut microbiota in turn modulates the immune system via the production of metabolites and/or MAMPs (38).

Our results show that although reconstitution of adaptive immunity can alter the abundance of some bacteria in the gut, it does not impact levels of *C. difficile* colonization. We found that in the RAG1$^{-/-}$ mice that developed serum IgG, there was a decreased abundance of *Akkermansia*. Another group has also observed this result, however we were surprised to see the same trend in our model as our mice were also subjected to antibiotic therapy and infection with *C. difficile.* In the two mice that received splenocytes but did not have detectable serum IgG, the abundance of the *Akkermansia* OTU was very low (figure 3.10 A).

There are numerous reasons why this could be the case, the first being that a lack of serum IgG does not preclude successful transfer of T cells which maybe responsible for modulating levels of *Akkermansia* in wild-type mice. Additionally fecal IgG or IgA from the mice that had successful transfers may have been transmitted via coprophagy in sufficient quantities to modulate the levels of *Akkermansia* in the IgG negative mice that were sharing their cage. Since the relative abundance of OTU3 was not significantly different between the groups in the pre-treatment samples we can conclude that the differences we observed were a result of the experimental conditions not merely baseline differences in their microbiota (figure 3.10 B). *Akkermansia* has been implicated in the modulation of health processes such as regulation of host metabolism so further studies are necessary to fully elucidate the factors that regulate its abundance in the gut (39, 40).

Based on our repeated observations that altered communities early in the experimental timeline was associated with clearance of *C. difficile* we used Random Forest to eventually identify just three OTUs that discriminate between mice that clear vs. remain colonized with 98% accuracy. Previous work using a similar approach identified OTUs present on the day of challenge that were predictive of levels of colonization day one post-infection, however we are the first group to assess if the composition of the murine gut microbiota before any treatment might affect the outcome of C*. difficile* infection (41). Of the three OTUs we identified, two belonged to the family *Lachnospiraceae* and were enriched in mice that would go on to clear *C. difficile* infection, while the third

OTU belonged to the *Lactobacillus* family and was more abundant in mice would remain colonized. Our group has previously observed that high levels of *Lachnospiraceae* is associated with protection from severe disease in a murine model of CDI (42). Furthermore we have also reported that mono-association of germ-free mice with a single *Lachnospiraceae* isolate partially restored colonization resistance (43). It is tempting to speculate multiple *Lachnospiraceae* isolates might be able to fully restore colonization resistance. However, it remains to be seen if the same mechanisms, which prevent initial colonization of *C. difficile*, play a role in clearance of *C. difficile.*

Our results suggest that community resilience is intrinsic to the pre-treatment membership. Additionally these data allude to the possibility of predicting those that will be at risk for persistent colonization before antibiotic therapy. However a crucial first step is to determine if predictive OTUs are different across perturbations such as various classes of antibiotic therapy. Finally, our findings have implications for the design of future preclinical studies testing the efficacy of vaccines or other manipulations of adaptive immunity on levels of colonization as “cage effects” or inherent differences in the baseline community structure of animals within cages may bias findings. Experimental approaches that can be implemented to account for the role of microbiota include co-housing, using multiple cages for each experimental condition, and the use of littermate controls (44).

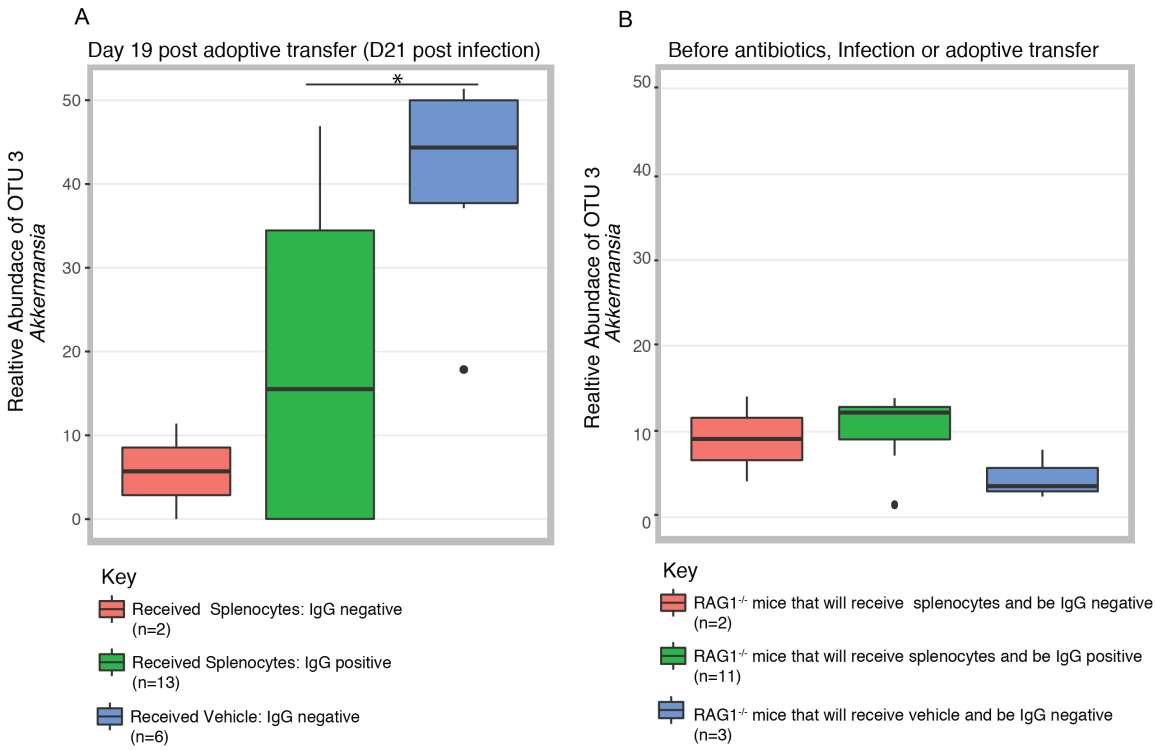

Figure 3.10. Akkermansia (OTU 3) relative abundance
A. Relative abundance of OUT 3 in all the mice on day 21-post infection in the adoptive transfer experiment. Mice that received splenocytes but did not develop detectable total serum IgG have low levels of this OTU unlike the mice that received vehicle. There is a significant difference in the abundance of OTU 3 in the mice that received vehicle compared to the mice that had successful transfers of WT splenocytes P=0.0199 by Wilcoxon test.
B. Relative abundance of OTU 3 before any treatment took place.

References

1. **Lessa FC, Mu Y, Bamberg WM, Beldavs ZG, Dumyati GK, Dunn JR, Farley MM, Holzbauer SM, Meek JI, Phipps EC, Wilson LE, Winston LG, Cohen JA, Limbago BM, Fridkin SK, Gerding DN, McDonald LC.** 2015. Burden of *Clostridium difficile* Infection in the United States. New England Journal of Medicine **372:**825-834.

2. **Chalmers JD, Akram AR, Singanayagam A, Wilcox MH, Hill AT.** 2016. Risk factors for *Clostridium difficile* infection in hospitalized patients with community-acquired pneumonia. The Journal of infection **73:**45-53.

3. **Theriot CM, Koenigsknecht MJ, Carlson PE, Hatton GE, Nelson AM, Li B, Huffnagle GB, Li J, Young VB.** 2014. Antibiotic-induced shifts in the mouse gut microbiome and metabolome increase susceptibility to *Clostridium difficile* infection. Nature communications **5:**3114-3114.

4. **Carter GP, Rood JI, Lyras D.** 2010. The role of toxin A and toxin B in *Clostridium difficile*-associated disease. Gut Microbes **1:**58-64.

5. **Pruitt RN, Chumbler NM, Rutherford SA, Farrow MA, Friedman DB, Spiller B, Lacy DB.** 2012. Structural determinants of *Clostridium difficile* toxin A glucosyltransferase activity. Journal of Biological Chemistry **287:**8013-8020.

6. **Leslie JL, Huang S, Opp JS, Nagy MS, Kobayashi M, Young VB, Spence JR.** 2015. Persistence and Toxin Production by *Clostridium difficile*

within Human Intestinal Organoids Result in Disruption of Epithelial Paracellular Barrier Function. Infection and Immunity **83:**138-145.

7. **Jiang ZD, Ajami NJ, Petrosino JF, Jun G, Hanis CL, Shah M, Hochman L, Ankoma-Sey V, DuPont AW, Wong MC, Alexander A, Ke S, DuPont HL.** 2017. Randomised clinical trial: faecal microbiota transplantation for recurrent *Clostridum difficile* infection - fresh, or frozen, or lyophilised microbiota from a small pool of healthy donors delivered by colonoscopy. Alimentary pharmacology & therapeutics **45:**899-908.

8. **Brandt LJ, Aroniadis OC, Mellow M, Kanatzar A, Kelly C, Park T, Stollman N, Rohlke F, Surawicz C.** 2012. Long-Term Follow-Up of Colonoscopic Fecal Microbiota Transplant for Recurrent *Clostridium difficile* Infection. Am J Gastroenterol **107:**1079-1087.

9. **Dowle C.** 2016. Faecal microbiota transplantation: a review of FMT as an alternative treatment for *Clostridium difficile* infection. Bioscience Horizons: The International Journal of Student Research **9:**hzw007-hzw007.

10. **Kyne L, Warny M, Qamar A, Kelly C.** 2001. Association between antibody response to toxin A and protection against recurrent *Clostridium difficile* diarrhoea. Lancet **357:**189-193.

11. **Wilcox MH, Gerding DN, Poxton IR, Kelly C, Nathan R, Birch T, Cornely OA, Rahav G, Bouza E, Lee C, Jenkin G, Jensen W, Kim Y-S, Yoshida J, Gabryelski L, Pedley A, Eves K, Tipping R, Guris D, Kartsonis N,**

Dorr M-B. 2017. Bezlotoxumab for Prevention of Recurrent *Clostridium difficile* Infection. New England Journal of Medicine **376:**305-317.

12. **Giannasca PJ, Zhang ZX, Lei WD, Boden JA, Giel MA, Monath TP, Thomas WD.** 1999. Serum antitoxin antibodies mediate systemic and mucosal protection from *Clostridium difficile* disease in hamsters. Infection and immunity **67:**527-538.

13. **Perez J, Springthorpe, V. S. & Sattar, S. A. .** 2011. Clospore: a liquid medium for producing high titers of semi-purified spores of *Clostridium difficile*. J. AOAC Int. **94:**618–626

14. **Trindade BC, Theriot CM, Leslie JL, Carlson Jr PE, Bergin IL, Peters-Golden M, Young VB, Aronoff DM.** 2014. *Clostridium difficile*-induced colitis in mice is independent of leukotrienes. Anaerobe **30:**90-98.

15. **Seekatz AM, Theriot CM, Molloy CT, Wozniak KL, Bergin IL, Young VB.** 2015. Fecal Microbiota Transplantation Eliminates *Clostridium difficile* in a Murine Model of Relapsing Disease. Infect Immun **83:**3838-3846.

16. **Kozich JJ, Westcott SL, Baxter NT, Highlander SK, Schloss PD.** 2013. Development of a Dual-Index Sequencing Strategy and Curation Pipeline for Analyzing Amplicon Sequence Data on the MiSeq Illumina Sequencing Platform. Applied and Environmental Microbiology **79:**5112-5120.

17. **Schloss PD, Westcott SL, Ryabin T, Hall JR, Hartmann M, Hollister EB, Lesniewski RA, Oakley BB, Parks DH, Robinson CJ, Sahl JW, Stres B,**

Thallinger GG, Van Horn DJ, Weber CF. 2009. Introducing mothur: Open-Source, Platform-Independent, Community-Supported Software for Describing and Comparing Microbial Communities. Applied and Environmental Microbiology **75:**7537-7541.

18. **Quast C, Pruesse E, Yilmaz P, Gerken J, Schweer T, Yarza P, Peplies J, Glöckner FO.** 2013. The SILVA ribosomal RNA gene database project: improved data processing and web-based tools. Nucleic Acids Research **41:**D590-D596.

19. **Edgar RC, Haas BJ, Clemente JC, Quince C, Knight R.** 2011. UCHIME improves sensitivity and speed of chimera detection. Bioinformatics **27:**2194-2200.

20. **Wang Q, Garrity GM, Tiedje JM, Cole JR.** 2007. Naive Bayesian classifier for rapid assignment of rRNA sequences into the new bacterial taxonomy. Appl Environ Microbiol **73:**5261-5267.

21. **Westcott SL, Schloss PD.** 2017. OptiClust, an Improved Method for Assigning Amplicon-Based Sequence Data to Operational Taxonomic Units. mSphere **2**.

22. **Segata N, Izard J, Waldron L, Gevers D, Miropolsky L, Garrett WS, Huttenhower C.** 2011. Metagenomic biomarker discovery and explanation. Genome Biology **12:**R60.

23. **R Core Team.** 2017. R: A Language and Environment for Statistical Computing. R Foundation for Statistical Computing, Vienna, Austria.

24. **Jari Oksanen FGB, Michael Friendly, Roeland Kindt, Pierre Legendre, Dan McGlinn, Peter R. Minchin, R. B. O'Hara, Gavin L. Simpson, Peter Solymos, M. Henry H. Stevens, Eduard Szoecs and Helene Wagner.** 2017. vegan: Community Ecology Package., R package version 2.4-3. ed, CRAN.

25. **Breiman L.** 2001. Random Forests. Machine Learning **45:**5-32.

26. **Liaw A, Wiener M.** 2002. Classification and regression by randomForest. R news **2:**18-22.

27. **Huang BFF, Boutros PC.** 2016. The parameter sensitivity of random forests. BMC Bioinformatics **17:**331.

28. **Strobl C, Malley J, Tutz G.** 2009. An Introduction to Recursive Partitioning: Rationale, Application and Characteristics of Classification and Regression Trees, Bagging and Random Forests. Psychological methods **14:**323-348.

29. **Bruxelle JF, Mizrahi A, Hoys S, Collignon A, Janoir C, Péchiné S.** 2016. Immunogenic properties of the surface layer precursor of *Clostridium difficile* and vaccination assays in animal models. Anaerobe **37:**78-84.

30. **Ghose C, Eugenis I, Sun X, Edwards AN, McBride SM, Pride DT, Kelly CP, Ho DD.** 2016. Immunogenicity and protective efficacy of recombinant *Clostridium difficile* flagellar protein FliC. Emerging Microbes & Infections **5:**e8.

31. **Lawley TD, Clare S, Walker AW, Stares MD, Connor TR, Raisen C, Goulding D, Rad R, Schreiber F, Brandt C, Deakin LJ, Pickard DJ, Duncan SH, Flint HJ, Clark TG, Parkhill J, Dougan G.** 2012. Targeted restoration of the intestinal microbiota with a simple, defined bacteriotherapy resolves relapsing *Clostridium difficile* disease in mice. PLoS Pathog **8:**e1002995.

32. **Round JL, Mazmanian SK.** 2009. The gut microbiome shapes intestinal immune responses during health and disease. Nature reviews. Immunology **9:**313-323.

33. **Rooks MG, Garrett WS.** 2016. Gut microbiota, metabolites and host immunity. Nat Rev Immunol **16:**341-352.

34. **Theriot CM, Bowman AA, Young VB.** 2016. Antibiotic-Induced Alterations of the Gut Microbiota Alter Secondary Bile Acid Production and Allow for *Clostridium difficile* Spore Germination and Outgrowth in the Large Intestine. mSphere **1**.

35. **Zhang H, Sparks JB, Karyala SV, Settlage R, Luo XM.** 2015. Host adaptive immunity alters gut microbiota. ISME J **9:**770-781.

36. **Kamada N, Sakamoto K, Seo SU, Zeng MY, Kim YG, Cascalho M, Vallance BA, Puente JL, Nunez G.** 2015. Humoral Immunity in the Gut

Selectively Targets Phenotypically Virulent Attaching-and-Effacing Bacteria for Intraluminal Elimination. Cell Host Microbe **17:**617-627.

37. **Kamada N, Kim Y-G, Sham H, Vallance B, Puente J, Martens E, Núñez G.** 2012. Regulated virulence controls the ability of a pathogen to compete with the gut microbiota. Science (New York, N.Y.) **336:**1325-1329.

38. **McDermott AJ, Huffnagle GB.** 2014. The microbiome and regulation of mucosal immunity. Immunology **142:**24-31.

39. **Plovier H, Everard A, Druart C, Depommier C, Van Hul M, Geurts L, Chilloux J, Ottman N, Duparc T, Lichtenstein L, Myridakis A, Delzenne NM, Klievink J, Bhattacharjee A, van der Ark KCH, Aalvink S, Martinez LO, Dumas M-E, Maiter D, Loumaye A, Hermans MP, Thissen J-P, Belzer C, de Vos WM, Cani PD.** 2017. A purified membrane protein from Akkermansia muciniphila or the pasteurized bacterium improves metabolism in obese and diabetic mice. Nat Med **23:**107-113.

40. **Everard A, Belzer C, Geurts L, Ouwerkerk JP, Druart C, Bindels LB, Guiot Y, Derrien M, Muccioli GG, Delzenne NM, de Vos WM, Cani PD.** 2013. Cross-talk between Akkermansia muciniphila and intestinal epithelium controls diet-induced obesity. Proc Natl Acad Sci U S A **110:**9066-9071.

41. **Schubert AM, Sinani H, Schloss PD.** 2015. Antibiotic-Induced Alterations of the Murine Gut Microbiota and Subsequent Effects on Colonization Resistance against *Clostridium difficile*. mBio **6**.

42. **Reeves AE, Theriot CM, Bergin IL, Huffnagle GB, Schloss PD, Young VB.** 2010. The interplay between microbiome dynamics and pathogen dynamics in a murine model of *Clostridium difficile* Infection. Gut microbes **2:**145-158.

43. **Reeves AE, Koenigsknecht MJ, Bergin IL, Young VB.** 2012. Suppression of *Clostridium difficile* in the gastrointestinal tracts of germfree mice inoculated with a murine isolate from the family Lachnospiraceae. Infection and immunity **80:**3786-3794.

44. **Stappenbeck TS, Virgin HW.** 2016. Accounting for reciprocal host–microbiome interactions in experimental science. Nature **534:**191-199.

CHAPTER IV

HUMAN INTESTINAL ORGANOIDS A NOVEL MODEL TO STUDY *C. DIFFICILE* – HUMAN EPITHELIUM INTERACTIONS

The contents of this chapter have been published as:

Leslie JL* Huang S*, Opp JS, Nagy MS, Kobayashi M, Young VB, Spence JR (2015). Persistence and toxin production by *Clostridium difficile* within human intestinal organoids result in disruption of epithelial paracellular barrier function. *Infect. Immun.* 83(1): 137-145
* Equal contribution

Summary

Clostridium difficile is the leading cause of infectious nosocomial diarrhea. The pathogenesis of *C. difficile* infection (CDI) results from the interactions between the pathogen, the intestinal epithelium, host immune system and the gastrointestinal microbiota. Previous studies of the host- pathogen interaction in CDI have utilized either simple cell monolayers or in vivo models. While much has been learned utilizing these approaches, little is known about the direct interaction of the bacterium with a complex host epithelium. Here, we asked if human intestinal organoids (HIOs), which are derived from pluripotent stem cells and demonstrate small intestinal morphology and physiology, could be used to study the pathogenesis of the obligate anaerobe *C. difficile*. Vegetative *C. difficile,* microinjected into the lumen of HIOs, persisted in a viable state for up to twelve hours. Upon colonization with *C. difficile* VPI 10463 the HIO epithelium is

markedly disrupted, resulting in loss of paracellular barrier function. Since similar effects were not observed when HIOs were colonized with the nontoxigenic *C. difficile* strain F200, we directly tested the role of toxin using TcdA and TcdB purified from VPI 10463. We show that injection of TcdA replicates the disruption of the epithelial barrier function and structure observed in HIOs colonized with the viable *C. difficile.*

Introduction

Clostridium difficile is an anaerobic, spore-forming bacterium that is the leading cause of infectious nosocomial diarrhea and is responsible for over 14,000 deaths annually (1). Human exposure to *C. difficile* results in a range of manifestations, from asymptomatic colonization, to diarrhea, to lethal toxic megacolon. Various models have been used to study *C. difficile* infection (CDI), including in vitro models using transformed cell lines and a variety of *in vivo* models (2-5). *In vitro* cell culture models are limited in their ability to recapitulate complexities of the human gastrointestinal tract, and detailed, real-time study of the mucosal epithelium during infection in an animal model is technically challenging.

Human intestinal organoids (HIOs) are three-dimensional spheroids of human epithelium generated through directed differentiation of human pluripotent stem cells (hPSCs), which include human embryonic stem cells (hESCs) and induced pluripotent stem cells (iPSCs). HIOs contain both mesenchymal and epithelial tissues that are structurally arranged around a central luminal cavity.

The epithelial compartment of the HIO possesses an array of small intestinal cell types, including absorptive enterocytes and secretory Paneth, goblet and enteroendocrine cells, in addition to Lgr5+ intestinal stem cells (6). HIOs have been used to model features of embryonic development, viral infection and inflammatory bowel disease(7-9). Due to their similarity to the human gastrointestinal tract, HIOs serve as a tractable and physiologically relevant model of the human intestine.

We sought to use HIOs to study the interaction between *C. difficile* and a complex human epithelium. We developed a real-time functional assay to demonstrate that HIOs have a robust and effective epithelial barrier, which limits paracellular diffusion. In addition, we developed microinjection techniques to introduce *C. difficile* into the lumen of HIOs and found that viable *C. difficile* persists within the HIOs. Colonization of HIOs with *C. difficile* strain VPI 10463 results in disruption of the organoid epithelium. These effects were apparently dependent on the primary virulence factors of *C. difficile,* the toxins TcdA and TcdB (10) since colonization with a nontoxigenic *C. difficile* strain did not disrupt the HIO epithelium while microinjection of purified TcdA recapitulated the effects mediated by toxigenic VPI 10463. These results demonstrate that HIOs can be used for detailed molecular and cellular investigation of the pathogenic interactions between *C. difficile* and human intestinal epithelium.

Experimental Procedures

Manuscript

All authors had access to the study data and reviewed and approved the final manuscript.

Human intestinal organoid growth/propagation

3-D human intestinal organoids (HIOs) were generated by directed differentiation of human pluripotent stem cells (hPSCs) as previously described (6, 9, 11). HIOs were generated from the H9 hESC line (WA09, NIH registry # 0062) and all hESC work described was approved by the University of Michigan human pluripotent stem cell oversight committee (hPSCRO). Briefly, hESCs were differentiated into endoderm using 100ng/mL ActivinA for three days, and then further differentiated into CDX2+ intestinal tissue using 2μM Chir99021 (Stemgent cat# 04-0004-10)+ 500ng/mL FGF4 for four to six days. The FGF4 used to differentiate the intestinal tissue was either obtained from R&D Systems (cat# 235-F4) or purified in the lab as previously described (12). During intestinal specification, 3D spheroids emerged in the culture dish. Spheroids were collected and embedded in Matrigel (BD Bioscience cat# 354234) and expanded for 30-60 days in Intestinal Growth Media (IGM) containing Dulbecco's modified Eagle medium (DMEM)-F12 medium (12634-010; Gibco by Life Technologies) supplemented with L-glutamine, 15mM HEPES, B27 supplement (Gibco by Life Technologies cat# 17504-044), penicillin/streptomycin and growth

factors containing 100 ng/ml Noggin (R&D Systems cat# 6057-NG), 100ng/ml EGF (R&D Systems cat#236-EG) and 5% R-Spondin2 conditioned media (13). The media was replaced every 4 days. One- to two-month-old cystic HIOs that were > 1mm in diameter were used for experiments.

Clostridium difficile isolates

Two strains of *C. difficile* were used in this study, strain VPI 10463 (ATCC 43255) a toxigenic strain, which produces both TcdA and TcdB and a nontoxigenic clinical isolate F200, described previously (4).

Growth of *Clostridium difficile in vitro*

For all experiments, both strains were grown in a vinyl anaerobic chamber (Coy Laboratory Products) at 37°C in brain- heart infusion (BHI) broth plus 100 mg liter^{-1} L-cysteine. For all microinjection experiments, overnight cultures were back-diluted 1:10 and grown for three hours at 37°C. For strain VPI 10463, after three hours the culture was further diluted to a starting OD_{600} of 0.01. F200 did not grow well following a second dilution, so the initial 1:10 back dilution was used to start the growth curve for the injections. The OD_{600} of the cultures was measured in the anaerobic chamber using a hand held spectrophotometer (Biochrom WPA CO8000 cell density meter, cat# 80-3000-45). After six hours of growth from a starting OD of 0.01 the mean OD_{600} of VPI 10463 used to colonize the HIOs was 0.5. After nine hours from the first 1:10 dilution the mean OD_{600} for F200 used to colonize the HIOs was 0.67. To prepare bacterial

supernatants, the cultures described above of either strain VPI 10463 or F200 were passed through 0.22μm filter to remove the bacterial cells and then FD4 was added to a final concentration 1mM.

Microinjection of HIOs

HIOs were gently removed from the Matrigel in which they were grown by cutting around each HIO using a 30-gauge needle. A cut 1000 microliter pipette tip with a large bore that did not mechanically disrupt the HIO was used to remove released HIOs from the well and to transfer them to a petri dish. HIOs were dividend into experimental groups, and each group of HIOs was re-embedded into fresh Matrigel in wells of a 24-well tissue culture plate. Thin wall glass capillaries (World precision Instruments cat# TW100F-4) were pulled using a Narishige PN-30 micropipette puller. The tips of the glass capillaries were cut with a scalpel and the capillaries were passed into an anaerobic chamber. In the anaerobic chamber, the capillaries were filled with either *C. difficile*+FD4 or filtered supernatant+FD4 using Eppendorf microloader tips (Eppendorf, cat# 5242956003). The filled capillaries were then passed out of the chamber and loaded on to the microinjector (Sutter Instrument Company, XenoWorks Analog Microinjector cat# BRI). FD4 was used in all microinjection experiments to aid in visualizing the injections. Even under ambient lighting, the green of the FD4 was sufficient for us to ascertain if each injection was successful. For example, if a HIO displayed a noticeable outflow of green (FD4) immediately following injection, it was excluded from the experiment. Once all the

HIOs were injected, the wells were washed twice with DMEM/F12 media (Gibco by Life Technologies, cat# 1263-028). Following the washes, 500µL of IGM with growth factors was added to each well and the HIOs were imaged using a fluorescent stereomicroscope (Olympus SZX16) at 1x magnification. The HIOs were incubated at 37°C in a 5% CO2 humidified incubator. Images were taken at indicated time points post injection. Disruption of barrier integrity was visualized by the loss of the FD4 in the lumen of the HIOs.

Clostridium difficile quantitation from HIOs

For these experiments *C. difficile* was grown and individual HIOs were injected as described above. At 0, 2, and 12 hours post injection each HIO was removed with a 1000µL genomic tip (Art by Molecular BioProducts, cat# 2079G) and transferred into a sterile 1.7 mL eppendorff tube. The tube was immediately passed into an anaerobic chamber. In the chamber, 500µL of anaerobic 1X PBS (Gibco by Life Science, cat# 10010-023) was added to each tube and the HIO was disrupted using a 1000µL tip. This HIO/PBS mixture was used for subsequent dilutions. To determine the level of vegetative *C. difficile*, samples were plated on BHI plus 100 mg liter^{-1} L-cysteine. Plates were incubated in the anaerobic chamber for 24 hours a 37°C at which point colonies were counted.

Vero cell cytotoxicity assay

The activity of the toxins used in the barrier function assay was determined using a cell rounding based cytotoxicity assay.African green monkey

kidney (Vero) cells (ATCC CCL-81) were grown to a confluent monolayer in T-75 Flasks in DMEM (Gibco by Life Technologies cat #11965), supplemented with 10% heat inactivated fetal bovine serum (Gibco by Life Technologies cat #16140) and 1% penicillin-streptomycin (Gibco by Life Technologies cat #15140). To remove the cells from the flask, they were washed with 1X PBS followed by treatment with 1mL of 0.25% trypsin. The trypsin was inactivated by the addition of 10mL of the supplemented DMEM. The cells were then transferred to a conical tube and spun at 1000 rpm for 5 minutes to pellet the cells. For this assay, 1x105 cells in 90µL of DMEM were seeded in each well of a 96-well plate (Corning cat# 3596) and incubated for 4 hours. Filtered culture supernatant or purified TcdA or TcdB were serially diluted 1:10 in 1X PBS. As a control, the diluted sample was then added to an equal volume of either a 1:25 dilution of anti-toxin sera (TechLab, cat# T5000) or PBS and incubated at room temperature for one hour. Following the incubation, 10µL of the sample was added to the Vero cells and the plate was incubated overnight at 37°C in a 5% humidified incubator. The next day plates were viewed at 10x magnification for cell rounding. The cytotoxic titer was defined as the reciprocal of the highest dilution that produced rounding in 80% of the cells.

Injection of purified toxins

HIOs were prepared and injected as described above. For these experiments purified *C. difficile* toxin A (TcdA) or B (TcdB) from strain VPI 10463 were purchased (List Biological Laboratories cat# 152C or#155D), reconstituted

at a concentration of 1µg/µL, aliquoted and stored a -80°C. Due to lot-to-lot variation, each new lot was tested for activity using the Vero cell cytotoxicity assay. Each HIO was injected with approximately 2µL of either 12.8ng/µL TcdA or 25.6ng/µL TcdB with 1mM FD4. For each experiment, new aliquot of toxin was thawed and used.

Determining pixel intensity of FD4 in injected HIOs

To determine pixel intensity of the HIOs ImageJ software was used (14). For each well of HIOs a brightfield and fluorescent image was taken. These two images of the same well were used to determine pixel intensity. First the fluorescent image of the well was opened in ImageJ and converted to 16 bit gray scale. Then the brightfield image of the same well was opened in ImageJ and synchronized to the gray scale image. Using the brightfield image, the perimeter of the HIO in the well was outlined manually and this region was used to determine the mean gray value of the HIO in the fluorescent image. These steps were repeated for each HIO in the well for all treatments. The percent pixel intensity is defined as the mean gray value of an HIO at a given time point divided by the mean gray value of that same HIO at T=0 multiplied by 100.

Basolateral barrier function assay

Intact HIOs were placed into wells of a 24 well dish containing 500µL IGM with growth factors. Purified *C. difficile* TcdA or TcdB were diluted in IGM. The HIOs were incubated in a well containing 400ng/mL of either TcdA or TcdB for

two hours at 37°C. After two hours, the HIOs were exposed to 0.1mM FD4 for an additional one-hour at 37°C. Negative and positive control HIOs were processed in the same manner as toxin-treated HIOs. For positive controls, 2mM EGTA was added with the FD4 in the final hour of incubation. Following the incubation, HIOs were washed for five to ten minutes with 1X PBS to remove excess FD4. Following the wash, HIOs were imaged using a fluorescent stereomicroscope (Olympus SZX16). Disruption of barrier integrity was visualized by the presence of the FD4 in the lumen of the HIOs.

Immunofluorescence staining and confocal microscopy

HIOs collected from the barrier function assays were fixed in 4% paraformaldehyde (PFA) at room temperature for 15-30 minutes, washed 3 times with PBS. HIOs were placed in optimal cutting temperature (O.C.T) compound (Sakura, cat# 4583) for 20 minutes, and then placed at -80°C to freeze. Frozen sections were cut at 10< µm for immunostaining followed by confocal microscopy. Immunostaining was carried out as previously described (6). Antibody information and dilutions can be found in Table 4.1. All immunofluorescence images were taken on a Nikon A1 confocal microscope.

Induction of apoptosis with TNFα and IFNγ

To induce apoptosis, as detected by cleaved caspase 3, HIOs were incubated in 1000 ng/mL of TNF (PeproTech cat# AF-300-01A or R&D Systems cat# 210-TA-010 note: cytokines from either company were efficient in this

assay) plus 1000 ng/mL of IFNγ (PeproTech cat# AF-300-02) for 24 hours. HIOs with disrupted barrier function were fixed, embedded, and sectioned as described.

Image Processing and Manipulation

Minimal image processing was used. Image manipulation was limited to uniform changes of brightness and/or contrast and to the use of a digital zoom in the inset of Figure 4. 3 B.

Statistical Analysis: Statistical analysis was performed using Prism 6 GraphPad software. The Mann-Whitney test was used to compare each group to the control. Statistical significance was set at a *P* value of <0.05.

Table 4.1: Antibodies Used in Chapter Four

Primary Antibodies	**Vendor & Catalog #**	**Application & dilution**
Mouse anti-ZO1	Life Technologies #33-9100	WB: 1:250 IF: 1:100
Rabbit anti-Occludin	Life Technologies #71-1500	WB: 1:1,000 IF: 1:250
Mouse anti-E-Cadherin	BD Biosciences #610651	WB: 1:10,000 IF: 1:500
Mouse anti-Actin	ABcam #ab11003	WB: 500
Mouse anti-Acetylated Tubulin	Sigma-Aldrich #T7451	IF: 1:1,000
Alexa Fluor 546 phalloidin	Life Technologies #A22283	IF: 1:100
Rabbit anti-Cleaved Caspase-3 (Asp175)	Cell Signaling #9664	IF: 1:500
Secondary Antibodies	**Vendor & Cat#**	**Application & dilution**
Donkey Anti-Mouse IgG-Cy3	Jackson ImmunoResearch Lab #715-165-150	IF: 1:1,000
Donkey Anti-Rabbit IgG-Alexa Fluor 488	Jackson ImmunoResearch Lab #711-545-152	IF: 1:1,000
Donkey anti-Mouse IgG-Alexa Fluor 647	Jackson ImmunoResearch Lab #715-605-150	IF: 1:1,000

Results

HIOs have a functional epithelium with an intact paracellular barrier. Beyond nutrient absorption, a key function of the gastrointestinal epithelium is as a barrier that prevents free passage of antigens from the lumen of the gastrointestinal tract to the rest of the body (15). To assess if HIOs possess a functional epithelial barrier we microinjected fluorescein isothiocyanate (FITC)-dextran with average molecular weight of 4KDa (FD4) into the lumen of HIOs and monitored fluorescence over the course of eighteen hours. FD4 is used to examine permeability of the epithelial paracellular barrier in a variety of *in vitro* polarized monolayers and in vivo assays (16, 17). In this assay, an intact barrier confines the FD4 in the HIO lumen maintaining green fluorescence while loss of paracellular barrier integrity results in measureable loss of fluorescence due to the diffusion of FD4 out of the lumen. We observed that FD4-injected HIOs maintained fluorescence over the course of eighteen hours (n=5) (figure 4.1 A).

To quantitate barrier function over time, we measured the fluorescence of each HIO throughout the assay and compared the fluorescence at each time point to the initial fluorescence at time zero (T=0). The fluorescence of each HIO was defined as the pixel intensity per HIO, normalized to the area of each HIO (pixel intensity/area). Eighteen hours following injection of FD4, HIOs maintained a median of 58.8% of the fluorescence observed at T=0. As a control, we added ethylene glycol tetraacetic acid (EGTA, 2mM), a calcium chelator known to disrupt tight junctions and adherens junctions to the culture media twelve hours

after injecting HIOs (n=5) with FD4. HIOs in the EGTA treatment group maintained a median of 90.4% of the fluorescence at twelve hours post FD4 injection. However, the addition of EGTA at this point resulted in a rapid loss of fluorescence such that the median fluorescence of the HIOs at T=18 was 18.3% of the intensity at T=0 (figure 4.1 B). By the conclusion of the experiment at eighteen hours post FD4 injection there was a statistically significant loss of pixel intensity in the EGTA treated HIOs compared to control HIOs. These results strongly support the notion that HIOs have a robust paracellular epithelial barrier that can be disrupted by chemical means, and also demonstrate that FD4 can be used to measure paracellular barrier function over time.

To confirm these results, we also performed a second “outside-in” barrier function experiment (figure 4.2 A). In this experiment, we added FD4 to the tissue culture media and reasoned that if the paracellular barrier were disrupted, leak would occur from the basal-to-apical (luminal) direction in addition to apical-to-basal leak demonstrated in figure 4.1. Indeed, when controls HIOs (n=10) were incubated in FD4, an intact barrier did not permit FD4 to diffuse into the HIO lumen. In contrast, when EGTA was added to the media, 100% of HIOs had a disrupted epithelial barrier, and FD4 was observed in the lumen after one hour (n=12 individual HIOs) (figure 4.2 B). These results indicate that HIOs have a robust paracellular barrier that restricts movement across the epithelium in both the luminal/basolateral and basolateral/luminal direction.

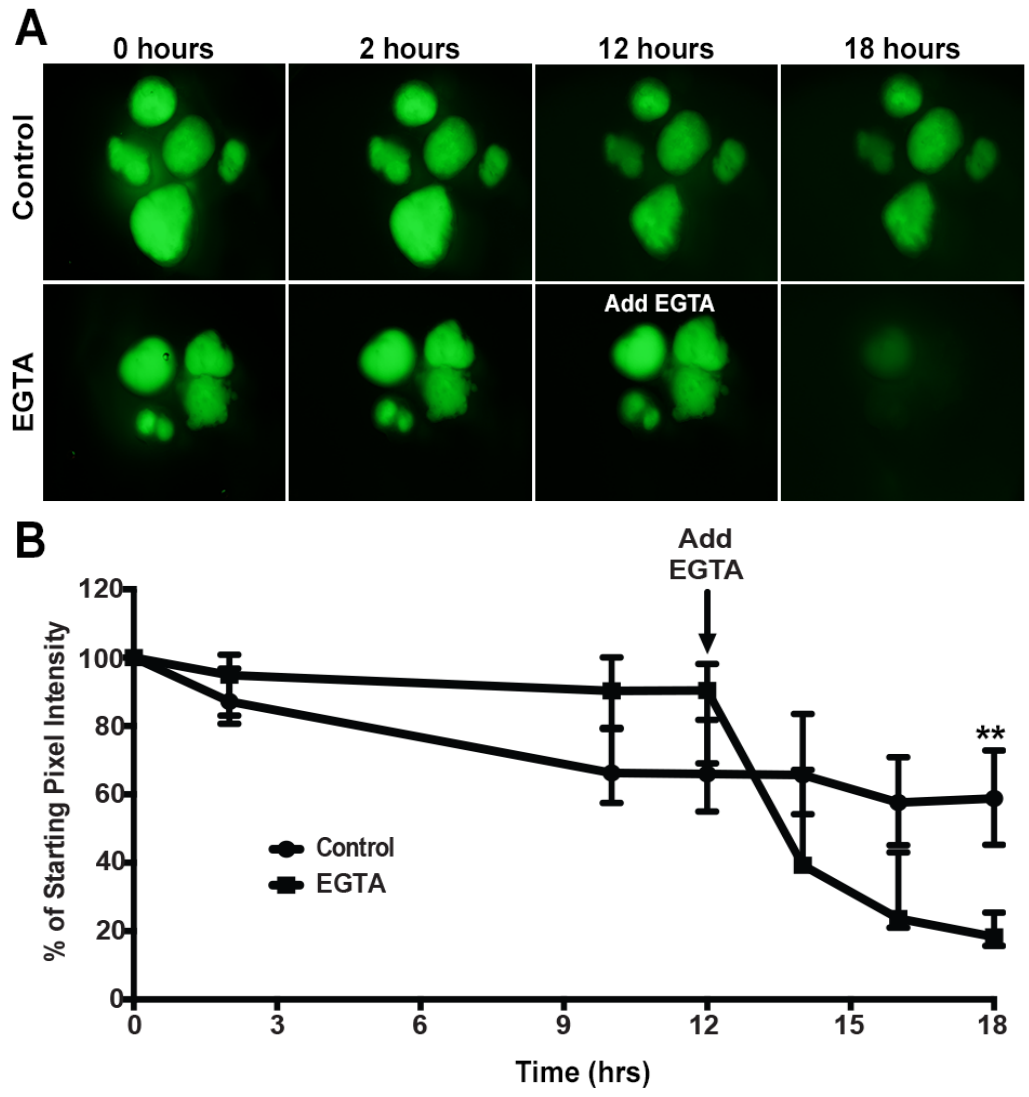

Figure 4.1 Assessment of HIO epithelial barrier function.
A. Representative images of FD4 dynamics in HIOs following injection. HIOs (n=5 per treatment) were injected with FD4 and imaged at 0,2, 10, 12, 14, 16, and 18 hours post injection. HIOs retained the majority of injected FD4 within the lumen over 18 hours. The addition of EGTA to the media 12 hours after injection resulted in rapid loss of FD4 from the lumen indicating loss of epithelial paracellular barrier function. Images represent the results from at least three independent experiments.
B. Quantitation of barrier disruption by determination of the fraction of initial FD4 fluorescence retained or lost over time. Points represent the median and bars represent the interquartile range. Eighteen hours after injection control HIOs retained significantly more FD4 than the EGTA treated HIOs (p=0.0079, Mann-Whitney test).

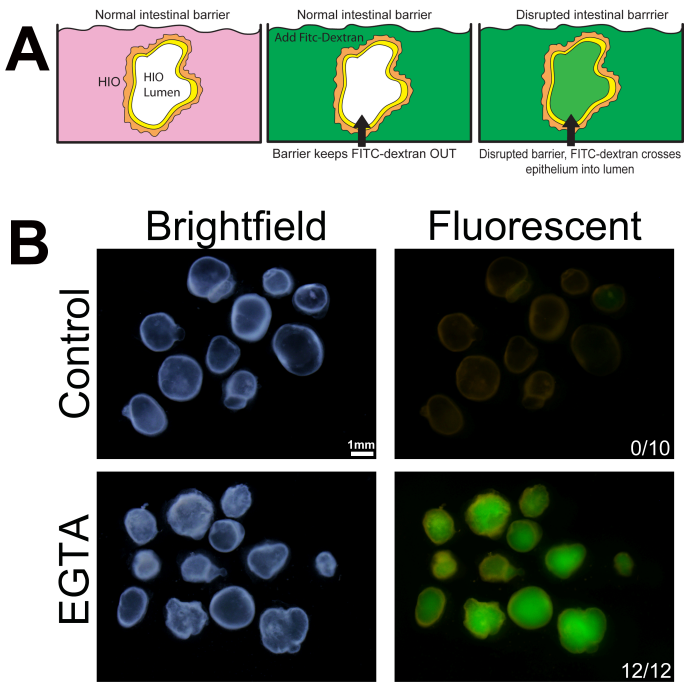

Figure 4.2. "Outside-in" barrier function experiment
To confirm that HIOs had a paracellular barrier function, FD4 was added to the media outside of the HIOs.
A. Schematic of the barrier function assay. Following treatment, FD4 is added to the media containing the HIOs. HIOs with intact epithelium prevent the diffusion of FD4 into the lumen where as those with a disrupted epithelium cannot exclude FD4.
B. Brightfield images indicate the location of the HIOs. Untreated HIOs exclude FD4; EGTA HIOs treated lose barrier function and appear green

Viable *C. difficile* persists in the lumen of HIOs and damages the epithelium.

To investigate the interaction between *C. difficile* and human epithelium we microinjected *C. difficile* strain VPI 10463 into the lumen of HIOs. To assess the viability of vegetative *C. difficile* in HIOs, injected organoids were mechanically disrupted and cultured under anaerobic conditions. Immediately following the injection (T=0), the mean vegetative colony forming units per HIO (CFU/HIO) was $2x10^4$ (figure 4.3 A). By T=2 hours post injection the mean CFUs/HIO had decreased, as some of the initial inoculum died. Twelve hours post injection the mean CFU/HIO was $1x10^2$ suggesting that viable, vegetative *C. difficile* was able to persist within the HIOs for at least twelve hours.

Histopathologic examination of HIOs twelve hours post injection revealed the epithelium was markedly disrupted with sloughing of cells with pyknotic nuclei into the lumen (figure 4.3 B). In addition, there were numerous rod shaped bacteria in the lumen with what appear to be sub-terminal bacterial spores.

Epithelial damage is the hallmark of *C. difficile* infection in the intestine and this is mediated by the virulence factors toxin A and B (TcdA and TcdB). To investigate if the epithelial damage observed in HIOs colonized with VPI 10463 was due to toxin, we microinjected a nontoxigenic *C. difficile* strain (F200). As with VPI 10463, viable F200 persisted within the HIO for 12 hours. However, the epithelium of HIOs colonized with F200 appeared intact (figure 4.3 C).

These results suggest that the VPI 10463 produces toxin in the HIO lumen. However, it is known that *C. difficile* can produce and release toxin into

the culture media during in vitro growth. Using the barrier function assay as readout of epithelial damage, we determined if the toxigenic strain VPI 10463 was producing toxin within the HIO. HIOs injected with VPI 10463 lost barrier integrity by twelve hours post injection, resulting 22% of the starting fluorescence (figure 4. 4 A, B). Importantly, barrier function was maintained in HIOs injected with the nontoxigenic F200 isolate of *C. difficile.* Similar to our previous observations (figure 4.1), twelve hours after the injection, the control HIOs (n=5) maintained barrier integrity as visualized by the presence of green fluorescence, retaining 66% of the initial fluorescence. As a control for the release toxins into culture supernatant during in vitro growth, HIOs were injected with a volume of filter sterilized bacterial culture supernatant equal to that used for injection of intact bacteria. Filtered supernatant from VPI 10463 or F200 culture media had no effect on HIO barrier function (figure 4. 4 A, B). We did, however measure detectable cytotoxicity in VPI 10463 supernatant using an *in vitro* Vero cell cytotoxicity assay, suggesting that this strain released toxin into the supernatant, but that quantities were not sufficient to disrupt barrier function within the twelve-hour time frame of our assay (figure 4.5). These results suggest that viable *C. difficile* persists within the lumen of HIOs and that the epithelial damage associated with VPI 10463 is due to the *in situ* production of toxin.

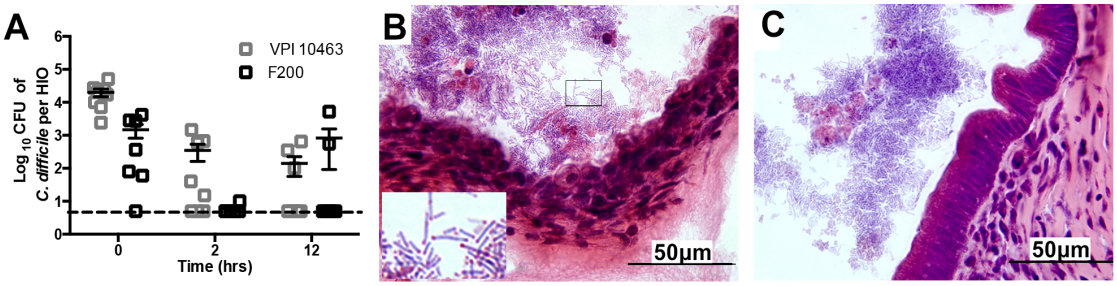

Figure 4.3. Vegetative *C. difficile* persists in the HIO lumen.
A. HIOs injected with either *C. difficile* strain VPI 10463 or F200 were collected at 0, 2, and 12 h post injection and plated on BHI with cysteine to quantitate the number of vegetative CFU per HIO. *C. difficile* was able to persist in the lumen of HIOs for 12 h. Points on the graph represent individual HIOs, and the dashed line represents the limit of detection. Bars indicate the means and SEM.
B. Twelve hours after colonization, HIOs injected with *C. difficile* were fixed and stained using hematoxylin and eosin. The epithelium of the HIO colonized with strain VPI 10463 is severely disrupted, and large rods with what appear to be subterminal spores are visible (inset) within the HIO (inset is a 3.25× digital zoom of the boxed region).
C. An HIO colonized with the nontoxigenic strain F200 has an intact epithelium despite the presence of large rod-shaped bacteria in the lumen of the HIO.

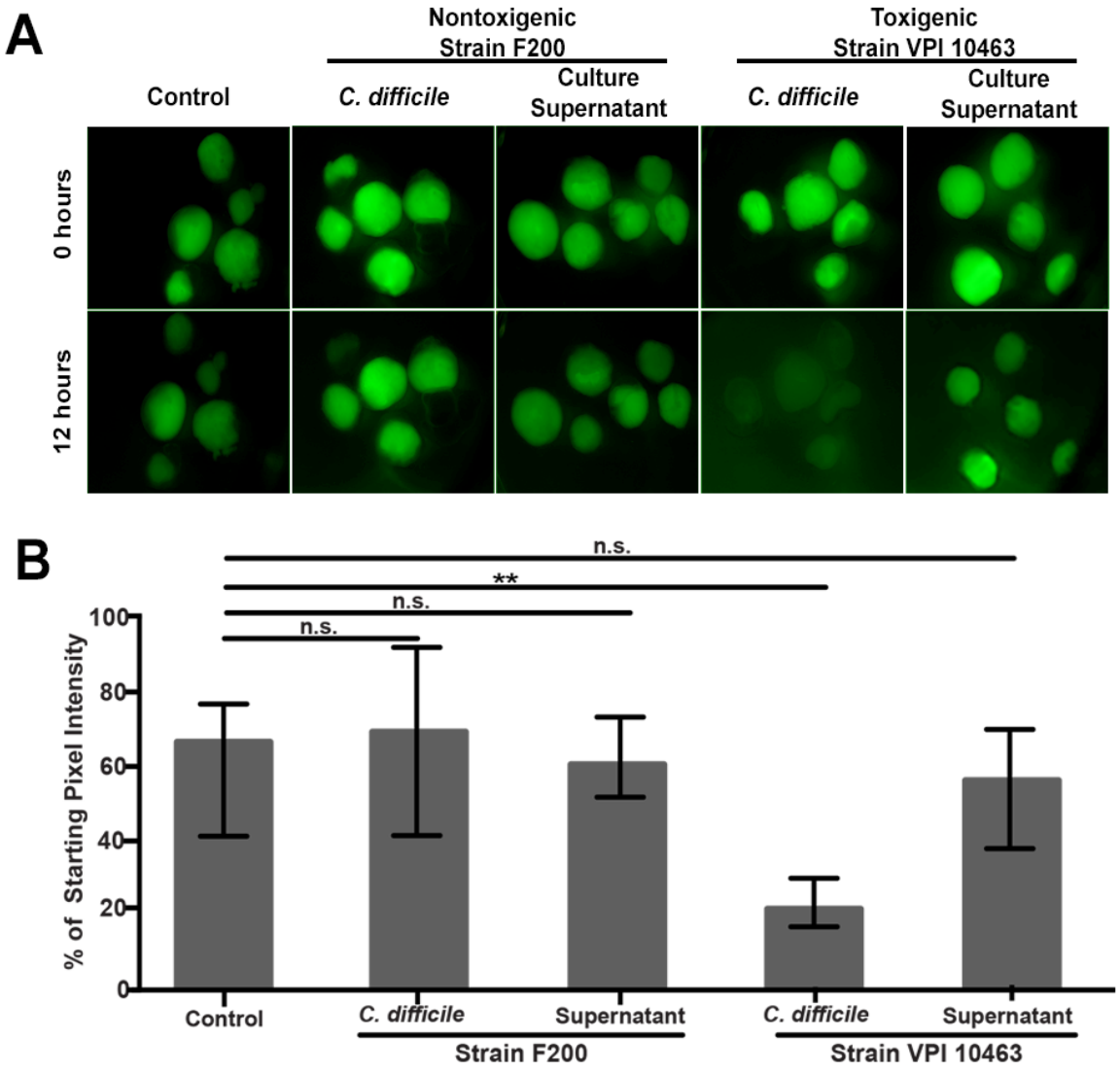

Figure 4.4. Injection of toxigenic but not nontoxigenic *C. difficile* results in loss of HIO barrier function.

A. HIOs were injected with FD4 alone (control) (*n* = 5), a nontoxigenic strain (F200) of *C. difficile* (*n* = 5), filtered culture supernatant from that strain (*n*= 6), a toxigenic *C. difficile* strain (VPI 10463) (*n* = 5), or filtered culture supernatant from the toxigenic strain (*n* = 5). Only VPI 10463-injected HIOs lost barrier function. Images are representative of three independent experiments using 5 to 6 HIOs per group.

B. Quantification of epithelial barrier disruption by measuring retention of injected FD4 after 12 h. Bars represent the medians and the interquartile ranges. Only the HIOs colonized with the toxigenic strain (VPI 10463) lost a significantly greater amount of FD4 from the lumen, indicating significant epithelial damage (*P* = 0.0079 by Mann-Whitney test).

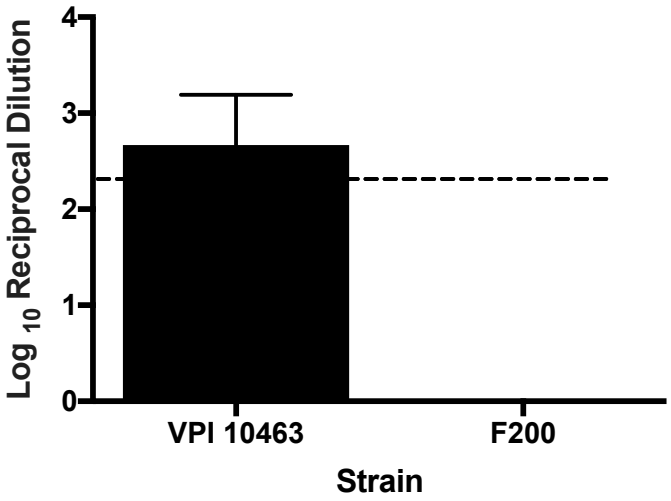

Figure 4.5. Toxin activity of filtered supernatants
C. difficile culture supernatant was filtered to remove the bacteria and toxin activity was assessed using a Vero cell cytotoxicity assay. The culture filtrate from strain VPI 10463 had detectable cytotoxicity (black bar), however this level was not sufficient to disrupt HIO barrier function when injected into HIOs. Strain F200 (the nontoxigenic strain) had no cytotoxicity. The plot is of the mean with the SD of two independent experiments. Dashed line is the LOD of 2.3.

Purified *C. difficile* toxins disrupt HIO paracellular barrier function.

Epithelial damage and loss of barrier function in HIOs injected with *C. difficile* was dependent on the ability of the strain to produce toxin. Since F200 is a naturally occurring nontoxigenic strain and not an isogenic mutant of VPI 10463, we directly determined the effect of TcdA or TcdB purified from VPI10463 on HIO barrier function. FD4 was combined with purified TcdA or TcdB and the mixture was injected into the lumen of HIOs. Compared to controls in which 100% of HIOs (n=5) retained barrier function, TcdA had a strong effect that resulted in a loss of barrier function in 100% of HIOs (n=5) while TcdB had a less potent effect on the HIOs and did not appear to robustly disrupt the epithelial barrier (n=5) (figure 4.6 A). Importantly, at the same concentration, TcdA and TcdB had similar cytotoxicity on Vero cells in vitro (figure 4.7). When we quantitated the relative fluorescence over time, HIOs injected with TcdA lost a greater amount of fluorescence compared to HIOs injected with either TcdB or FD4 alone (figure 4.6 B).

C. difficile toxins are known to inactivate the Rho family GTPases, leading to the disruption of cytoskeleton and cellular junctions. To determine if these effects were seen in the epithelium of HIOs treated with *C. difficile* toxins, we examined several junctional and cytoskeletal proteins. These include proteins of the adherens junctions (AJs) and tight junctions (TJs), which are crucial for the maintenance of epithelial barrier function (18). In controls, E-cadherin, a cellular transmembrane AJ protein, is localized to the basolateral surfaces of epithelial cells and is absent from the apical surface (figure 4.8 A, top panel). In HIOs

injected with TcdA, E-cadherin is redistributed and can be seen on the apical surface of the epithelium where as in HIOs injected with TcdB, E-cadherin localization does not appear to be different from controls (Figure 5A,middle and bottom panels). In addition to E-cadherin, we also examined cellular localization of Zonula occludens protein 1 (ZO-1) and Occludin (OCLN), both components of cellular TJs. In control HIOs, ZO-1 is present at the TJ near the apical surface of the epithelium, whereas OCLN is seen at the TJ and along the lateral surface of the cell (figure 4.8 B, top panel). Similar to what was observed with E-cadherin, TcdA treated HIOs had dramatic redistributed of tight junction proteins where as TcdB treated HIOs were not different from controls (figure 4.8 B, middle and bottom panels). Reports by others have demonstrated that OCLN is internalized via endocytosis upon disruption of the TJ, and can be visualized in endocytic vesicles. We did not observe obvious enodcytic vesicles containing OCLN, however, this is likely due to differences in tissue processing conditions that are required to visualize vesicles (19). Lastly, we used Phalloidin staining to assess the organization of F-actin, and acetylated alpha tubulin (AcTub) immunofluorescence to visualize stabilized microtubules within the cell (figure 4. 8 C). In controls, F-actin was strongly localized to the apical surface of the epithelium and weak staining was seen along the lateral and basal surface of the epithelium (figure 4.8 C top panel). Similarly, AcTub staining was strongest on the apical side of the cell, but was also weakly present throughout the cell and on the basal surface (figure 4.8 C, top panel). Compared to FD4 injected controls, HIOs treated with TcdA had a marked reduction of F-actin with areas where

staining was undetectable. In addition, HIOs treated with TcdA displayed a severe disruption of AcTub at the apical border of the epithelial cells (figure 4.8, middle panel), consistent with previous reports (20). In contrast, TcdB treated HIOs showed F-actin distribution and apical AcTub staining that was similar to controls, whereas AcTub immunofluorescence on the basal side of the cells appeared to be disrupted, indicating that TcdB had a mild effect on the basal side of the HIO epithelium (figure 4.8 C, bottom panel). In conclusion, examination of the cellular effects of purified *C. difficile* toxin on HIO epithelium demonstrated that this model recapitulates the hallmark effects of toxin host epithelium.

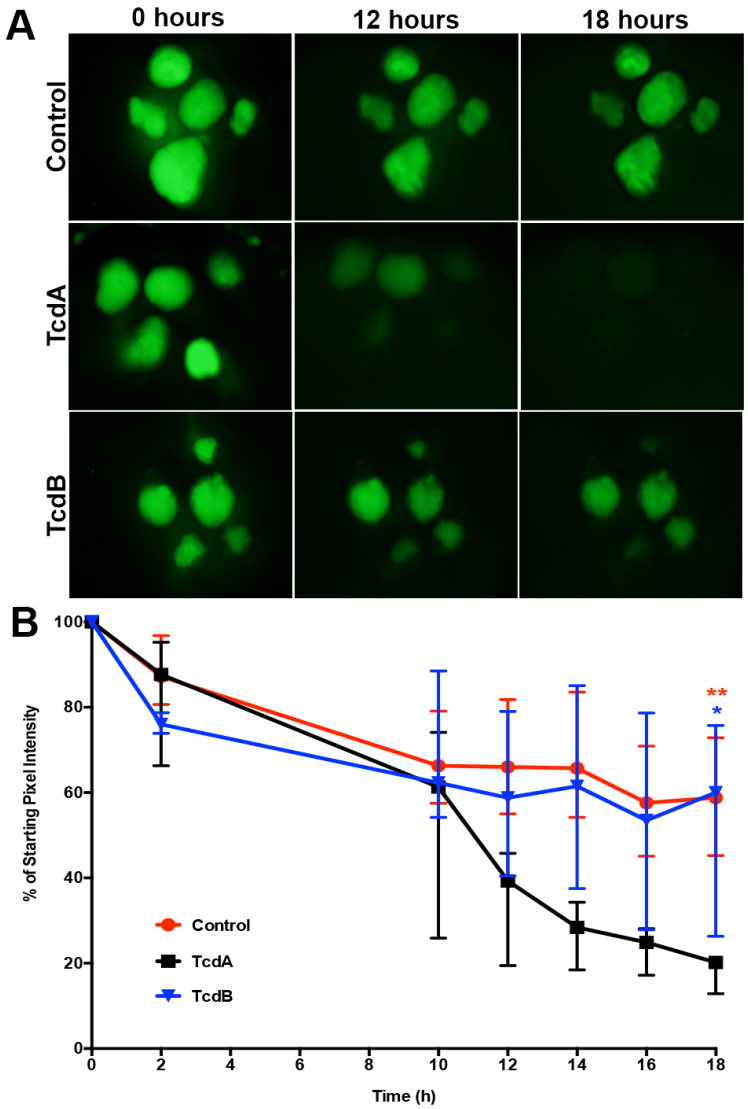

Figure 4.6 Purified TcdA and TcdB injected into the lumen of HIOs disrupt paracellular barrier function.

A. Representative images of FD4 leakage from the lumen of HIOs treated with C. difficile toxin. HIOs (n = 5 per treatment) were injected with FD4 alone (top), with purified TcdA (middle), or with TcdB (bottom). In this system, TcdA is more potent than TcdB. Images are representative of at least three independent experiments using 5 to 6 HIOs per group.

B. Quantitation of fluorescence of each HIO relative to time zero. Injection of purified TcdA into HIOs causes significantly greater loss of paracellular barrier function than injection with either TcdB (blue asterisk, P = 0.0159) or FD4 alone (red asterisks, P = 0.0079). Points represent the median percentages, and bars represent the interquartile ranges. The data were analyzed using the Mann-Whitney test. Control data presented in panels A and B are the same as those used in figure 4.1, as these assays were preformed at the same time.

.

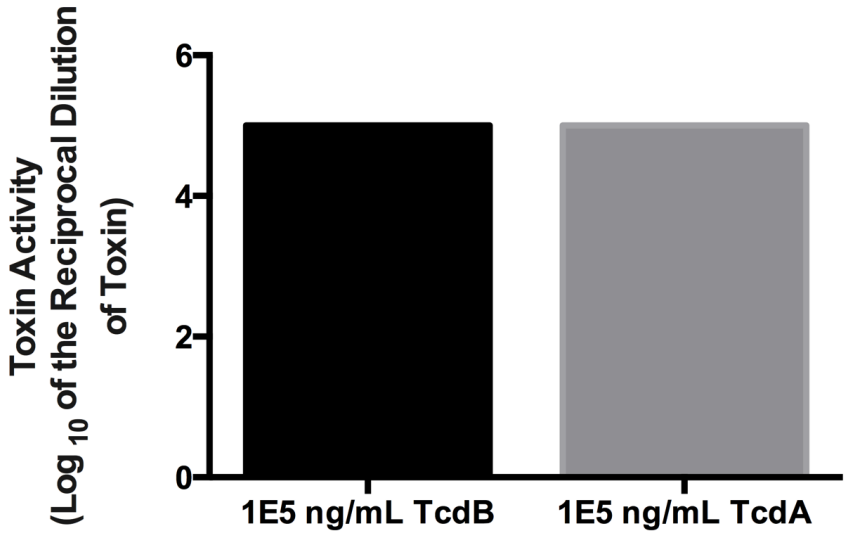

Figure 4.7. Toxin activity of purified TcdA and TcdB used in injections. Purified toxin was tested in cell cytotoxicity assay. At the same concentration, TcdB and TcdA had similar activity on Vero cells

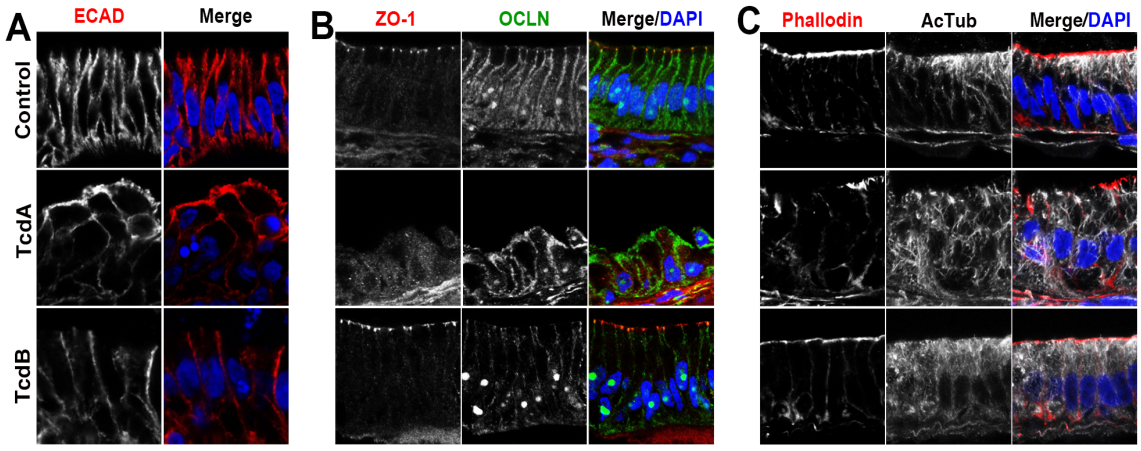

Figure 4.8. Cellular effects of injection of HIOs with TcdA or TcdB
HIOs were injected with FD4 alone (control), TcdA, or TcdB and monitored for disruption of barrier function. At 18 h postinjection, the HIOs were fixed and stained.
A. The normal basolateral distribution of the adherens junction protein E-cadherin (ECAD) is disrupted following injection of TcdA. In these HIOs, ECAD is redistributed and can be seen on the apical surface of the epithelium. HIOs injected with TcdB maintain a basolateral distribution of ECAD similar to that of the controls.
B. Altered localization of TJ proteins ZO-1 and OCLN following injection with TcdA. In control HIOs, ZO-1 is present at the apical surface of the epithelium, whereas OCLN is seen at the lateral surface of the cell. In HIOs injected with TcdA, apical ZO-1 at TJs is lost and OCLN no longer is restricted to the lateral surface, while TcdB-injected HIOs have ZO-1 and OCLN immunofluorescence similar to those of the control. DAPI, 4′,6-diamidino-2-phenylindole.
C. HIOs were stained with phalloidin to assess the organization of F-actin and acetylated alpha tubulin (AcTub) to visualize stabilized microtubules. In control HIOs, F-actin is strongly localized to the apical surface of the epithelium, while AcTub immunofluorescence is strongest on the apical and basal sides of the cell. Compared to control HIOs injected with TcdA, epithelial cells displayed a reduction of F-actin staining, with areas where staining was undetectable, and showed a severe disruption of AcTub at the apical border. In contrast, in HIOs injected with TcdB, phalloidin staining was similar to that of the controls and AcTub immunofluorescence was mostly similar to that of the controls, with a mild reduction of immunofluorescence on the basal side of the cells.

Basolateral addition of purified toxins disrupts HIO barrier function.

Studies have suggested that TcdA acts to disrupt the localization of tight junction proteins, which then allows for TcdB to act on the basolateral side of the cell (21). Moreover, a “fence and gate” model has recently been proposed whereby *C. difficile* toxins cause a redistribution of basal-lateral proteins to the apical surface so that the bacteria can bind to the cell surface (2). However, the receptors for TcdA and TcdB have not been definitively identified, and it has not been conclusively shown that toxins preferentially affect the apical versus basal surfaces of the epithelium. Therefore, to test a differential effect of apical (Figure 5) versus basal exposure to toxin, we added FD4 along with TcdA or TcdB to the tissue culture media in order to expose HIOs to toxin on the basal side of the epithelium (figure 4.9). In this experiment, since FD4 was added outside the HIO, inward leak and fluorescence inside the HIO lumen indicates a disrupted epithelial barrier. Consistent with apical exposure (figure 4.8), and compared controls, TcdA was again more potent than TcdB at disrupting barrier function (figure 4.9). While barrier function remained intact in 100% of control HIOs (n=10), TcdA disrupted barrier function in 100% of HIOs (n=13) and the barrier was disrupted in only 23% of TcdB treated HIOs (n=22). Importantly, barrier disruption in toxin treated HIOs was not due to apoptosis (figure 4.10). Taken together, these results indicate that the *C. difficile* toxins TcdA and TcdB have the ability to interact with both the apical and basolateral aspects of the epithelium of human intestinal organoids.

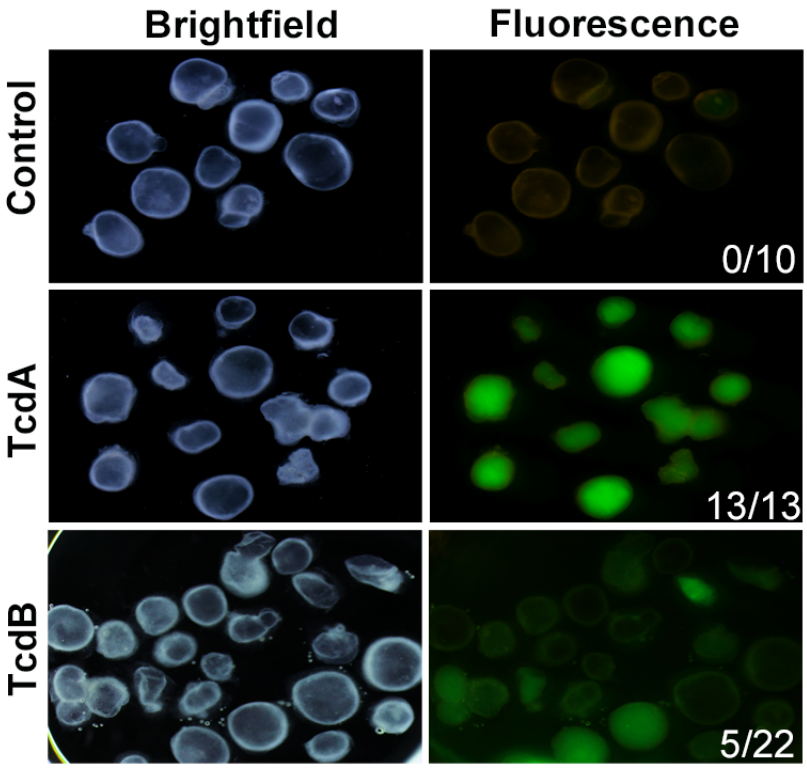

Figure 4. 9 Basolateral exposure to purified toxins causes loss of barrier function.
Purified TcdA or TcdB was added to tissue culture media containing HIOs, followed by the addition of FD4. In this assay, the loss of paracellular barrier function was indicated by diffusion of FD4 into the lumen of HIOs, while HIOs with an intact epithelium excluded FD4. Bright-field images show the location of the HIOs. Images taken under fluorescent light indicate barrier function status. None (0/10) of the untreated HIOs lost barrier function, whereas 100% (13/13) of HIOs treated with TcdA lost barrier function, while only 23% of HIOs treated with TcdB lost barrier function. The results shown are representative of five independent experiments.

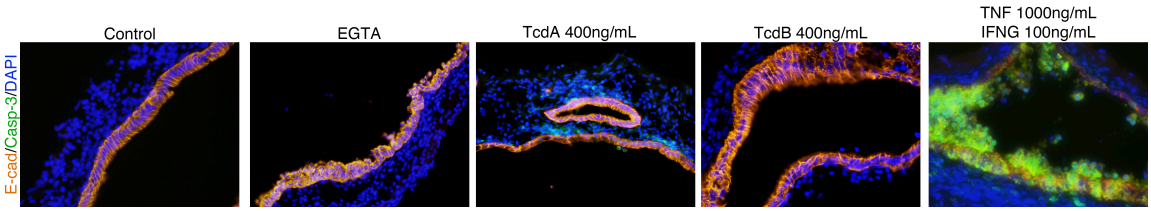

Figure 4.10 Loss of barrier function following treatment with TcdA or TcdB is not due to caspase-3 mediated apoptosis.
Controls, EGTA treated, and 400ng/ml of TcdA or TcdB treated HIO were stained for cleaved caspase-3 an indicator of apoptotic cell death. Treatment with the cytokines TNFalpha and INF-gamma induces massive cell death and serves as a positive control.

Discussion

The pathogenesis of CDI is multifaceted and involves interactions between the host, the gut microbiota and *C. difficile* (22-24). In order to study the effect of *C. difficile* colonization on human epithelium, we developed techniques to colonize the HIO lumen with viable vegetative *C. difficile*. The vegetative cell is sensitive to oxygen leading to the concept that the environmentally stable spore is responsible for transmission (25). Our data suggests that the vegetative cell can be tolerant of oxygen in the lumen of HIOs as viable *C. difficile* persists despite cultivating the HIOs in ambient oxygen conditions. While it may be surprising that *C. difficile* can persist in HIOs grown at ambient oxygen levels, many anaerobes can tolerate oxygen under conditions that limit toxicity of reactive oxygen species (26, 27). Preliminary measurements using an oxygen micosensor indicate that the lumen of HIOs has lower than ambient oxygen levels, with the luminal oxygen concentrations ranging from 5-15% (data not shown). A recent report suggests that some strains of *C. difficile* may be able to grow even at these high levels of oxygen (28).

Recently, others have utilized mouse-derived enteroids (epithelium-only organoids) to study host-microbe interactions (29, 30). A key difference between those reports and the data presented here is that our system utilizes organoids derived from human cells rather than mouse intestinal crypts. In addition, this is the first report demonstrating that organoids can be colonized with an obligate anaerobe.

A caveat of our model is that while HIOs are more similar to the human small intestine, CDI manifests clinically as colitis. However, the small intestinal epithelium is relevant to study *C. difficile* pathogenesis as patients with ileal pouch anal anastomoses will develop clinical CDI. Additionally, animal ileal loop models have historically been used to understand the pathogenesis of this infection with respect to the activity of the toxins on the host.

Many previous studies of *C. difficile* virulence and pathogenesis have focused on the glucosyltransferase toxins TcdA and TcdB. Depending on which system has been used to study these toxins, the relative activities of TcdA and TcdB differ. Previous studies in cell culture lines demonstrate that TcdB has greater cytotoxicity than TcdA (31, 32). However, TcdA has been reported to be more potent than TcdB in animal models, which recapitulate the diverse cell types and structure of the gastrointestinal tract (33, 34). The greater activity of TcdA in the organoid may reflect the fact that the organoid epithelium responds more like the intestinal epithelium *in situ* instead of like *in vitro*-cultured cell lines. One caveat to consider in light of our observations is the growth conditions for the HIOs, which includes media containing EGF, Noggin and R-Spondin2. Previous studies have shown the EGF can reduce TcdA and TcdB induced damage in the colonic mucosa (35). Thus, it is possible that EGF present in the media is able to attenuate the effect of one toxin (TcdB) more than another (TcdA), a possibility that will be tested in the future. However, our finding that TcdA caused greater disruption of HIO epithelial barrier function than TcdB is consistent with the finding that TcdA (but not TcdB) can inactivate the Ras family

GTPase Rap, which regulates cell-cell junctions (36). Our FD4-based assay measures disruption of intercellular junctions, which allows paracellular leak, and is consistent with the described activity of TcdA. Finally our results showing that TcdA can disrupt barrier function when added apically and both TcdA and TcdB can disrupt barrier function when exposed to the basolateral surface demonstrate that toxins can interact with receptors on both surfaces. As yet, the definitive receptor for either of these toxins is not known, however, basolateral activity of toxins have been previously reported, and so it is possible that receptors exist on both apical and basolateral cell surfaces (37). The HIO system may represent a new avenue to search for this important molecular target.

The gastrointestinal epithelium is an interface between the host and the environment and is crucial for many aspects of health including nutrient absorption, maintenance of immune homeostasis as well as a selective barrier against antigens (38, 39). Defects in intestinal epithelial barrier function have been associated with the pathogenesis of inflammatory bowel diseases, celiac disease and enteric infections (40). Herein, we demonstrated that HIOs have an intact polarized epithelium with paracellular barrier function, which can be used for detailed, real-time studies of both normal physiological barrier function as well as barrier dysfunction in the context of chemical perturbations or infection. As such, this system represents the first robust three-dimensional, non-transformed, primary human intestinal system to study the effects of *C. difficile* Infection and will be a valuable tool to study epithelial barrier defects in a variety of injury and disease context

References

1. **Hall AJ, Curns AT, McDonald LC, Parashar UD, Lopman BA.** 2012. The roles of *Clostridium difficile* and norovirus among gastroenteritis-associated deaths in the United States, 1999-2007. Clinical infectious diseases : an official publication of the Infectious Diseases Society of America **55:**216-223.

2. **Kasendra M, Barrile R, Leuzzi R, Soriani M.** 2013. *Clostridium difficile* toxins facilitate bacterial colonization by modulating the fence and gate function of colonic epithelium. The Journal of infectious diseases.

3. **Goulding D, Thompson H, Emerson J, Fairweather NF, Dougan G, Douce GR.** 2009. Distinctive profiles of infection and pathology in hamsters infected with *Clostridium difficile* strains 630 and B1. Infection and immunity **77:**5478-5485.

4. **Theriot CM, Koumpouras CC, Carlson PE, Bergin II, Aronoff DM, Young VB.** 2011. Cefoperazone-treated mice as an experimental platform to assess differential virulence of *Clostridium difficile* strains. Gut microbes **2:**326-334.

5. **Lizer JT, Madson DM, Schwartz KJ, Harris H, Bosworth BT, Kinyon JM, Ramirez A.** 2013. Experimental infection of conventional neonatal pigs with *Clostridium difficile*: A new model. J Swine Health and Production **21:**22-29.

6. **Spence JR, Mayhew C, Rankin S, Kuhar M, Vallance J, Tolle K, Hoskins E, Kalinichenko V, Wells S, Zorn A, Shroyer N, Wells J.** 2011.

Directed differentiation of human pluripotent stem cells into intestinal tissue *in vitro*. Nature **470:**105-109.

7. **Du A, McCracken KW, Walp ER, Terry NA, Klein TJ, Han A, Wells JM, May CL.** 2012. Arx is required for normal enteroendocrine cell development in mice and humans. Developmental Biology **365:**175-188.

8. **Finkbeiner SR, Zeng X-L, Utama B, Atmar RL, Shroyer NF, Estes MK.** 2012. Stem cell-derived human intestinal organoids as an infection model for rotaviruses. mBio **3**.

9. **Xue X, Ramakrishnan S, Anderson E, Taylor M, Zimmermann EM, Spence JR, Huang S, Greenson JK, Shah YM.** 2013. Endothelial PAS domain protein 1 activates the inflammatory response in the intestinal epithelium to promote colitis in mice. Gastroenterology **145:**831-841.

10. **Kuehne SA, Cartman ST, Heap JT, Kelly ML, Cockayne A, Minton NP.** 2010. The role of toxin A and toxin B in C*lostridium difficile* infection. Nature **467:**711-713.

11. **McCracken KW, Cata EM, Crawford CM, Sinagoga KL, Schumacher M, Rockich BE, Tsai Y-H, Mayhew CN, Spence JR, Zavros Y, Wells JM.** 2014. Modelling human development and disease in pluripotent stem-cell-derived gastric organoids. Nature **516:**400-404.

12. **Sugawara S, Ito T, Sato S, Sato Y, Kasuga K, Kojima I, Kobayashi M.** 2014. Identification of site-specific degradation in bacterially expressed human

fibroblast growth factor 4 and generation of an aminoterminally truncated, stable form. Appl Biochem Biotechnol **172:**206-215.

13. **Bell SM, Schreiner CM, Wert SE, Mucenski ML, Scott WJ, Whitsett JA.** 2008. R-spondin 2 is required for normal laryngeal-tracheal, lung and limb morphogenesis. Development **135:**1049-1058.

14. **Schneider CA, Rasband WS, Eliceiri KW.** 2012. NIH Image to ImageJ: 25 years of image analysis. Nat Meth **9:**671-675.

15. **Peterson LWA, David.** 2014. Intestinal epithelial cells: regulators of barrier function and immune homeostasis. Nature Reviews Immunology **14:**141153.

16. **Bergstrom KS, Kissoon-Singh V, Gibson DL, Ma C, Montero M, Sham HP, Ryz N, Huang T, Velcich A, Finlay BB, Chadee K, Vallance BA.** 2010. Muc2 protects against lethal infectious colitis by disassociating pathogenic and commensal bacteria from the colonic mucosa. PLoS pathogens **6**.

17. **Sappington PL, Yang R, Yang H, Tracey KJ, Delude RL, Fink MP.** 2002. HMGB1 B box increases the permeability of Caco-2 enterocytic monolayers and impairs intestinal barrier function in mice. Gastroenterology **123:**790-802.

18. **Bruewer M, Hopkins AM, Hobert ME, Nusrat A, Madara JL.** 2004. RhoA, Rac1, and Cdc42 exert distinct effects on epithelial barrier via selective

structural and biochemical modulation of junctional proteins and F-actin. American journal of physiology. Cell physiology **287:**35.

19. **Shen L, Turner JR.** 2005. Actin depolymerization disrupts tight junctions via vaveolae-mediated endocytosis. Molecular Biology of the Cell **16:**3919-3936.

20. **Nam H, Kang J, Kim S-K, Ahn K, Seok H, Park S, Chang J, Pothoulakis C, Lamont J, Kim H.** 2010. *Clostridium difficile* toxin A decreases acetylation of tubulin, leading to microtubule depolymerization through activation of histone deacetylase 6, and this mediates acute inflammation. The Journal of biological chemistry **285:**32888-32896.

21. **Du T, Alfa MI.** 2004. Translocation of *Clostridium difficile* toxin B across polarized Caco-2 cell monolayers is enhanced by toxin A. The Canadian journal of infectious diseases **15:**83-88.

22. **Madan R, Guo X, Naylor C, Buonomo EL, Mackay D, Noor Z, Concannon P, Scully KW, Pramoonjago P, Kolling GL, Warren CA, Duggal P, Petri WA.** 2013. Role of leptin-mediated colonic inflammation in defense against *Clostridium difficile* colitis. Infection and immunity **82:**341-349.

23. **Reeves AE, Theriot CM, Bergin IL, Huffnagle GB, Schloss PD, Young VB.** 2010. The interplay between microbiome dynamics and pathogen dynamics in a murine model of *Clostridium difficile* Infection. Gut microbes **2:**145-158.

24. **Robinson CD, Auchtung JM, Collins J, Britton RA.** 2014. Epidemic *Clostridium difficile* strains demonstrate increased competitive fitness compared to nonepidemic isolates. Infection and Immunity **82:**2815-2825.

25. **Deakin LJ, Clare S, Fagan RP, Dawson LF, Pickard DJ, West MR, Wren BW, Fairweather NF, Dougan G, Lawley TD.** 2012. The *Clostridium difficile* spo0A gene is a persistence and transmission factor. Infection and immunity **80:**2704-2711.

26. **Rolfe RD, Hentges DJ, Campbell BJ, Barrett JT.** 1978. Factors related to the oxygen tolerance of anaerobic bacteria. Applied and Environmental Microbiology **36:**306-313.

27. **Brusa T, Canzi E, Pacini N, Zanchi R, Ferrari A.** 1989. Oxygen tolerance of anaerobic bacteria isolated from human feces. Current Microbiology **19:**39-43.

28. **Green L, Worthington T, Hilton A, Lambert P.** 2012. 22nd European Congress of Clinical Microbiology and Infectious Diseases, London, United Kingdom

29. **Lukovac S, Belzer C, Pellis L, Keijser BJ, de Vos WM, Montijn RC, Roeselers G.** 2014. Differential modulation by *Akkermansia muciniphila* and *Faecalibacterium prausnitzii* of host peripheral lipid metabolism and histone acetylation in mouse gut organoids. mBio **5**.

30. **Wilson SS, Tocchi A, Holly MK, Parks WC, Smith JG.** 2014. A small intestinal organoid model of non-invasive enteric pathogen-epithelial cell interactions. Mucosal Immunol.

31. **Chaves-Olarte E, Weidmann M, Eichel-Streiber C, Thelestam M.** 1997. Toxins A and B from *Clostridium difficile* differ with respect to enzymatic potencies, cellular substrate specificities, and surface binding to cultured cells. The Journal of clinical investigation **100:**1734-1741.

32. **Riegler M, Sedivy R, Pothoulakis C, Hamilton G, Zacherl J, Bischof G, Cosentini E, Feil W, Schiessel R, LaMont JT.** 1995. *Clostridium difficile* toxin B is more potent than toxin A in damaging human colonic epithelium in vitro. The Journal of Clinical Investigation **95:**2004-2011.

33. **Hirota SA, Iablokov V, Tulk S, Schenck L, Becker H, Nguyen J, Al Bashir S, Dingle T, Laing A, Liu J, Li Y, Bolstad J, Mulvey G, Armstrong G, MacNaughton W, Muruve D, MacDonald J, Beck P.** 2012. Intrarectal instillation of *Clostridium difficile* toxin A triggers colonic inflammation and tissue damage: development of a novel and efficient mouse model of *Clostridium difficile* toxin exposure. Infection and immunity **80:**4474-4484.

34. **Triadafilopoulos G, Pothoulakis C, O'Brien MJ, LaMont JT.** 1987. Differential effects of *Clostridium difficile* toxins A and B on rabbit ileum. Gastroenterology **93:**273-279.

35. **Riegler M, Sedivy R, Sogukoglu T, Castagliuolo I, Pothoulakis C, Cosentini E, Bischof G, Hamilton G, Teleky B, Feil W, Lamont JT, Wenzl E.** 1997. Epidermal growth factor attenuates *Clostridium difficile toxin* A- and B-induced damage of human colonic mucosa, vol. 273.

36. **Pruitt RN, Chumbler NM, Rutherford SA, Farrow MA, Friedman DB, Spiller B, Lacy DB.** 2012. Structural determinants of *Clostridium difficile* toxin A glucosyltransferase activity. Journal of Biological Chemistry **287:**8013-8020.

37. **Nusrat A, von Eichel-Streiber C, Turner JR, Verkade P, Madara JL, Parkos CA.** 2001. *Clostridium difficile* toxins disrupt epithelial barrier function by altering membrane microdomain localization of tight junction proteins. Infection and Immunity **69:**1329-1336.

38. **Groschwitz KRH, Simon P.** 2009. Intestinal barrier function: molecular regulation and disease pathogenesis. The Journal of allergy and clinical immunology **124:**3.

39. **Artis D.** 2008. Epithelial-cell recognition of commensal bacteria and maintenance of immune homeostasis in the gut. Nature reviews. Immunology **8:**411-420.

40. **Catalioto RM, Maggi CA, Giuliani S.** 2011. Intestinal epithelial barrier dysfunction in disease and possible therapeutical interventions. Current medicinal chemistry **18:**398-426.

CHAPTER V

DISCUSSION

The work outlined in the preceding chapters tested the central hypothesis that protection from *C. difficile* disease reflects the combined effects of host immunity and bacteria/bacteria competition. The major findings from this work are: 1) in a murine model, colonization-resistance to a lethal *C. difficile* infection can be restored by pre-colonization with a single bacterium, specifically a less virulent strain of *C. difficile*; 2) pre-colonization with the less virulent strain results in decreased levels of amino acids, such as glycine, which serve as spore co-germinant; 3) pre-colonization leads to decreased germination of the lethal strain, likely due to decreased availability of amino acid co-germinant. Surprisingly, while numerous studies have demonstrated that adaptive immunity is sufficient to protect from CDI (1-4), in the context of our experimental conditions, it was not required for either protection from acute disease when mice were pre-colonized with *C. difficile* strain 630 or for clearance of *C. difficile*. This chapter includes a summary of the main findings from each of the previous chapters in addition to next steps that should be taken to study the factors that provide protection from CDI.

Exploring How Intraspecific Interactions Prevent Colonization by a Lethal Strain of *C. difficile*

In chapter two, I developed a model of subclinical C*. difficile* infection and showed that colonization with one strain of *C. difficile* prevents infection by a highly virulent strain. Using mice deficient in both B and T cells as well as mice that lack a microbiota, I demonstrate that protection is independent of adaptive immunity and occurs via exclusion of the highly virulent strain.

Others had previously observed that colonization with one strain of *C. difficile* protects from challenge by a second strain (5-7). Borriello *et* al. suggested that prior colonization with a non-pathogenic strain limited colonization by a second strain by filling *C. difficile*'s preferred spatial niche in the gut (6, 8). In support of this hypothesis the proteinaceous surface layer of *C. difficile,* termed S-layer protein A (SlpA), was shown to bind to the intestinal epithelium (9). Furthermore, pretreatment of cells with purified SlpA from one strain significantly decreased adherence of another strain *in vitro* (10). Together these data led me to hypothesize that SlpA mediated adherence to the epithelium by *C. difficile* might contribute to the protection by preventing colonization of the invading strain.

I sought to test this hypothesis *in vivo* by treating susceptible mice with SlpA from *C. difficile* strain 630. I reasoned that SlpA might competitively inhibit adherence of the invading strain thereby limiting its colonization. To test this, I partially purified SlpA from overnight cultures of *C. difficile* strain 630 using a low pH glycine buffer as previously described (10, 11). While SlpA is expressed as a

single precursor-peptide, it is cleaved into two smaller peptides termed the low molecular weight (LMW) and high molecular weight (HMW) subunits. Both the LMW and HMW subunits of SlpA were clearly visible on a commasie stained gel after partial purification (figure 5.1).

Mice were made susceptible to CDI by administration of 0.5mg/mL of the antibiotic cefoperazone. Following 2 days off of the antibiotic, 100uL of 3mg/mL SlpA prep or 100uL of PBS was given to mice via orogastric administration 3 hours before infection and every 3 hours thereafter for a total of 5 treatments. Mice treated with PBS (mock) and one of the SlpA treated groups of mice were challenged with *C. difficile* strain VPI 10463. A third group of SlpA treated mice remained unchallenged to monitor the effect of SlpA alone.

Following pretreatment with SlpA, we did not detect a difference in levels of colonization of *C. difficile* strain VPI 10463 compared to mock treated animals (figure 5.2 B) Furthermore, all mice that were challenged with of *C. difficile* strain VPI 10463 developed signs of disease; overall there was no significant difference between the SlpA and mock-treated mice (figure 5.3 A,C).

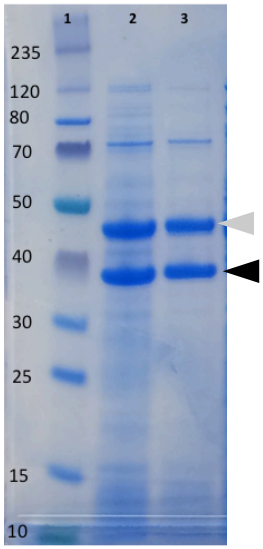

Figure 5.1 Commassie stained 10% Bis-Tris gel of preparations of C. *difficile* strain 630.
Lane numbers are labeled across the top of the gel. Lanes 1 is the protein standard, molecular weights are labeled on the far left side of the gel. Lanes 2,3 show SlpA partially purified by low pH glycine extraction. In lane 3, the grey arrow shows the HMW band and the black arrow shows the LMW band

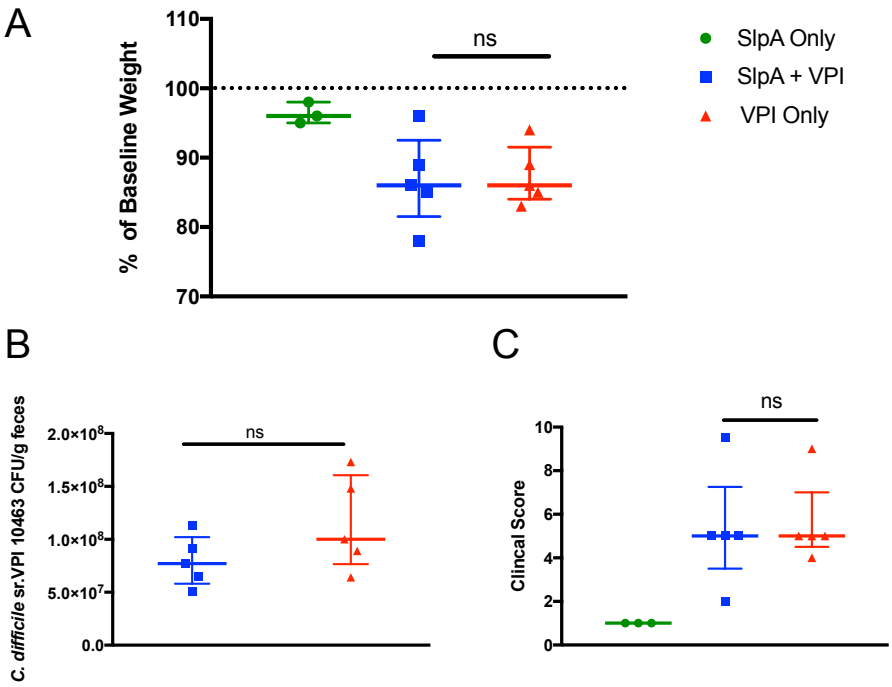

Figure 5.2 Administration of partially purified SlpA from *C. difficile* strain 630 does not protect mice from challenge with the lethal strain
A. Change in mouse body weight from day of infection to necropsy. Mice treated with SlpA only lost a small amount of weight (green). Mice treated with SlpA and then challenged with *C. difficile* strain VPI 10463 (blue) lost the same amount of weight as mice that were only infected with *C. difficile* strain VPI 10463 (red).
B. *C. difficile* strain VPI 10463 CFU in the feces twenty-four hours after infection. There was no difference in colonization between the mice treated with SlpA (blue) compared to untreated mice (red).
C. Clinical score of mice at time of necropsy. Mice only given SlpA had minimal signs of disease (green). Both the mice treated with SlpA (blue) and untreated mice infected *C. difficile* strain VPI 10463 showed signs of disease.

Together these data suggest that SlpA may not be the main driver of protection *in vivo*. However a major limitation of this experiment was that we had no method to confirm that the amount of SlpA given was sufficient to mimic colonization with *C. difficile* strain 630. An alternative tactic would be to challenge mice with *C. difficile* strain 630 deficient in SlpA and ask if this isolate no longer provides protection from challenge with VPI 10463. We did not pursue this approach as reports in the literature claim that *slpA* is an essential gene.

If this hypothesis were to be pursued in the future three things should be determined first: 1) *C. difficile* adheres to the gut epithelium *in vivo*, 2) pre-colonization with C*. difficile* strain 630 blocks adherence of strain VPI 10463, 3) SlpA mediates *C. difficile* adherence to mouse epithelium *in vivo*. While the data presented by no means rule out the role of SlpA in limiting colonization of *C. difficile,* they do not support it either.

In chapter two, we showed that pre-colonization decreases levels of the amino acid glycine, a co-germinant for *C. difficile* spores, leading to decreased germination of the lethal strain. These results provide a novel metabolite to target for restoration of colonization resistance to *C. difficile*. *C. difficile*, in addition to many other *Clostridium* species can ferment amino acid pairs, including glycine, in processes called Stickland reactions (12-14). Since glycine is both a signal for germination as well as a potential nutrient source for vegetative growth of *C. difficile* (15, 16), it is tempting to speculate that glycine is a preferred nutrient source for *C. difficile*. Interestingly SlpA was shown to bind human collagen I (9), which is rich in the amino acids proline and glycine. It is possible that following

toxin mediated disruption of the gut epithelium; SlpA facilitates colonization by binding to collagen, which might serve as a food source for the vegetative cell. If this were true, then SlpA may be more important for persistence of *C. difficile* rather than initial colonization.

While I utilized a virulent but low pathogenic strain of *C. difficile* in these studies due to its genetic tractability, in the clinic, non-toxigenic strains of *C. difficile* have been used to protect patients from disease (17). However, it is worrying that there have been reports of transfer of the toxin genes from a toxigenic strain into a non-toxigenic strain *in vitro* (18, 19). This suggests that ultimately non-toxigenic *C. difficile* may not the best therapy for CDI. It is likely that next generation probiotics will contain defined consortia of strains that confer colonization resistance and/or protect from toxin (20). Future work should focus on confirming the role of glycine in limiting colonization of *C. difficile* as well explore the use of other species capable of removing glycine from the gut as an alterative means to restore colonization resistance to *C. difficile.*

Exploring the Contribution of Adaptive Immunity in Clearance of C. difficile

In chapter three, using the murine model developed in chapter two, we show that adaptive immunity is also not required for clearance of *C. difficile* from the murine gut. While restoration of humoral immunity did result in changes in the abundance of some members of the microbiota it was not required for clearance of *C. difficile*. Furthermore, combining data from multiple experiments we found that three OTUs present in the indigenous pre-treatment community could classify mice that would go on to clear with over 90% accuracy. This finding is

important because it highlights the role of bacterial factors independent of adaptive immunity in modulating colonization of *C. difficile*. Furthermore, while those three OTUs were differential abundant before antibiotics they were not very abundant at the time of infection (data not shown). This raises the question of whether those OTUs directly inhibit *C. difficile* or if they are just biomarkers of a more resilient gut microbial community.

The most important finding from this study is that differences in the microbiota before the start a treatment may greatly impact the outcome of experiments. Moving forward preclinical studies should strive to use multiple cages of animals to minimize bias due to the variation of the gut microbiota of animals.

Summary and implications of chapter four

In chapter four I describe the use of human intestinal organoids as a model for studying both *C. difficile* persistence and toxin mediated epithelial damage. While the high oxygen levels in HIOs makes them imperfect models to study colonization, they are ideal for studying the cellular effects of the toxins on a complex epithelium. While the work in chapters two and three demonstrate that limiting colonization can prevent CDI, protection can also be mediated by modulation of toxin production and activity. Thus it is important to continue to study the factors that modulate toxin-mediated damage to the host epithelium. At the time of publication, we did not know that one TcdB receptor belongs to the Wnt receptor frizzled family of proteins (21). It would be in interesting and

informative to explore if different organoids culture conditions alters the observed effect of the toxins.

References

1. **Wullt M, Noren T, Ljungh A, Akerlund T.** 2012. IgG antibody response to toxins A and B in patients with *Clostridium difficile* infection. Clinical and vaccine immunology : CVI **19:**1552-1554.

2. **Allo M, Silva J, Fekety R, Rifkin G, Waskin H.** 1979. Prevention of clindamycin-induced colitis in hamsters by *Clostridium sordellii* antitoxin. Gastroenterology **76:**351-355.

3. **Giannasca PJ, Zhang ZX, Lei WD, Boden JA, Giel MA, Monath TP, Thomas WD.** 1999. Serum antitoxin antibodies mediate systemic and mucosal protection from *Clostridium difficile* disease in hamsters. Infection and immunity **67:**527-538.

4. **Marozsan A, Ma D, Nagashima K, Kennedy B, Kang Y, Arrigale R, Donovan G, Magargal W, Maddon P, Olson W.** 2012. Protection against *Clostridium difficile* infection with broadly neutralizing antitoxin monoclonal antibodies. The Journal of infectious diseases **206:**706-713.

5. **Wilson KH, Sheagren JN.** 1983. Antagonism of toxigenic *Clostridium difficile* by nontoxigenic *C. difficile*. The Journal of Infectious Diseases **147:**733-736.

6. **Borriello SP, Barclay FE.** 1985. Protection of hamsters against *Clostridium difficile* ileocaecitis by prior colonisation with non-pathogenic strains. Journal of Medical Microbiology **19:**339-350.

7. **Nagaro K, Phillips S, Cheknis A, Sambol S, Zukowski W, Johnson S, Gerding D.** 2013. Nontoxigenic *Clostridium difficile* protects hamsters against challenge with historic and epidemic strains of toxigenic BI/NAP1/027 *C. difficile*. Antimicrobial agents and chemotherapy **57:**5266-5270.

8. **Borriello S, Welch A, Barclay,Ä¶ F.** 1988. Mucosal association by *Clostridium difficile* in the hamster gastrointestinal tract. Journal of medical ,Ä¶.

9. **Calabi E, Calabi F, Phillips AD, Fairweather NF.** 2002. Binding of *Clostridium difficile* surface layer proteins to gastrointestinal tissues. Infection and Immunity **70:**5770-5778.

10. **Merrigan MM, Venugopal A, Roxas JL, Anwar F, Mallozzi MJ, Roxas BAP, Gerding DN, Viswanathan VK, Vedantam G.** 2013. Surface-layer protein A (SlpA) Is a major contributor to host-cell adherence of *Clostridium difficile*. PLOS ONE **8:**e78404.

11. **Dubreuil JD, Logan SM, Cubbage S, Eidhin DN, McCubbin WD, Kay CM, Beveridge TJ, Ferris FG, Trust TJ.** 1988. Structural and biochemical analyses of a surface array protein of *Campylobacter fetus*. J Bacteriol **170:**4165-4173.

12. **Nisman B.** 1954. THE STICKLAND REACTION. Bacteriological Reviews **18:**16-42.

13. **Jackson S, Calos M, Myers A, Self WT.** 2006. Analysis of Proline Reduction in the Nosocomial Pathogen *Clostridium difficile*. Journal of Bacteriology **188:**8487-8495.

14. **Fonknechten N, Chaussonnerie S, Tricot S, Lajus A, Andreesen JR, Perchat N, Pelletier E, Gouyvenoux M, Barbe V, Salanoubat M, Le Paslier D, Weissenbach J, Cohen GN, Kreimeyer A.** 2010. *Clostridium sticklandii*, a specialist in amino acid degradation:revisiting its metabolism through its genome sequence. BMC Genomics **11:**555.

15. **Bouillaut L, Self WT, Sonenshein AL.** 2013. Proline-dependent regulation of *Clostridium difficile* Stickland metabolism. Journal of bacteriology **195:**844-854.

16. **Sorg JA, Sonenshein AL.** 2008. Bile salts and glycine as cogerminants for *Clostridium difficile* spores. Journal of Bacteriology **190:**2505-2512.

17. **Gerding DN, Meyer T, Lee C, et al.** 2015. Administration of spores of nontoxigenic *Clostridium difficile* strain m3 for prevention of recurrent *C. difficile* infection: A randomized clinical trial. JAMA **313:**1719-1727.

18. **Villano S, Seiberling M, Tatarowicz W, Monnot-Chase E, Gerding D.** 2012. Evaluation of an oral suspension of VP20621, spores of nontoxigenic

Clostridium difficile strain M3, in healthy subjects. Antimicrobial agents and chemotherapy **56:**5224-5229.

19. **Brouwer MSM, Roberts AP, Hussain H, Williams RJ, Allan E, Mullany P.** 2013. Horizontal gene transfer converts non-toxigenic *Clostridium difficile* strains into toxin producers. Nature Communications **4:**2601.

20. **Andersen KK, Strokappe NM, Hultberg A, Truusalu K, Smidt I, Mikelsaar R-H, Mikelsaar M, Verrips T, Hammarström L, Marcotte H.** 2016. Neutralization of *Clostridium difficile* toxin B mediated by engineered *Lactobacilli* that produce single-domain antibodies. Infection and Immunity **84:**395-406.

21. **Tao L, Zhang J, Meraner P, Tovaglieri A, Wu X, Gerhard R, Zhang X, Stallcup WB, Miao J, He X, Hurdle JG, Breault DT, Brass AL, Dong M.** 2016. Frizzled proteins are colonic epithelial receptors for *C. difficile* toxin B. Nature **538:**350-355.